1-1-2011

Application of Digital Signal Processing to Underground Power Cables Fault Detection

Abhishek Pandey

APPLICATION OF DIGITAL SIGNAL PROCESSING TO UNDERGROUND POWER CABLES FAULT DETECTION

By

Abhishek Pandey

A Thesis
Submitted to the Faculty of
Mississippi State University
in Partial Fulfillment of the Requirements
for the Degree of Master of Science
in Electrical Engineering
in the Department of Electrical and Computer Engineering

Mississippi State, Mississippi

August 2011

APPLICATION OF DIGITAL SIGNAL PROCESSING TO UNDERGROUND POWER CABLES FAULT DETECTION

By

Abhishek Pandey

Approved:

Nicolas H. Younan James Worth Bagley Chair and Professor of Electrical and Computer Engineering and Department Head (Major Advisor and Director of thesis)	Stanislaw Grzybowski Professor of Electrical and Computer Engineering, Director High Voltage Laboratory, and Mississippi Power Professorship in ECE (Committee Member)
Jenny Q. Du Associate Professor of Electrical and Computer Engineering (Committee Member)	James E. Fowler Professor of Electrical and Computer Engineering (Graduate Coordinator)
Sarah Rajala Dean, Bagely College of Engineering	

Name: Abhishek Pandey

Date of Degree: August 6, 2011

Institution: Mississippi State University

Major Field: Electrical Engineering

Major Professor: Dr. Nicolas H. Younan

Title of Study: APPLICATION OF DIGITAL SIGNAL PROCESSING TO UNDERGROUND POWER CABLES FAULT DETECTION

Pages in Study: 84

Candidate for Degree of Master of Science

Underground power cables encounter various problems caused by manufacturing defects and/or environmental contact. In keeping with the Smart Grid vision, researchers must develop diagnostic techniques that can be utilized to facilitate the decision making processes regarding replacement prior to failure can occur, thereby minimizing impact to customers. Due to the impact of the aging infrastructure and in particular underground polymeric cables, various offline and online methods have been developed for the detection of the remaining life of underground cables. The offline methods require power outage, which can lead to further difficulty in their implementation. Signal processing techniques hold promise to provide real time or near real time diagnostics. In this thesis, three different signal processing techniques; fast Fourier transform, short-time Fourier transform, and wavelet transform; are investigated for identifying and classifying various fault types encountered in underground power cables based on cable current and voltage measurements.

DEDICATION

I would like to dedicate my thesis to my dad who had always been my inspiration in life. My mom, my brother, and my sister have always given encouragement as well, without which this project would not have been possible and Pummi for her relentless support.

ACKNOWLEDGEMENTS

I would like to thank Dr Younan for his immense support and guidance. His valuable suggestions have made this thesis possible. This project was financially supported by San Diego Gas & Electric. Thanks to Dr Tom Bialek and Ron Jordan for their support. Thanks to all my committee members, Dr Grzybowski and Dr Du, for their valuable time and help at various stages of the thesis. I would also like to thank Dr Fowler for standing by me through all my doubts and questions. Special thanks go also to Dr Taylor, Jr. for his friendly advice.

TABLE OF CONTENTS

LIST OF FIGURES

CHAPTER I

INTRODUCTION

1.1 Background

In general, underground power cables encounter various problems due to aging and faults; thus affecting electric service delivery and transmission infrastructure. The application of distributed generation in a micro-grid application, for example, is increasing, likely to be connected to the grid via power cables. While industry expectations are that power polymeric cables should have a thirty to forty year lifespan, experience has shown that certain vintages of cable are performing better than others. The development of predictive analytics in support of the modern grid helps to ensure that the equipment required to integrate distributed generation into the grid will operate in an optimal manner with minimal maintenance.

Predictive analytics are the next logical extension of the self-healing grid concept. Today, most equipment diagnostics are performed on de-energized equipment. In keeping with the smart grid vision, diagnostic techniques must be developed which can be utilized with the equipment on-line so that decisions regarding replacement prior to failure can occur; thus minimizing impact to customers. Due to the impact of an aging infrastructure, and in particular underground polymeric cables, various offline and online methods have been developed for the detection of the remaining life of underground cables. The offline methods require power outage, which can lead to further difficulty in their implementation. Other available methods can provide average life details [1] or

exact location details. Preliminary work performed by investigators indicates that predictive analytics hold promise in classifying the condition of power cables and other equipment insulation. In order to perform this diagnostic in real or near-real time, digital signal processing (DSP) methods are required.

It is well known that most of the tests conducted are based on voltage, current, and impedance values of the cable. Processing these experimental data will effectively provide us with some idea about the remaining life of a cable. Accordingly, advanced signal processing methods can be used for this purpose. Such methods include Fast Fourier Transform (FFT), Short-Time Fourier Transform (STFT), and Wavelet Transform (WT). In general, the Fourier transform is a simple and effective method for analyzing various types of experimental data. However, the Fourier transform provides only information about the frequency content (frequency spectrum) over the entire duration of the time domain signal. Thus, it is quite difficult to characterize the frequency content of the signal as time progresses. On the other hand, the STFT provides localization in both time and frequency that allows characterizing the frequency content of a time domain signal at each time instance. However, the localization in time and frequency is fixed, thus providing limited time and frequency resolutions. Accordingly, multiresolution analysis, such as the wavelet transform, would be a better method to perform this type of analysis. In general, the wavelet transform provides multiresolution analysis with variable window size, and it is thus better suited for such analysis. In general, variable window sizes provide good resolution in the time and frequency domains; thus helping not only in identifying the fault, but also in localizing it.

In this thesis, the analysis of underground power cables is performed using the fast Fourier transform, short-time Fourier transform, and the wavelet transform with the

objective of detecting fault and average life of the cable. Three types of cables are used in this experiment: a normal cable, a shorted cable, and a cable with holes. The impedance in each case is computed and all three signal processing methods are applied so that the resulting impedance magnitude and impedance phase can be examined in the frequency domain (FFT) and time/frequency domain (STFT and WT). This analysis is expected to unveil differences in the frequency response of the three different types of a cable and can eventually be used as a measure for fault detection and localization.

1.2 Motivation

There has been lot of work done on using signal processing techniques to do diagnostics for aging underground power cables. Lately wavelet analysis has been used as very efficient method for fault identification and localization. There is not much work done on fault classification using signal processing algorithms. Again phase responses from these algorithms has not been analysed much. Phase response obtained from different faulty cables could be used as a method in diagnostic analysis. Again not much work is done on exploring to find out effect of different types of windowing on the output of fault detection and classification. Different windowing techniques implemented on underground power cable could be an interesting result to see. We can explore a possibility of better windowing method and explore if there is a preferable windowing method for these different kinds of fault data.

1.3 Literature Review

Multiresolution analysis is one of the most frequent and widely used methods in signal processing applications. Various methods based on multiresolution analysis have been used for fault detection in power cables. J Moshtagh et al. [2] uses ATP to simulate

transient high frequency signals, fault current and voltage conditions. Then, they use wavelet transformation to extract useful information from fault data followed by fuzzy logic to accurately determine the localization of fault. Four types of faults are considered; core open circuit (CROC), core and sheath open circuit (CRSHOC), core with sheath short circuit (CRSHSC), and core and sheath through ground short circuit (CRSHGSC). A dyadic grid is used to implement the wavelet transform with the Haar being the mother wavelet. It should be noted that the selection of a mother wavelet is, in general, critical to fault detection, i.e., the closer the mother wavelet is to fault, the better the fault can be localized. A Fuzzy logic system is then used to localize and identify different type of faults.

Another method, introduced by C.K. Jung et al [3], uses the wavelet transform as a method for localization of fault. This method is based on localizing the transient coming out of reflection from the fault location. Instead of using directly the discrete wavelet transform (DWT), the stationary wavelet transform is used because the stationary wavelet transform has a redundancy property which is useful in locating transient in noisy environment. In this method, system modelling and simulation is done by ATP as well. The first step of the process is detecting the fault which is done by setting a threshold value. If the signal exceeds the threshold before and after the first spike, a fault has theoretically occurred. This fault could be present in any of the phases; hence it is detected by using a 4^{th} approximation of the phases. For example, if a, b, and c represent the corresponding phases, the faulty phase will have high approximation. The approximation from other phases will be near zero. The output generated by this method will have many spikes so it will be difficult to localize fault. These spikes are produced due to the reflection by faults and attenuation and reflection by the other end of the wire.

This noise could be removed by using a multiscale correlation algorithm. The distance of the fault is found by scaling the distance between the first and second peaks through calculation.

Various neural network methods and sensors methods [7] are also used to identify faults in power cables. Mousavi et al describes a pattern classification method for fault identification. In this method, data collection is performed online using a monitoring system installed onsite. Various steps of this procedure involve pre-processing, feature extraction, and classification into 4 classes. The pre-processing stage ensures that the abnormal signal is distinguishable from the normal signal. Feature extraction is done using a discrete wavelet analysis package. Raw feature extraction is done by dimensionality reduction, using the principal component analysis method. Finally, the problem is reduced to a classification problem with 2 groups and 4 classes. Classification is based on the k-nearest neighbour problem, where the K closest training data set is found and the majority class is assigned.

CHAPTER II

METHODOLOGY

The methodology applied in this study is based on implementing three different signal processing algorithms: Fourier transform, short time Fourier transform, and wavelet transform.

2.1 FFT:

The FFT [10] is a simple and effective method to analyze various types of experimental data. Since experimental data, in general, are limited in length and can be affected by the presence of measurement noise, various data windowing are first applied to the cable data prior to the application of the FFT. Mathematically, the Fourier transform can be represented by the following equations:

$$F(w) = \int_{-\infty}^{\infty} \mathrm{f(t)}\exp(-\mathrm{jwt})\,\mathrm{dt}$$

$$f(t) = \frac{1}{2\pi}\int_{-\infty}^{\infty} \mathrm{F(w)}\exp(\mathrm{jwt})\,\mathrm{dw} \qquad \text{Eq. 2.1}$$

The mathematical equations above show how FFT can be used to convert time domain data into frequency domain. In the frequency domain, it is easier to visualize fault diagnostics. The FFT, in general, is not good for time resolution and only frequency precision can be achieved by this method. This type of analysis is not good for types of signals where we would like to perform localization tasks. FFT is a handy tool for performing identification of faults as it is quite simple to implement. But a complete fault

analysis will always involve the localization of fault, which will require better signal processing tools than FFT.

2.2 STFT

As we discussed earlier, the FFT in general, is not a sufficient method for analyzing fault diagnostics. One method that comes into mind, which gives us some frequency and time resolutions, is the short time Fourier transform (STFT). The STFT is a windowed version of the Fourier transform, i.e., its implementation is based on applying the Fourier transform to a sliding window of the time domain signal. Accordingly, the window choice is important to the quality of the localization. In general, the STFT is a complex function of time and frequency and its magnitude is displayed in the time-frequency plane, i.e., in a form known as the spectrogram. Note that the frequency and time resolutions are inversely proportional to each other and there is a tradeoff between them. Thus, at any given instant of time, one can select a large window size and concentrate on the frequency resolution, or one can select a small window size so that we can get a better time resolution. Mathematically, the STFT is represented by the following equation

$$STFT\{x(n)\} \equiv X(m,w) = \sum_{-\infty}^{\infty} \mathrm{x[n]w[n-m]e^{-jwn}} \qquad \text{Eq. 2.2}$$

with w being a time window function.

The most common way to represent the STFT is the spectrogram, which is described by the square of the magnitude response of the STFT. The Spectrogram is represented mathematically as,

$$spectrogram\{x(t)\} \equiv |X(\tau,\omega)|^2 \qquad \text{Eq. 2.3}$$

The spectrogram is used in various signal processing applications, such as music and voice analysis. Some of the limitations of the spectrogram include the difficulty of extracting the original signal since it contains no phase information.

2.3 Wavelet

Since the STFT offers only limited resolution results in the frequency and/or in time domain, we can use multiresolution analysis as an answer to this problem. Wavelet analysis [11] provides us with numerous possibilities of selecting various mother wavelet functions. Most common mother wavelet functions used is Haar, Daubecheis, etc. In the Fourier transform, all the signals are represented as combination of sine functions. In the wavelet transform, any signal can be represented by a translated and scaled version of a mother wavelet. Although several mother wavelets are available, only the Daubechies mother wavelet was used in this analysis. The Daubechies mother wavelet is illustrated in 3D in Figure 2.1.

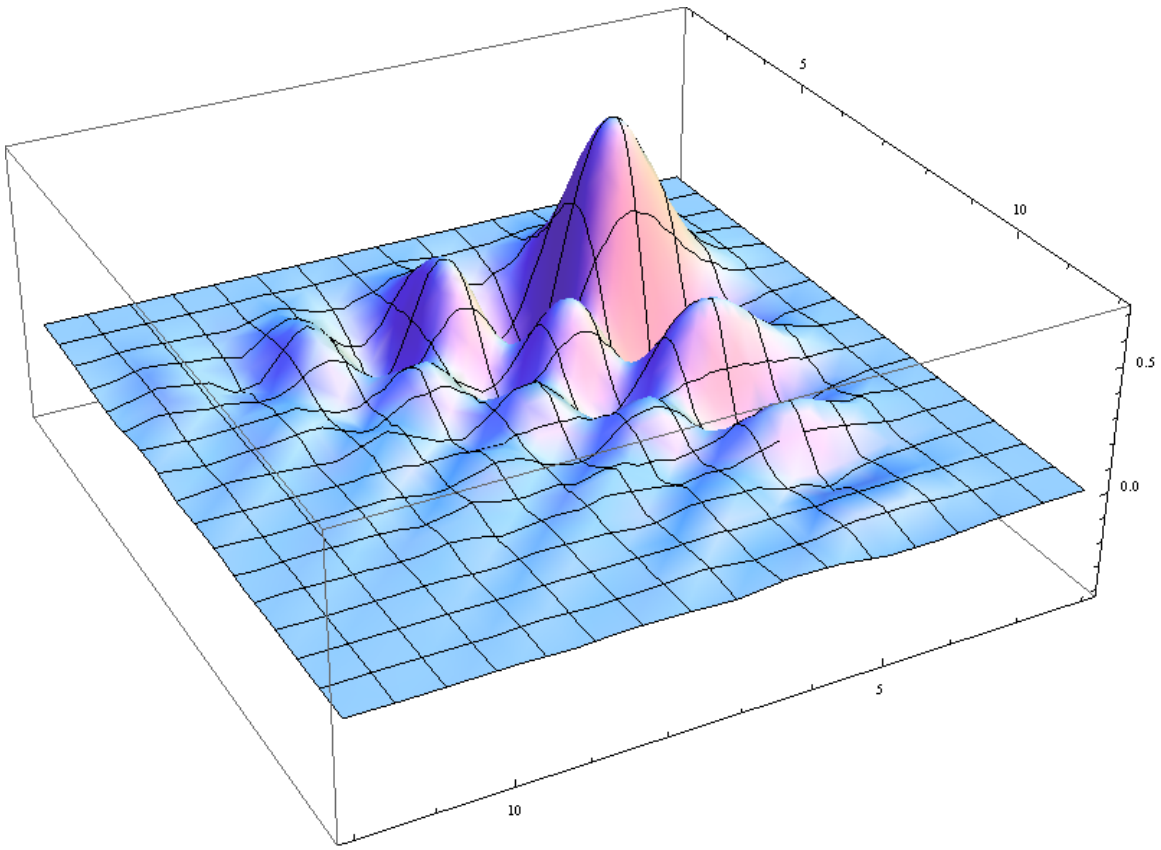

Figure 2.1 Example of Daubecheis mother wavelet

Unlike the STFT, the wavelet transform provides a multiresolution analysis that offers more flexibility in terms of frequency and time resolutions since it handles a variable size windowing. Wavelet is better suited for diagnostics detection as it provides better frequency resolution for lower frequencies and higher time resolution for higher frequencies. Since most of the fault signal produces high frequency component in case of fault, these high frequency components need to be localized so that fault location in power cables can be found.

The implementation of the wavelet transform requires the decomposition of the original signal, which is mathematically represented by the following equation:

$$y[n] = (x * g)[n] = \sum_{-\infty}^{\infty} x[k]g[n-k] \qquad \text{Eq. 2.4}$$

The original signal, x(n), is decomposed into high and low frequency components with impulse responses of g (low pass filtering) and h (high pass filtering), respectively, as follows:

$$y_{low}[n] = \sum_{-\infty}^{\infty} \mathrm{x[k]g[2n-k]}$$
$$y_{high}[n] = \sum_{-\infty}^{\infty} \mathrm{x[k]h[2n-k]} \qquad \text{Eq. 2.5}$$

Wavelet is implemented via a decomposition of a characteristic filter bank. First, a signal is decomposed into a high frequency band and a low frequency band. Then, a low pass signal is down-sampled by 2 and the low frequency band is further decomposed into high frequency and low frequency bands. This kind of stepwise analysis yields better resolution for the low frequency range. Figure 2.2 shows the decomposition of the characteristic filter banks into detail and approximation coefficients.

Figure 2.2 Wavelet decomposition

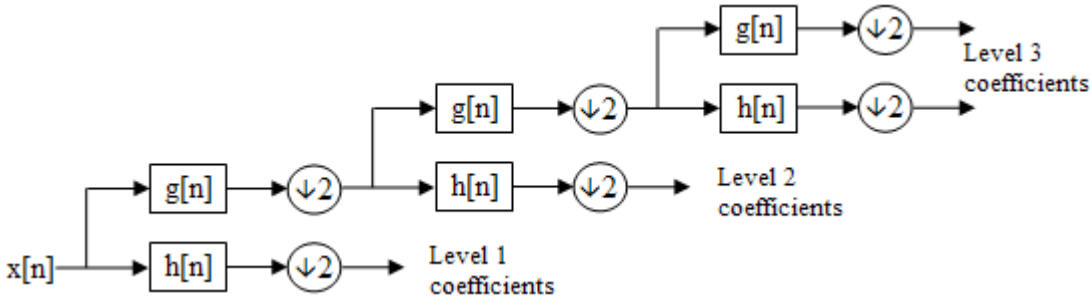

Figure 2.3 Filter bank showing a 3 filter bank level decomposition

Figure 2.3 shows a three level filter bank decomposition of the signal. Note that the level of decompositions of the signal is determined by the number of samples in the original signal. For example, a three level decomposition is possible for an 8 sample signal. The detail coefficients correspond to the high frequency components while the approximation coefficients correspond to the low frequency components. The approximation coefficients combined with different levels of the detail coefficients yields the original signal. For certain applications, which involve high frequency analysis, we cannot get a good frequency resolution as most of the wavelet schemes are based on focusing on low band frequencies.

The wavelet transform, in general, has many advantages. These include:

1) The wavelet transform gives flexibility in time and frequency resolutions by using multiresolution analysis. This is a benefit over the STFT, which has limited time and frequency resolutions.

2) The wavelet transform is a useful signal processing tool for analyzing transient behavior of a signal, as we can use different types of mother wavelet functions. The selection of the mother wavelet function is based on the type of tasks the wavelet analysis is used for.

3) Localization in both time and frequency can be easily achieved using the wavelet transform. Wavelet offer good time resolution which helps in a localization task as we can have selective time resolution in fault areas, which are easily identified by high frequency components generated by faults.

4) Wavelet is a tool which is very helpful in analyzing signals found in nature and surrounding. Most of the signals found in nature have very crucial and significant low frequency components. As we have seen, the wavelet transform provides a very good

frequency resolution for low frequency components when filter bank decomposition is performed. Thus, wavelet is the right tool to analyze signals found naturally in the world.

5) Compression of images is an important task performed by wavelet analysis. Since a filter bank decomposition of a signal reduces the original signal into detail and approximate coefficients, we can select any level of decomposition without much loss and get compressed image using wavelets. For example, a 32 sample original signal can be decomposed to 5 levels of filter bank decompositions, but we can stop only with 3 level of decompositions; thus saving calculation time and complexity. On the other hand, the disadvantages of using the wavelet transform include

1) The wavelet coefficients are real quantities; thus, there is no phase information provided, which is helpful in identifying faults in power cables, as seen from the implementation of the FFT and STFT.

2) The original wavelet analysis cannot be used for analyzing signals with very high frequency components. This is due to the inherent nature of the implementation of the wavelet transform, which divides a low frequency component into further low and high frequency components. Accordingly, the frequency resolution of the high frequency regions is not as great as the low frequency regions. Thus, we need to use a modified version of the wavelet transform to analyze signals with high frequency components.

3) Images compressed via the wavelet transform cannot be reversed to obtain the original image. This is because wavelet offers a lossy compression algorithm, which does not contain important detail components thrown during image compression.

2.4 Windowing

For all three methods, FFT, STFT, and wavelet analyses, five different types of windows [11] [12], rectangular, Hamming, Hanning, triangular, and Gaussian, of length N (total number of samples) are used. A brief description of each window is presented below.

Rectangular window: This windowing has sharp edges at the extremes and not good in general because of the ripple effects that are introduced in the frequency response. This window is represented in the time domain by following equation.

$$w(n) = 1, n = 0, 1, \dots, N-1, \quad \text{Eq. 2.6}$$

Hamming window: This window has a smoother frequency and time domain responses. It is good because of its smooth frequency response output. The output equation is given by:

$$w(n) = 0.54 - Cos\left(\frac{2\pi n}{N-1}\right), n = 0, 1, \dots, N-1 \quad \text{Eq. 2.7}$$

Hanning window: Similar to the Hamming window, a Hanning window has smooth time domain and frequency domain responses. The Hanning window is represented mathematically by:

$$w(n) = 0.5\left\{\cos\left(\frac{2\pi n}{N-1}\right)\right\}, \mathrm{n} = 0, 1, \dots, \mathrm{N}-1 \quad \text{Eq. 2.8}$$

Triangular window: This windowing technique has a sharp edge response and has limited applications. It is represented by:

$$w(n) = 2/N(\left\{\frac{N}{2} - abs\left(n - \frac{N-1}{2}\right)\right\}, \mathrm{n} = 0, 1, \dots, \mathrm{N}-1 \quad \text{Eq. 2.9}$$

Gaussian window: The Gaussian window is another windowing technique that has smooth time domain and frequency domain responses. The Gaussian window is represented mathematically by:

$$w(n) = e^{-\frac{1}{2}\left\{\left(\frac{n-\frac{N-1}{2}}{\alpha(N-1)/2}\right)^2\right\}}, \mathrm{n} = 0, 1, \ldots, \mathrm{N}-1 \qquad \text{Eq. 2.10}$$

where $\alpha <= 0.5$

CHAPTER III

RESULTS AND OBSERVATIONS

Results of the experiments are divided into three parts based on the order in which the experiments are carried out.

3.1 Experimental Data Description

Five set of data samples with sample sizes of N=5000 and N=50000 are used in this study for three different cable types: normal cable, cable with a hole drilled from the insulator shield to the conductor at the midpoint of the conductor, and shorted cable formed by inserting a copper wire in the hole, thus shorting the conductor and concentric neutral. Data sets with 50000 samples are down-sampled to 5000 for uniformity. All the data is obtained from an L=100 m, D=10.3 mm AL, 4.45 mm of XLPE cable (polymeric cable). Sampling of the data is done at time interval t = 0.00000001sec. With this type of cables, the overall capacitance to ground is 32 nF, the insulation resistance to ground is 3 GΩ, the conductor resistance is 30 mΩ, and the conductor inductance is 0.3 mH. A typical polymeric cable with the presence of different types of faults present is shown in Figure 3.1 below. Three types of cable data are provided; sending end voltage (cable end where an input voltage is applied), receiving end voltage (cable end where the input voltage is received) and current.

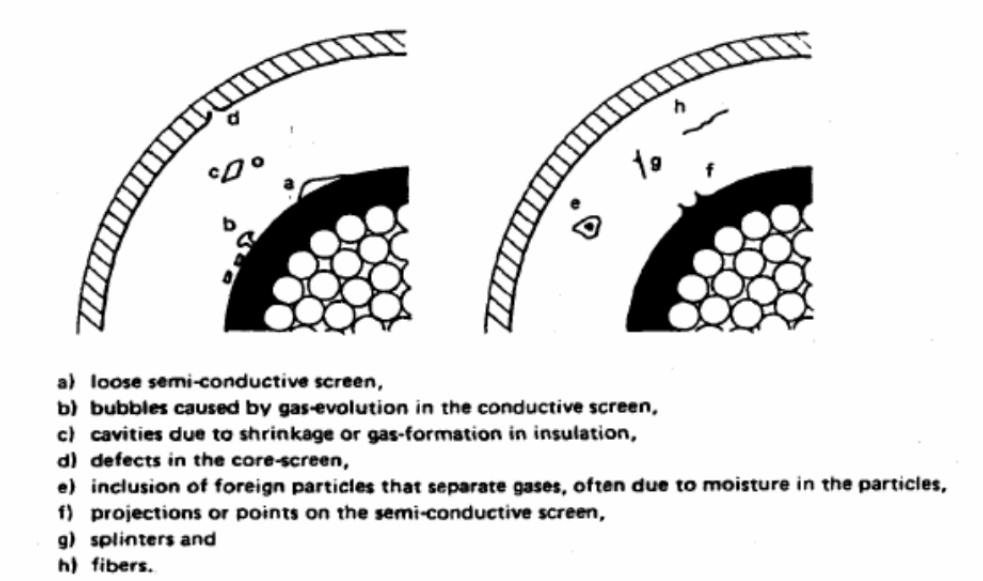

Figure 3.1 Defects in extruded cable dielectrics

3.2 FFT Test Results

For the FFT analysis, the cable impedance was computed directly from the current and voltage measurements in two ways:

1. In the first method, we directly calculate the impedance as the ratio of the sending end voltage over the current.
2. In the second method, the impedance is calculated as the ratio of the differential voltage over the current, where the differential voltage represents the difference between the sending end voltage and the receiving end voltage.

Note that for FFT computation, the data length required must satisfy $N=2^m$, with m being an integer. Since the data length is limited to 5000 samples, 4096 samples are used in this study. We also tried the concept of zero padding with 8192 samples and similar results were obtained.

The results provided below correspond to the impedance magnitude and impedance phase for the three types of cables considered in this study for different types

of windows. Figures 3.1 – 3.10 correspond to the magnitude and phase of the impedance as a function of frequency computed from the sending end voltage and Figures 3.11 – 3.20 correspond to the same, except the impedance is computed from the differential voltage. Although all types of windowing techniques seem to distinguish between the three different types of cables from the phase information, it is observed that the Gaussian window seems to have slightly better results in terms of both magnitude and phase responses compared to the other types of windows. Accordingly, the other sample data sets are examined using the Gaussian window. Figures 3.21 – 3.28 corresponds to the magnitude and phase responses for sample data sets 2 -5 with the impedance being calculated from the sending end voltage and Figures 3.29 – 3.36 correspond to the same with the impedance being calculated from the differential voltage.

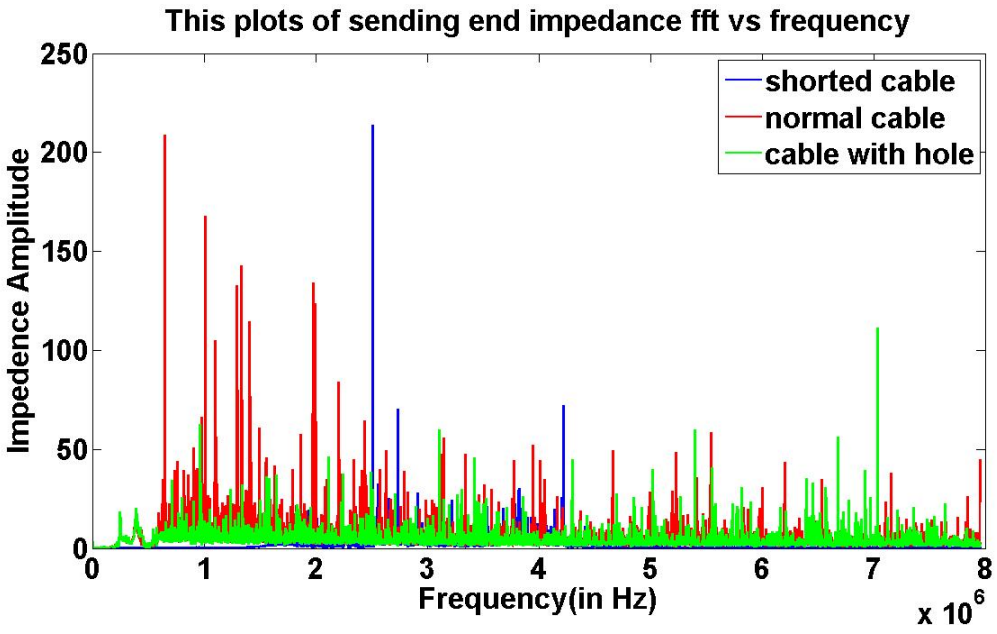

Figure 3.2 Impedance amplitude with a rectangular window (first sample, sending end voltage).

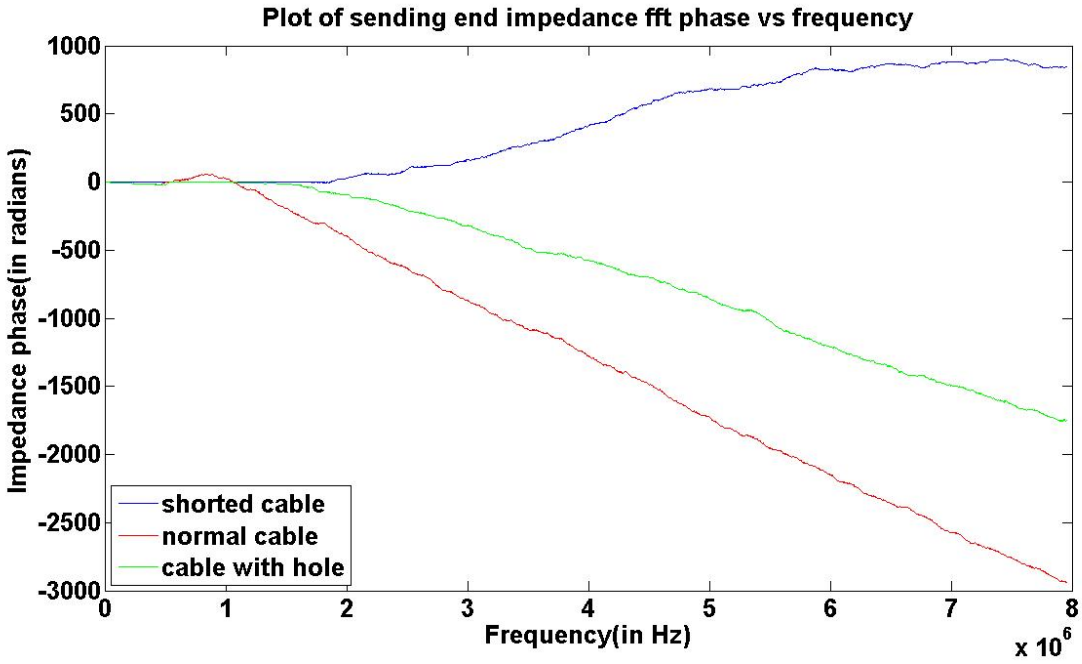

Figure 3.3 Impedance phase with a rectangular window (first sample, sending end voltage).

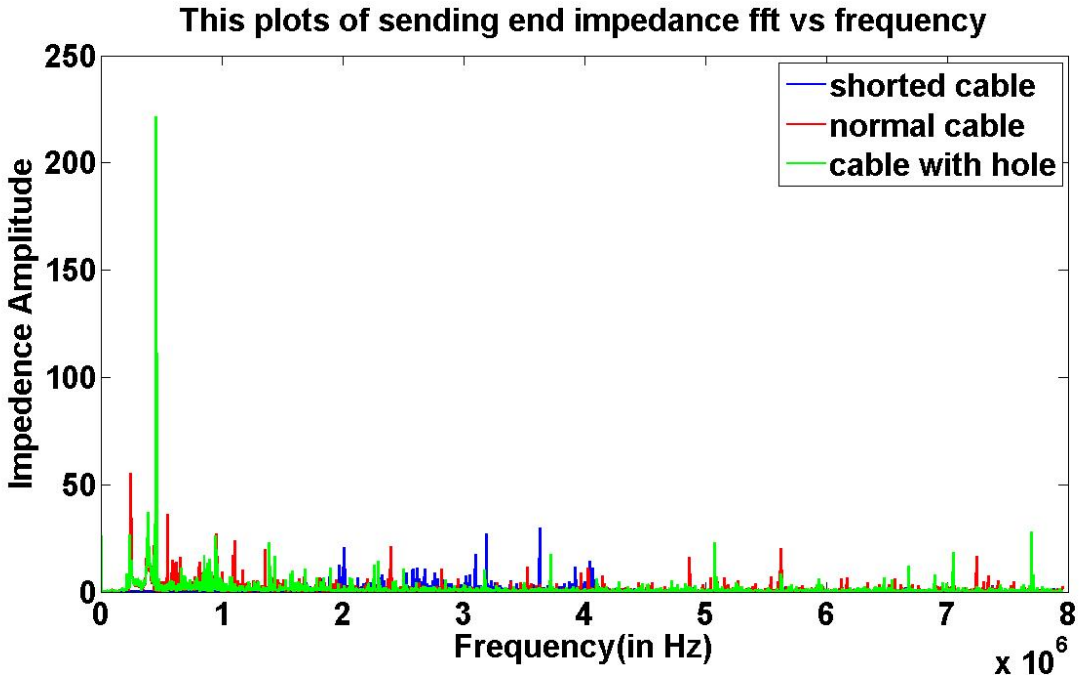

Figure 3.4 Impedance amplitude with a Hamming window (first sample, sending end voltage).

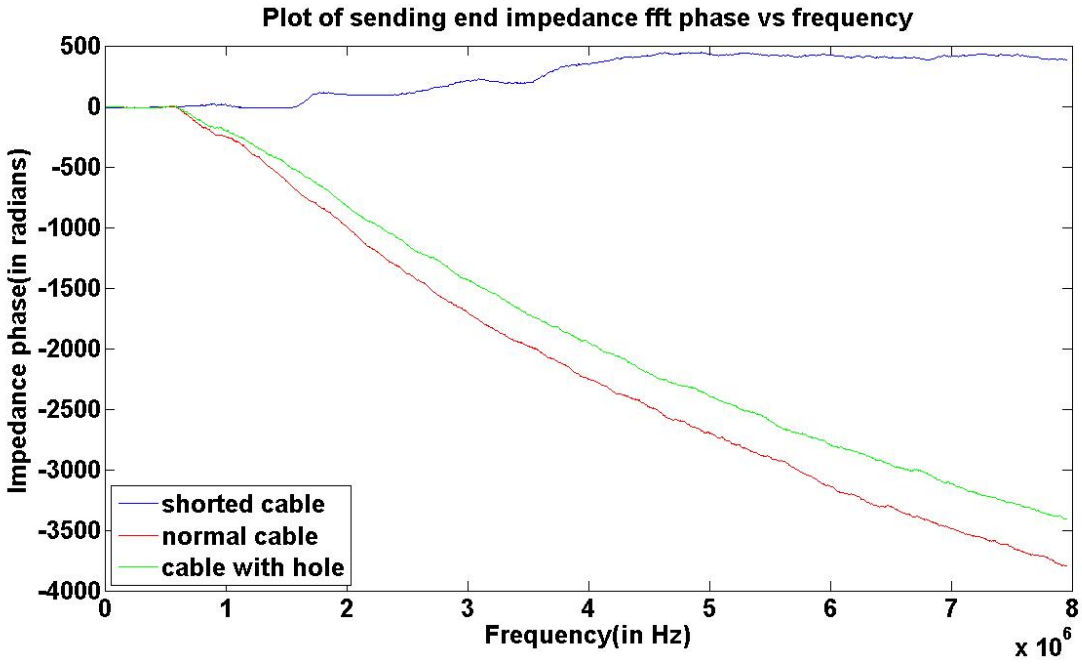

Figure 3.5 Impedance phase with a Hamming window (first sample, sending end voltage).

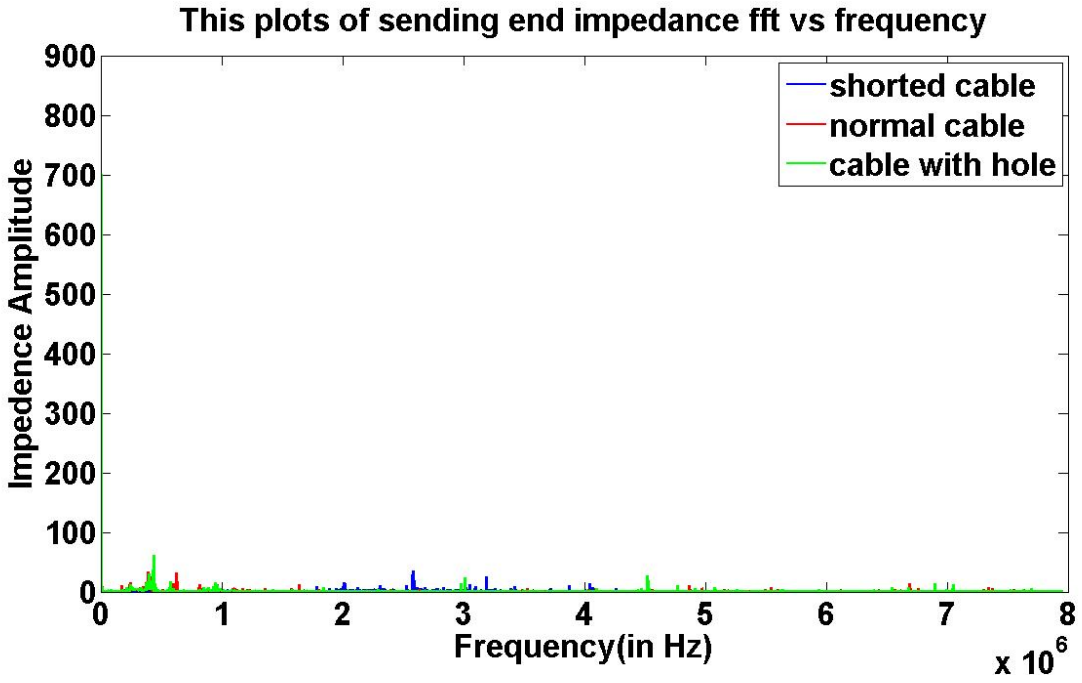

Figure 3.6 Impedance amplitude with a Hanning window (first sample, sending end voltage).

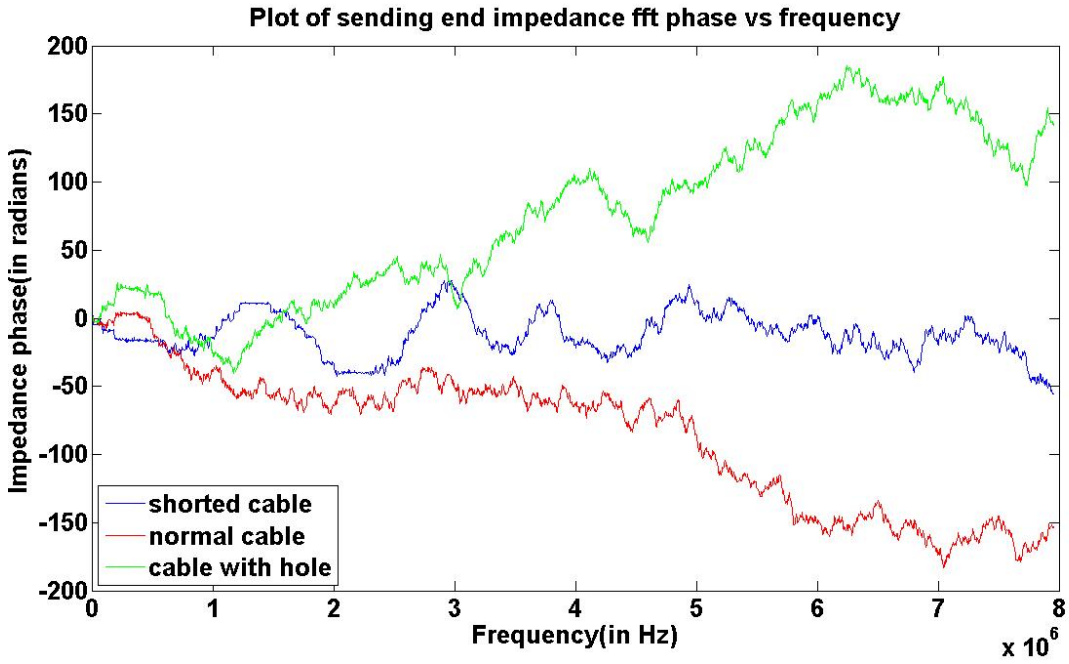

Figure 3.7 Impedance phase with a Hanning window (first sample, sending end voltage).

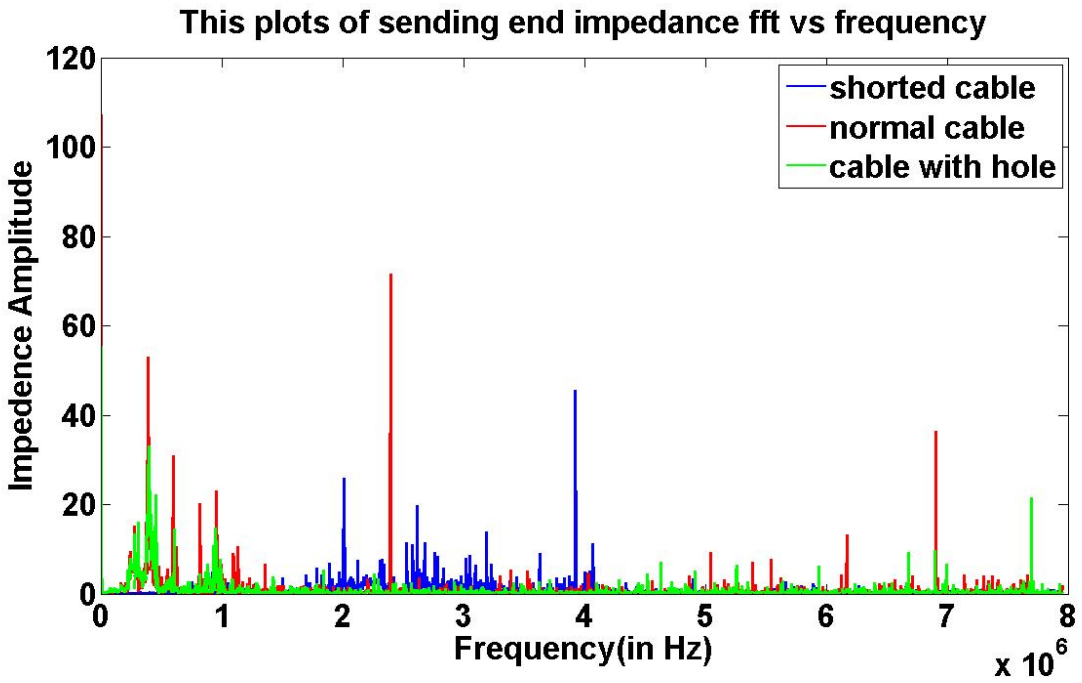

Figure 3.8 Impedance amplitude with a triangular window (first sample, sending end voltage).

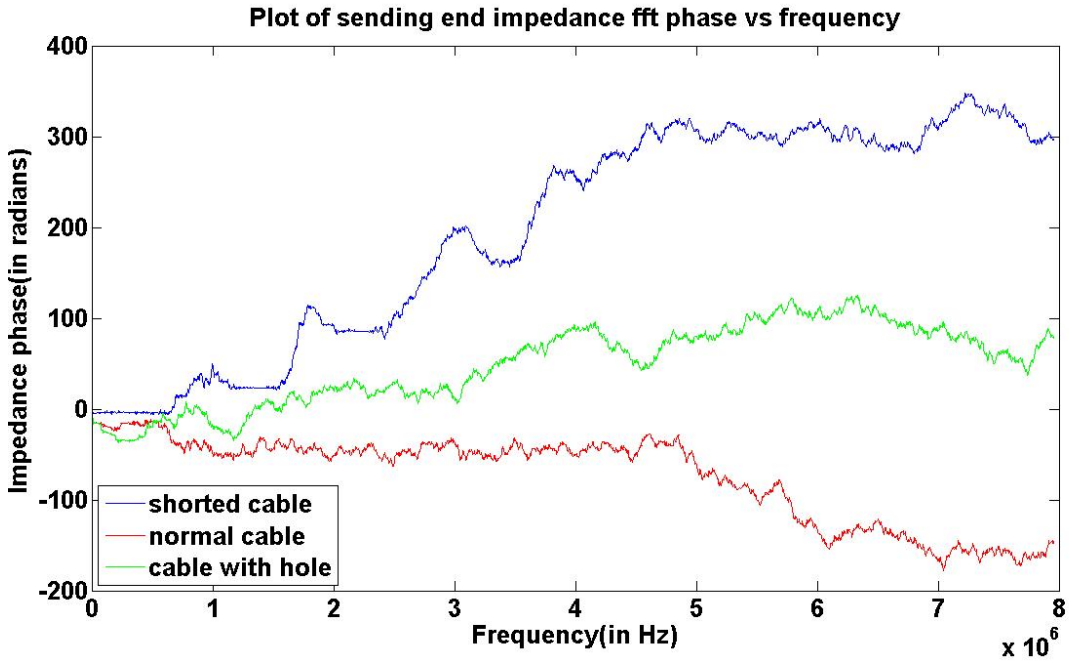

Figure 3.9 Impedance phase with a triangular window (first sample, sending end voltage).

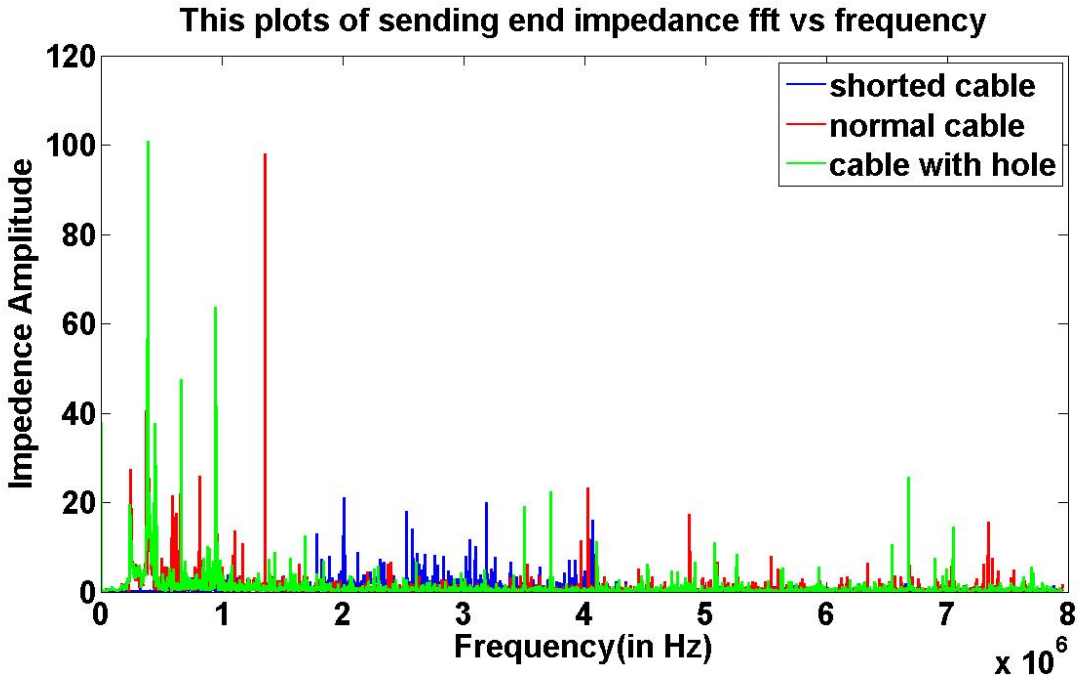

Figure 3.10 Impedance amplitude with a Gaussian window (first sample, sending end voltage).

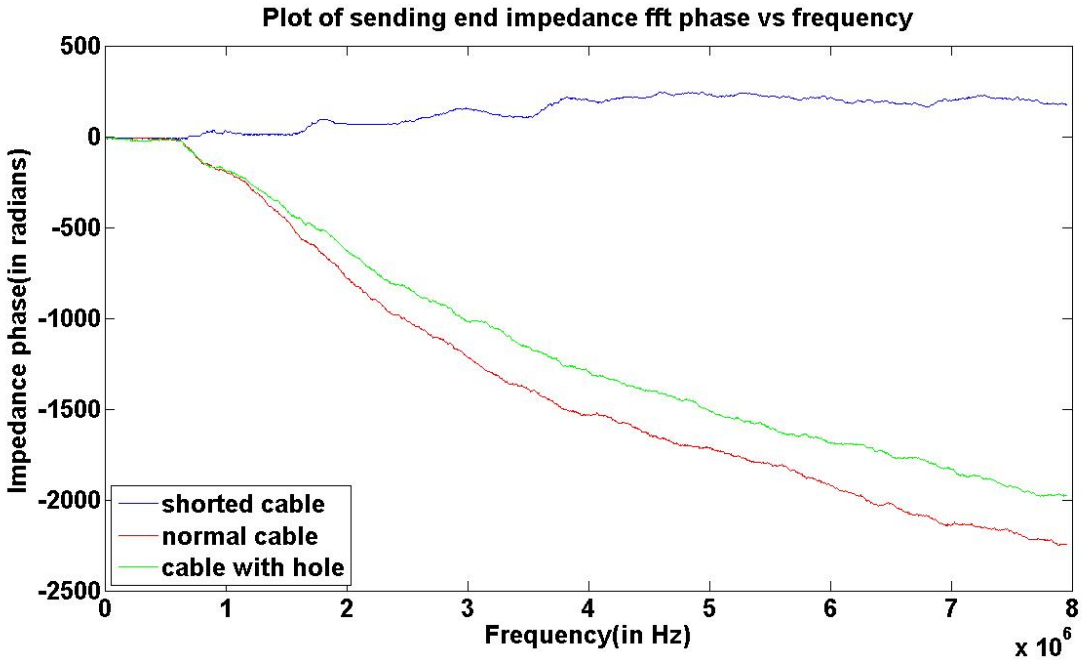

Figure 3.11 Impedance phase with a Gaussian window (first sample, sending end voltage).

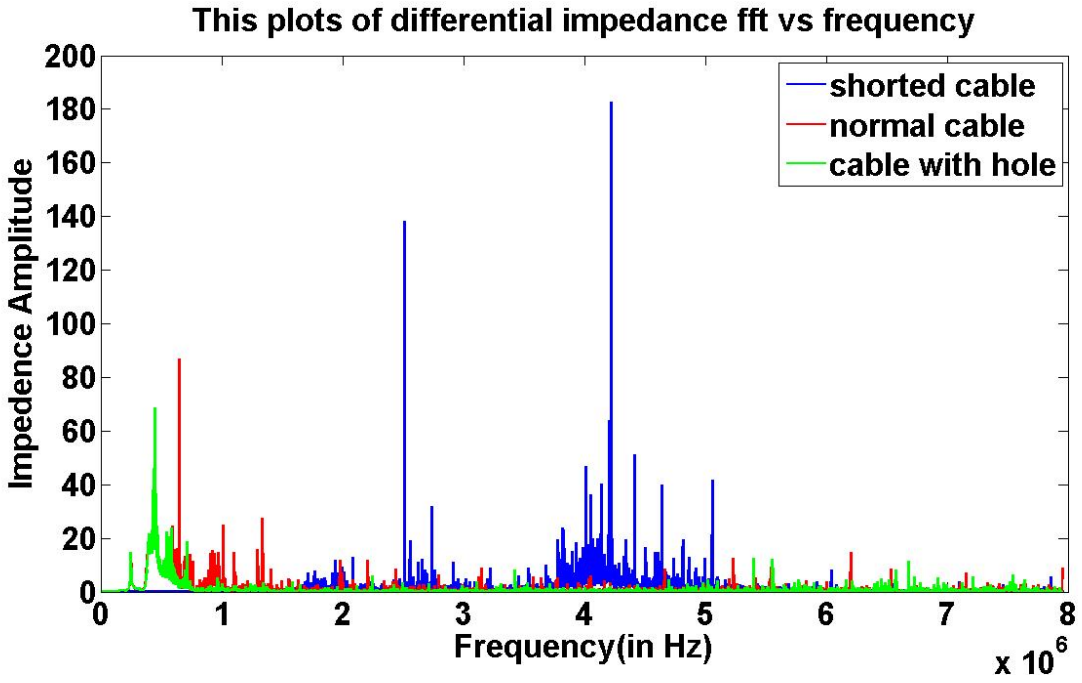

Figure 3.12 Impedance amplitude with a rectangular window (first sample, differential voltage).

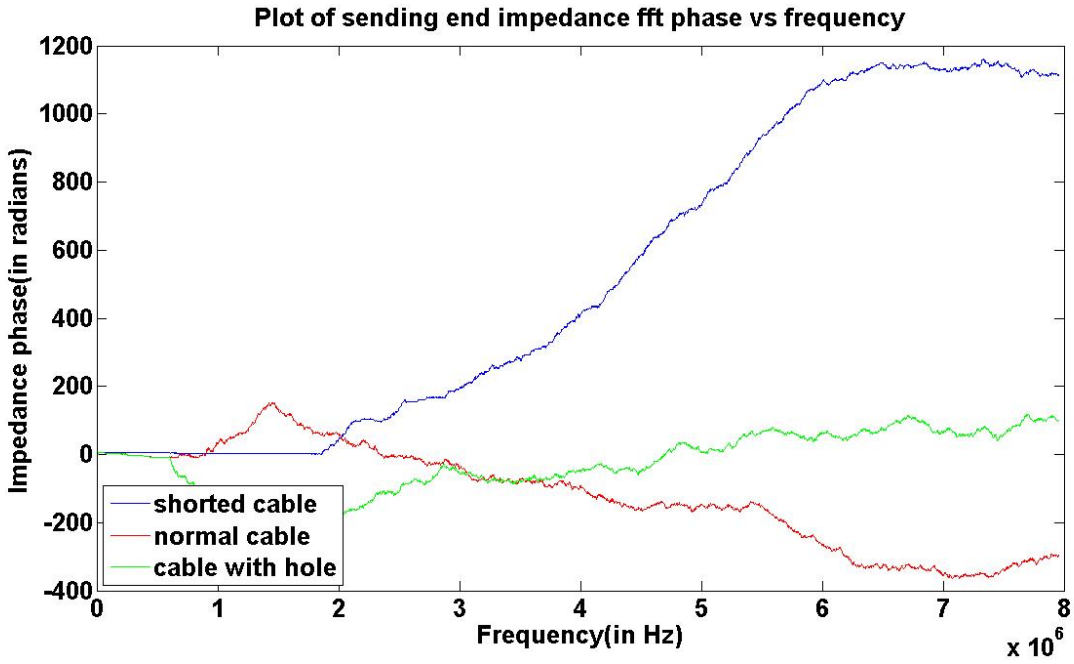

Figure 3.13 Impedance phase with a rectangular window (first sample, differential voltage).

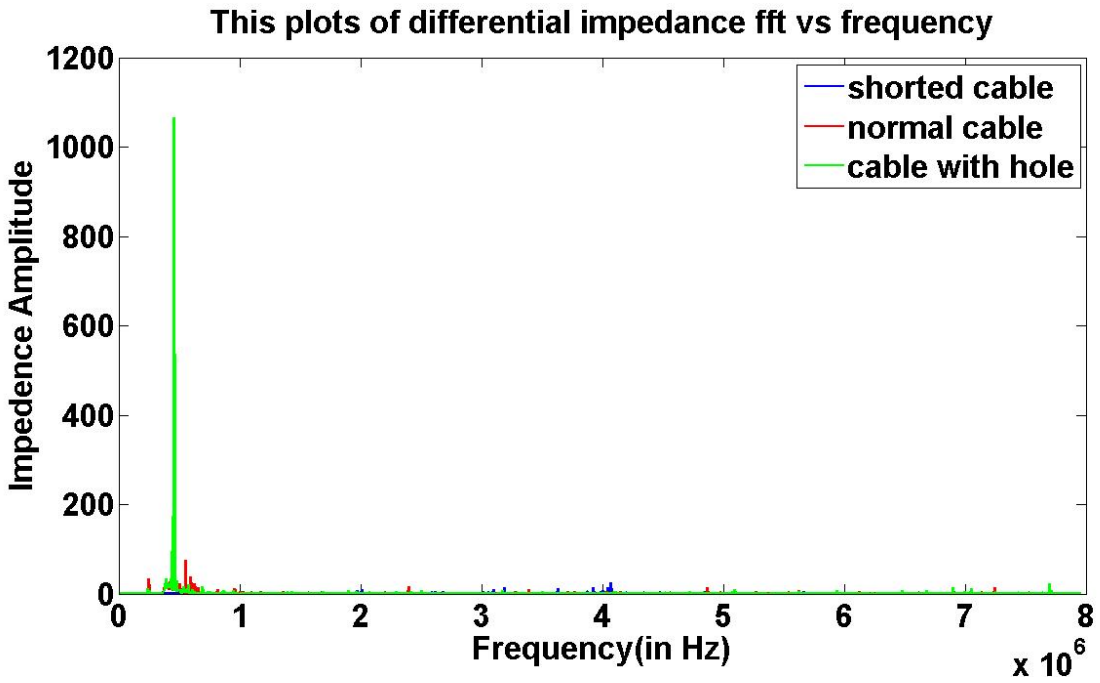

Figure 3.14 Impedance amplitude with a Hamming window (first sample, differential voltage).

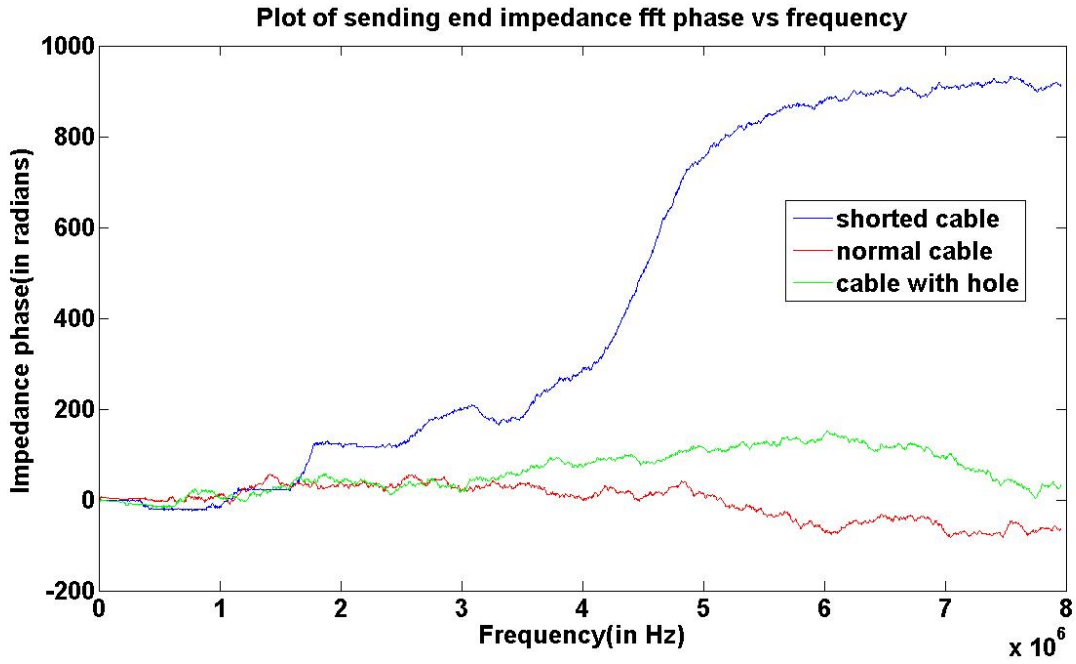

Figure 3.15 Impedance phase with a Hamming window (first sample, differential voltage).

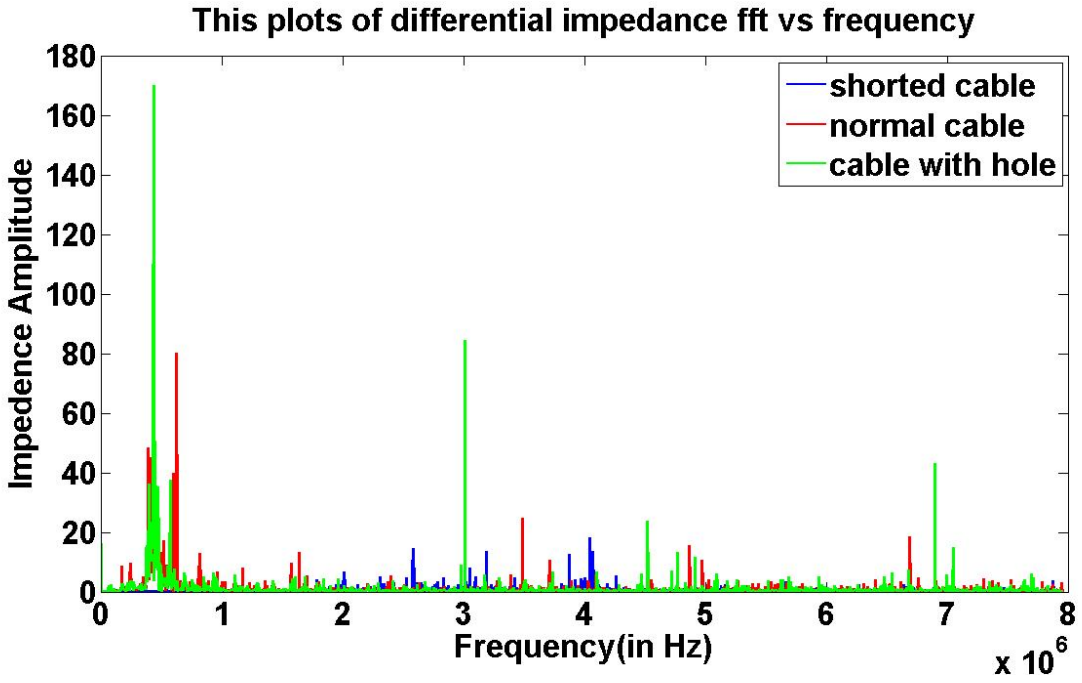

Figure 3.16 Impedance amplitude with a Hanning window (first sample, differential voltage).

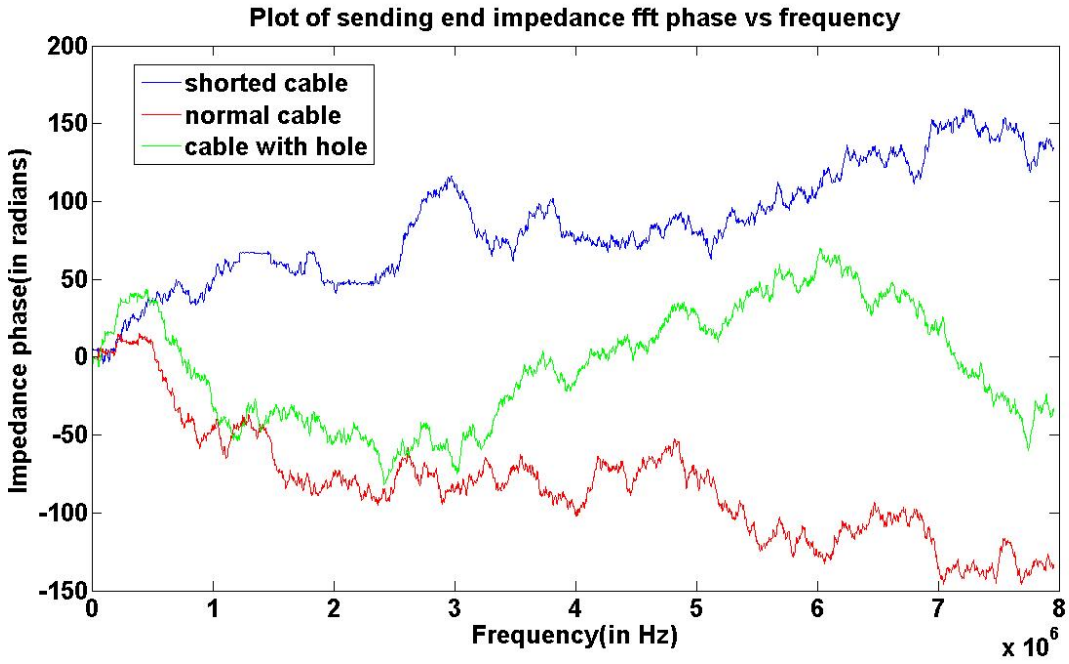

Figure 3.17 Impedance phase with a Hanning window (first sample, differential voltage).

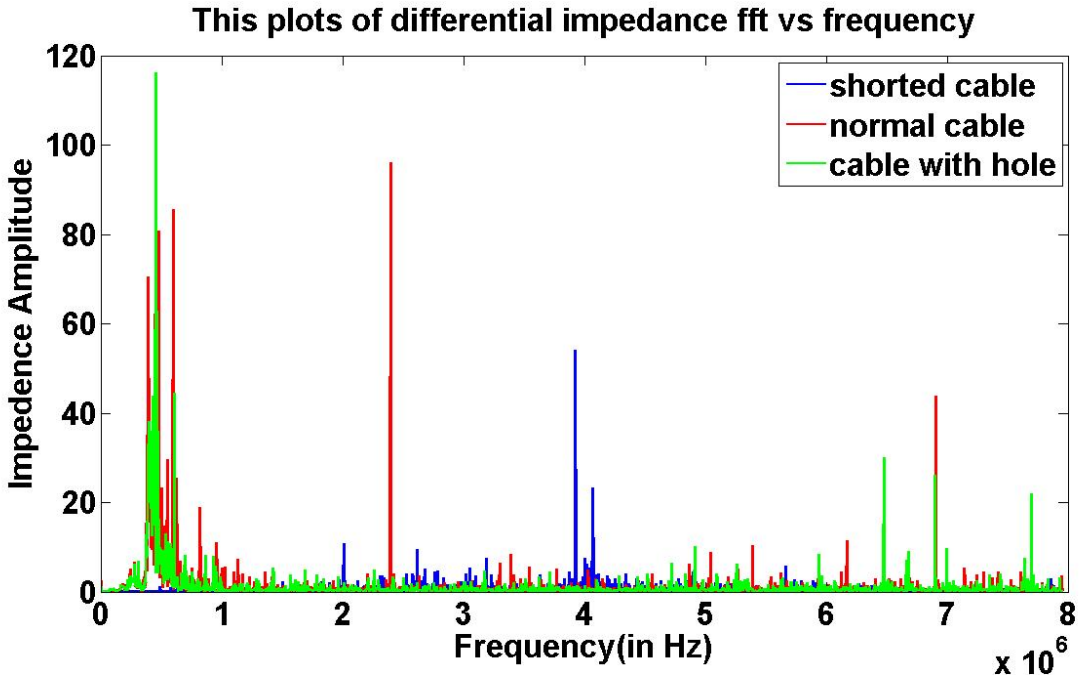

Figure 3.18 Impedance amplitude with a triangular window (first sample, differential voltage).

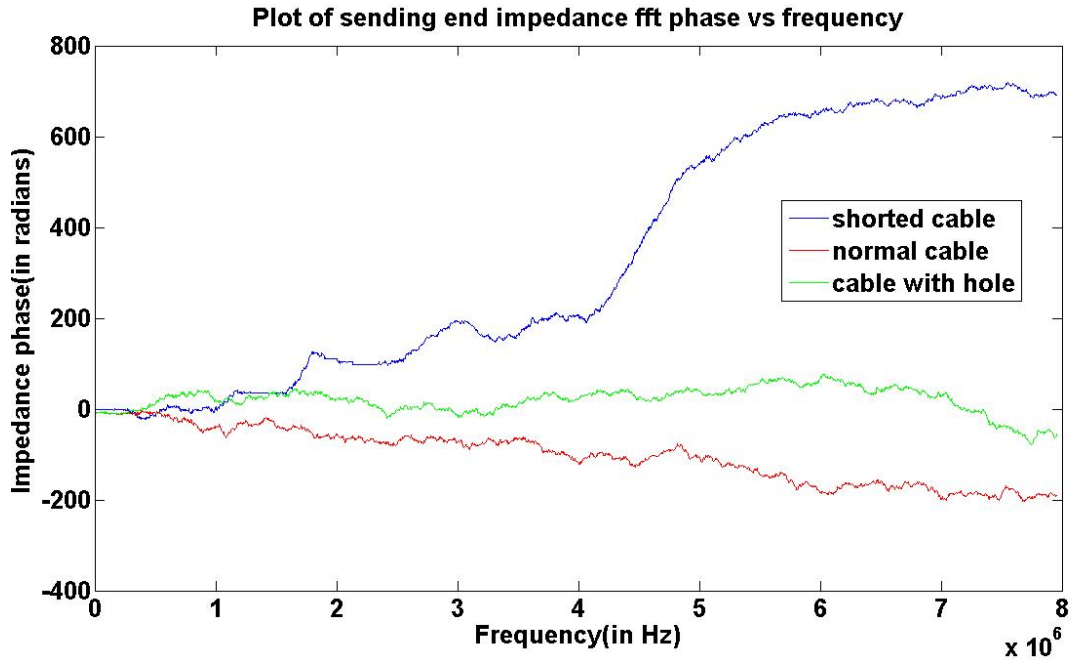

Figure 3.19 Impedance phase with a triangular window (first sample, differential voltage).

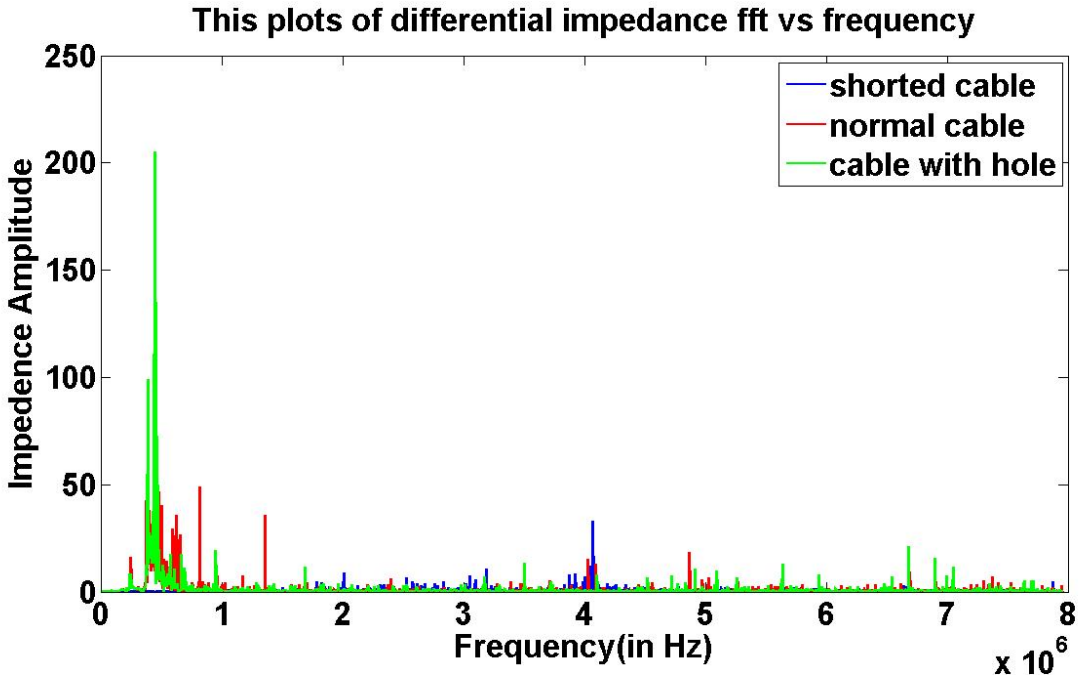

Figure 3.20 Impedance amplitude with a Gaussian window (first sample, differential voltage).

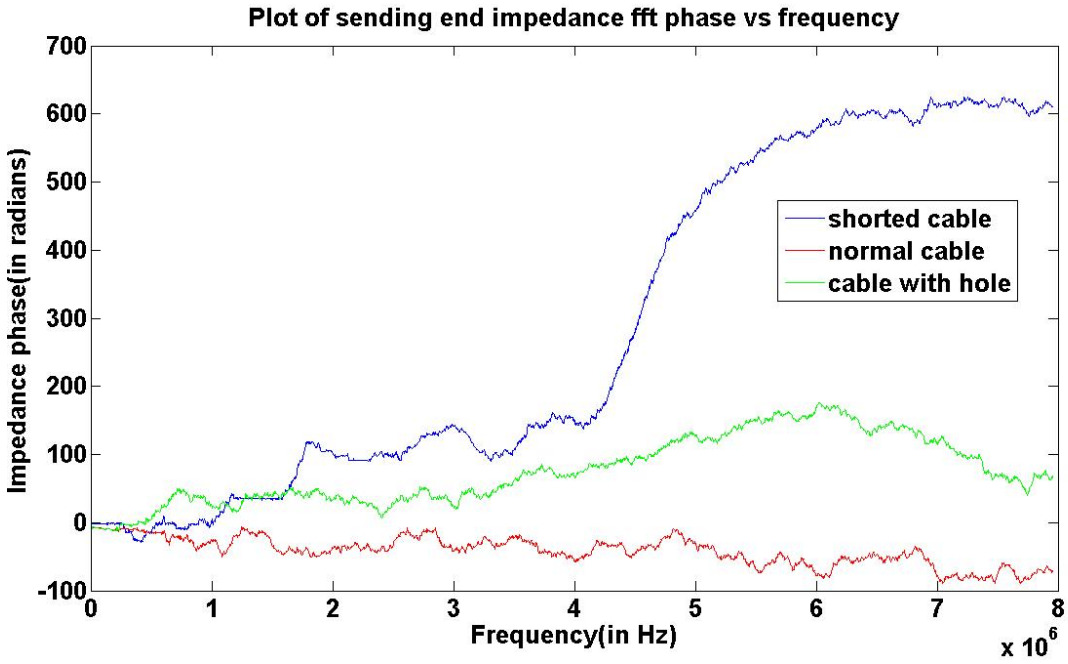

Figure 3.21 Impedance phase with a Gaussian window (first sample, differential voltage).

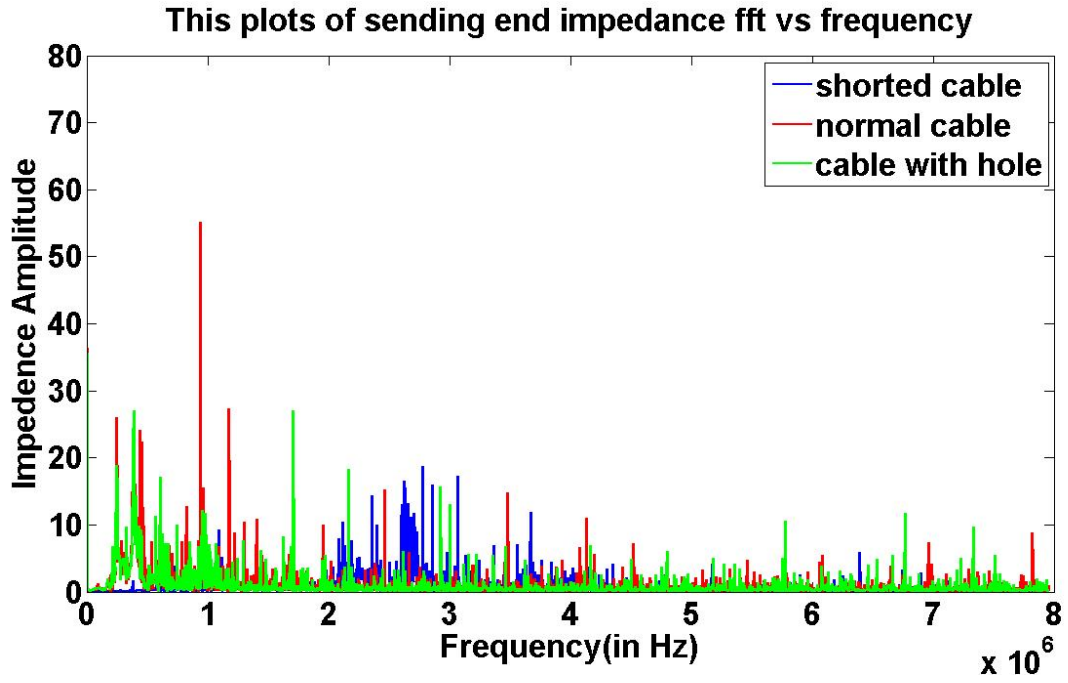

Figure 3.22 Impedance amplitude with a Gaussian window (second sample, sending end voltage).

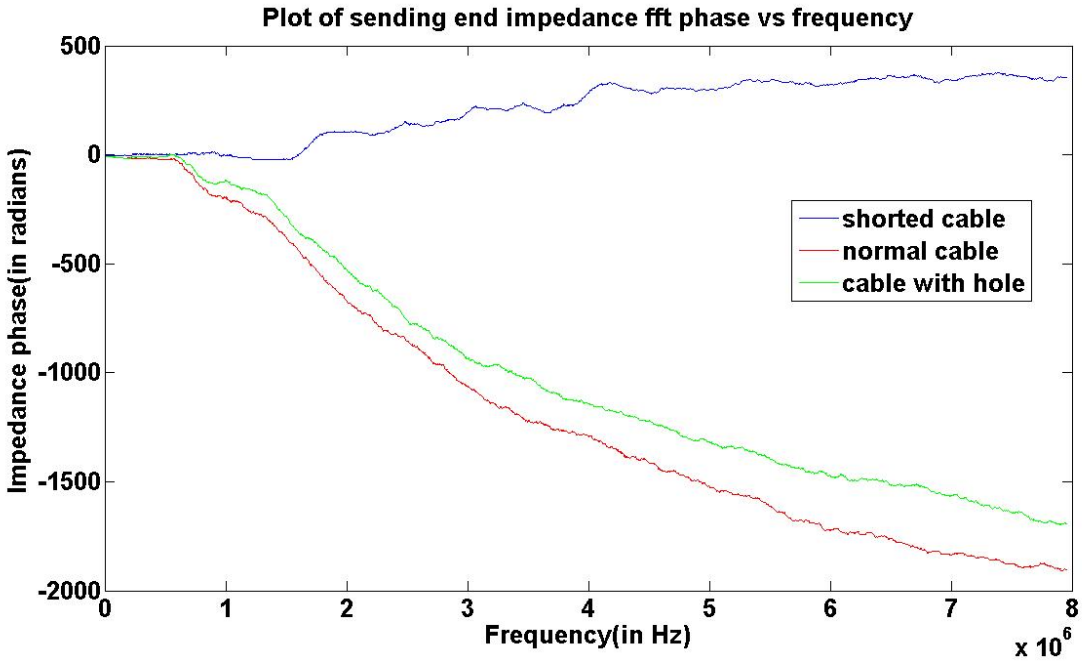

Figure 3.23 Impedance phase with a Gaussian window (second sample, sending end voltage).

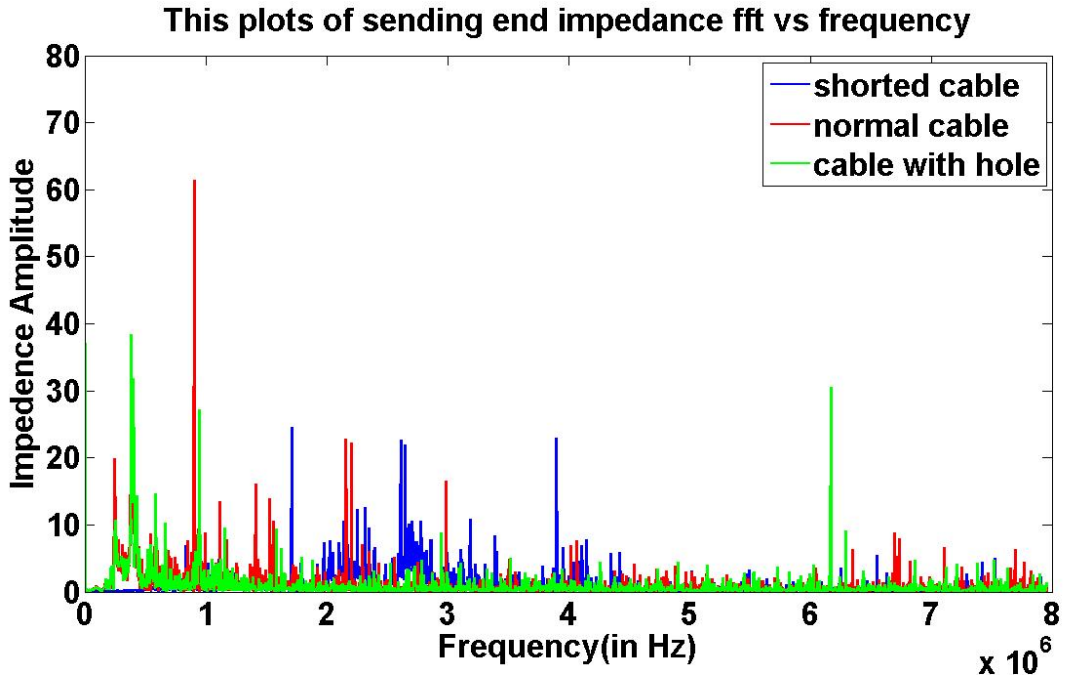

Figure 3.24 Impedance amplitude with a Gaussian window (third sample, sending end voltage).

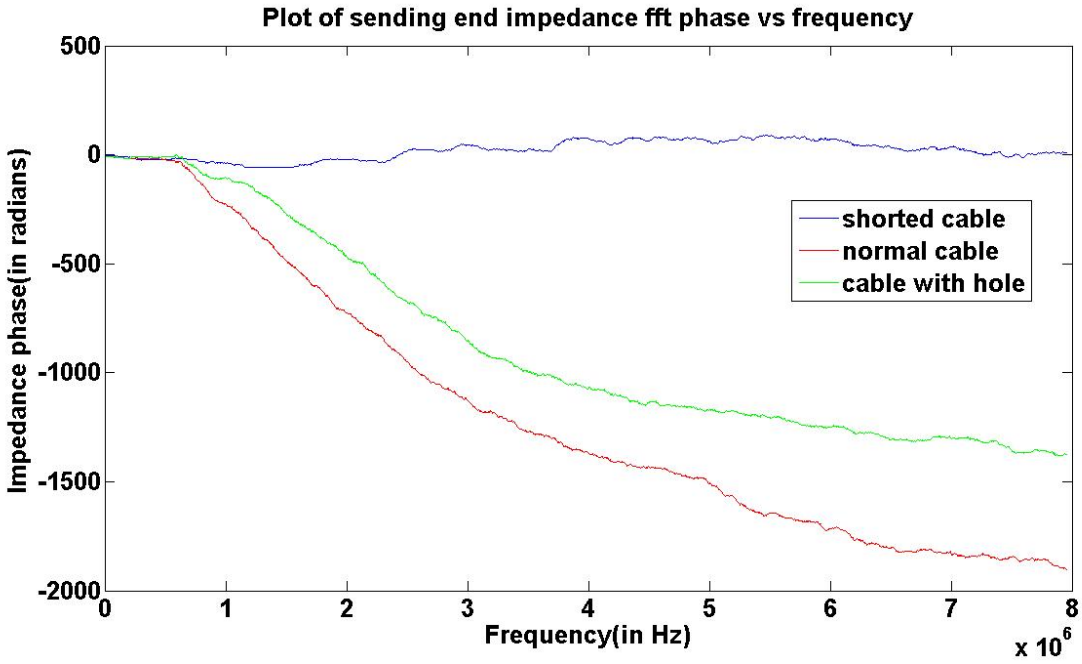

Figure 3.25 Impedance phase with a Gaussian window (third sample, sending end voltage).

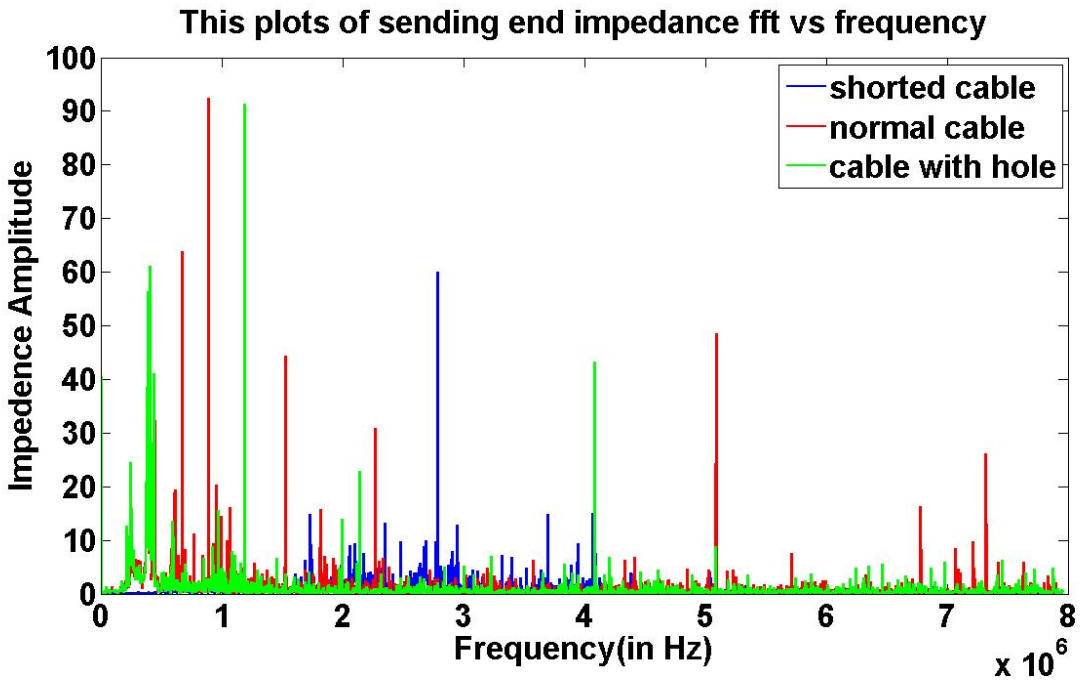

Figure 3.26 Impedance amplitude with a Gaussian window (fourth sample, sending end voltage).

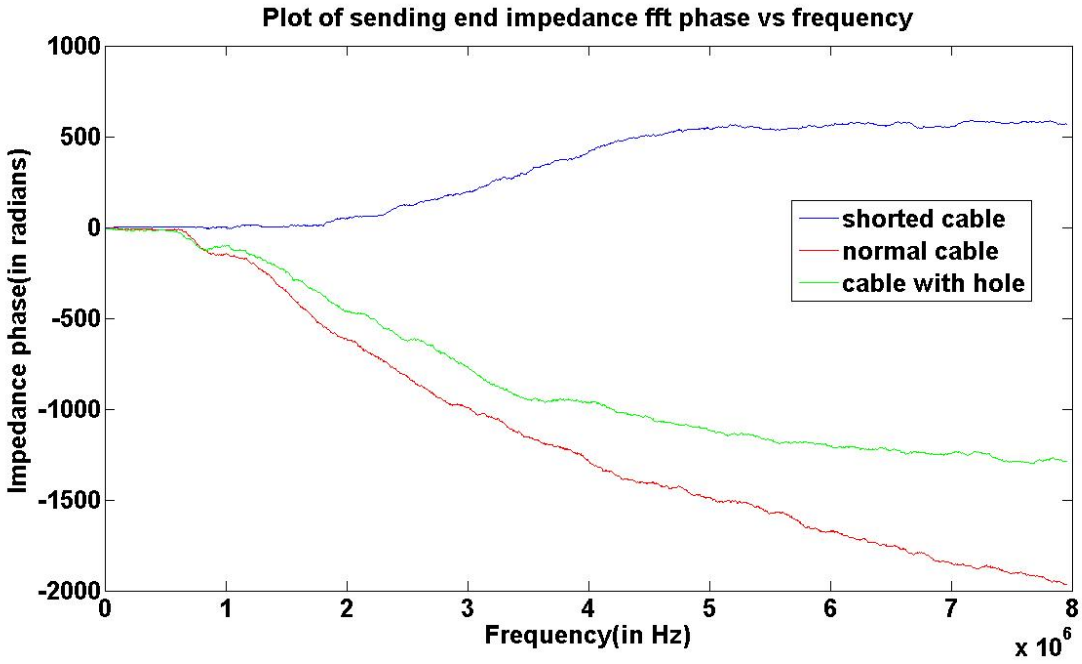

Figure 3.27 Impedance phase with a Gaussian window (fourth sample, sending end voltage).

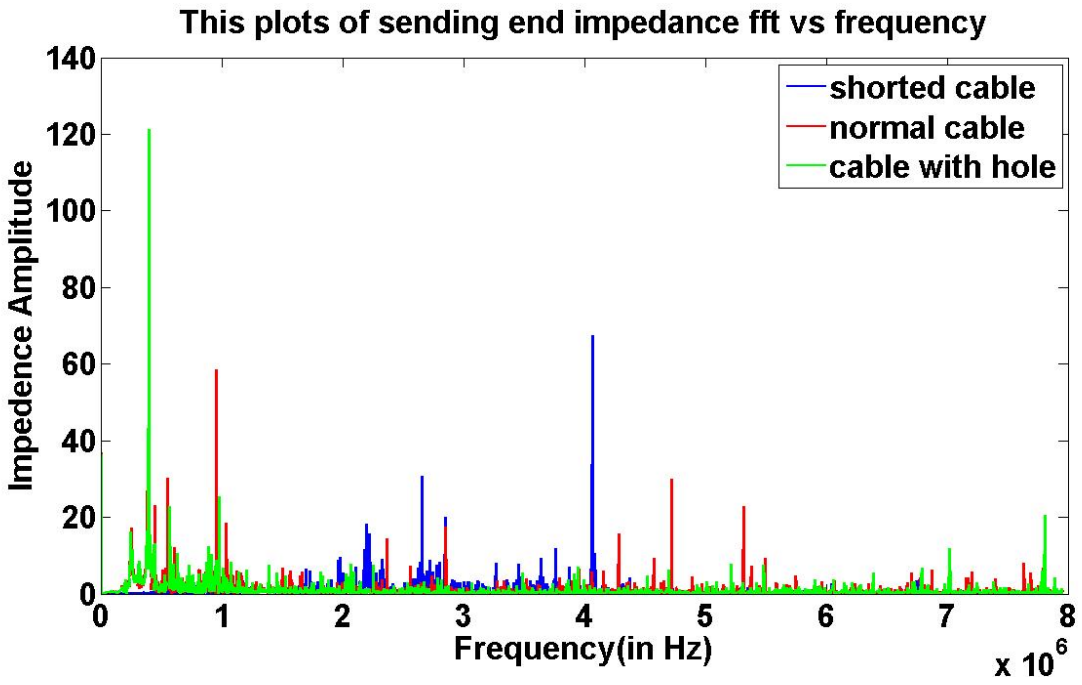

Figure 3.28 Impedance amplitude with a Gaussian window (fifth sample, sending end voltage).

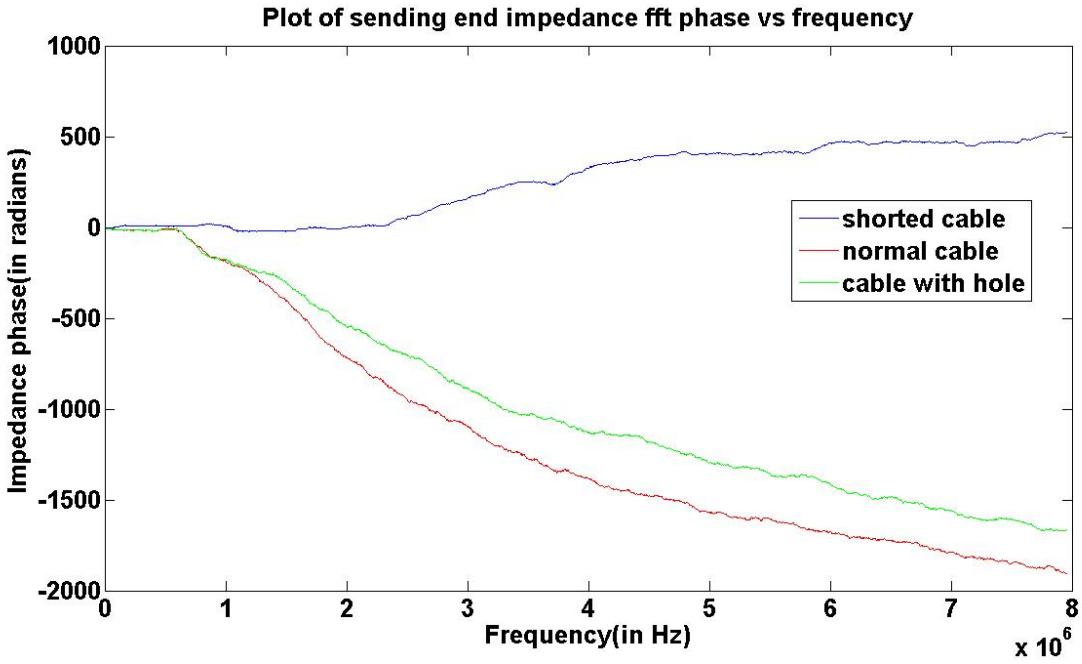

Figure 3.29 Impedance phase with a Gaussian window (fifth sample, sending end voltage).

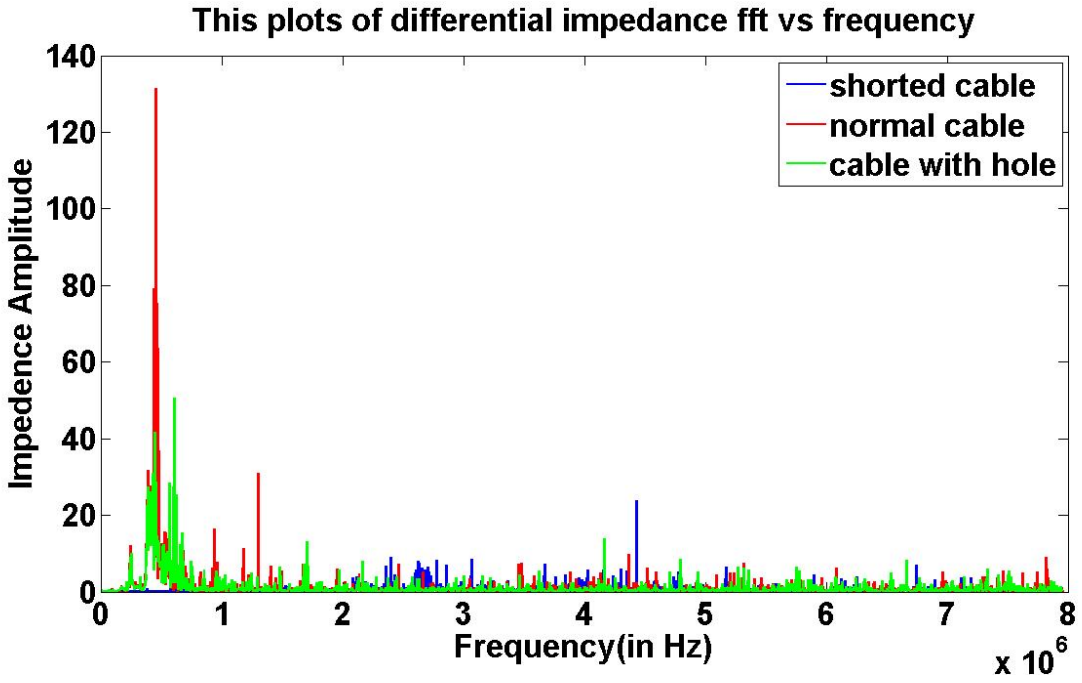

Figure 3.30 Impedance amplitude with a Gaussian window (second sample, differential voltage).

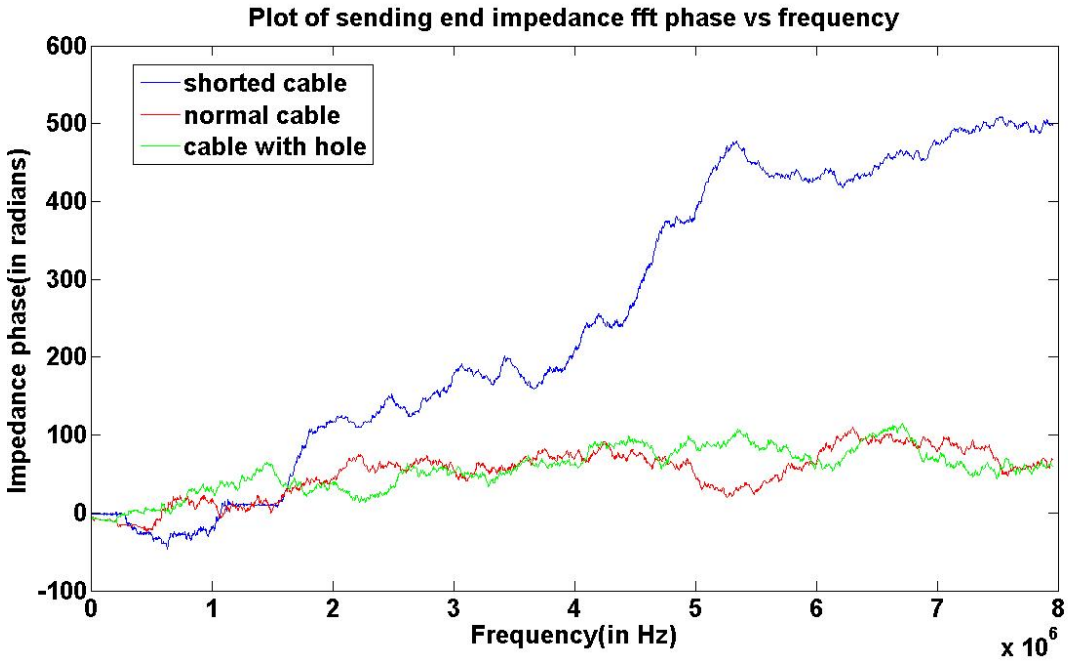

Figure 3.31 Impedance phase with a Gaussian window (second sample, differential voltage).

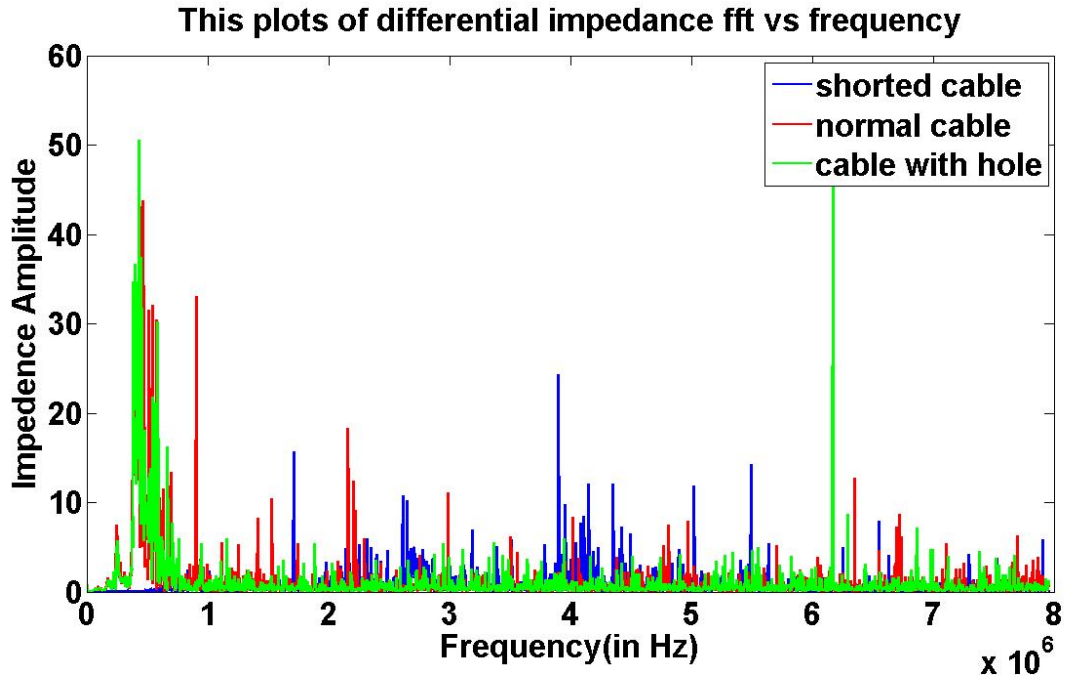

Figure 3.32 Impedance amplitude with a Gaussian window (third sample, differential voltage).

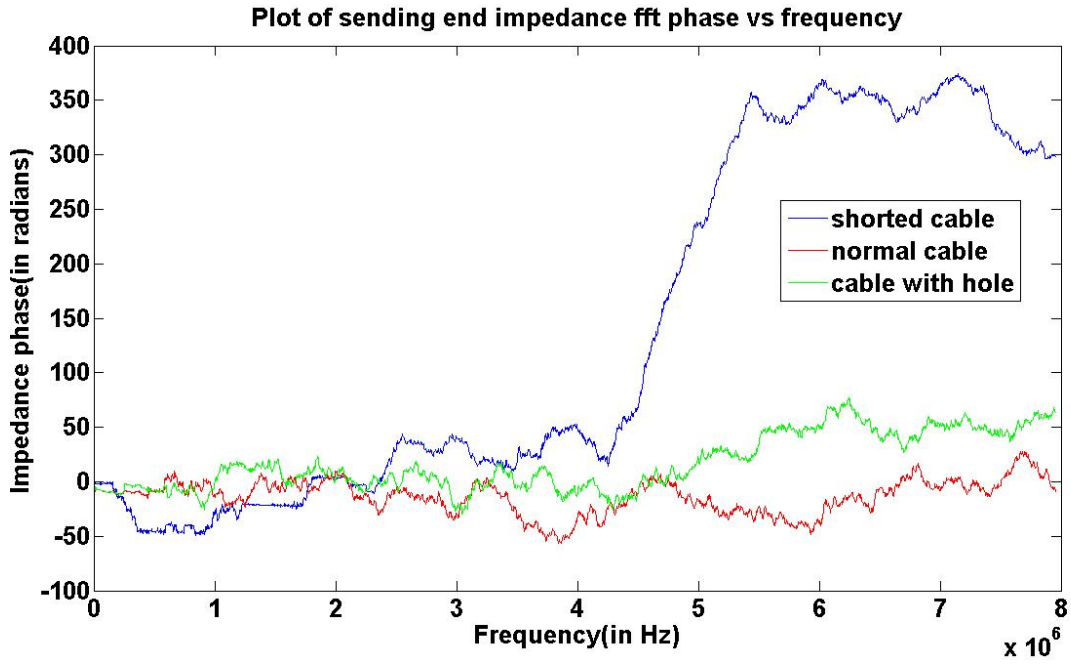

Figure 3.33 Impedance phase with a Gaussian window (third sample, differential voltage).

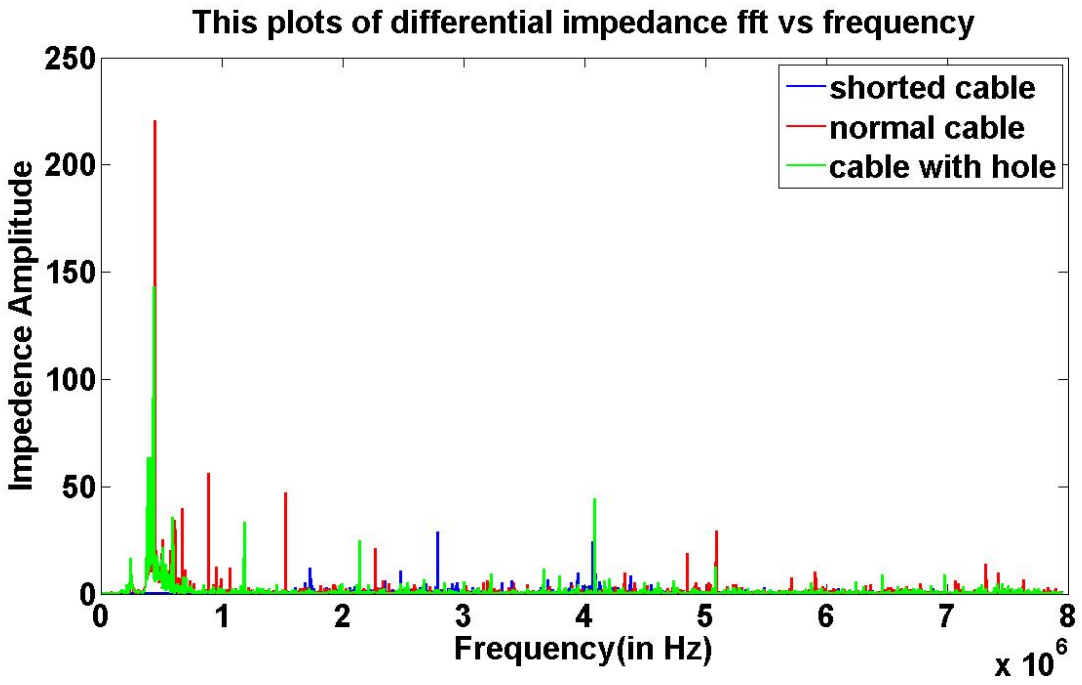

Figure 3.34 Impedance amplitude with a Gaussian window (fourth sample, differential voltage).

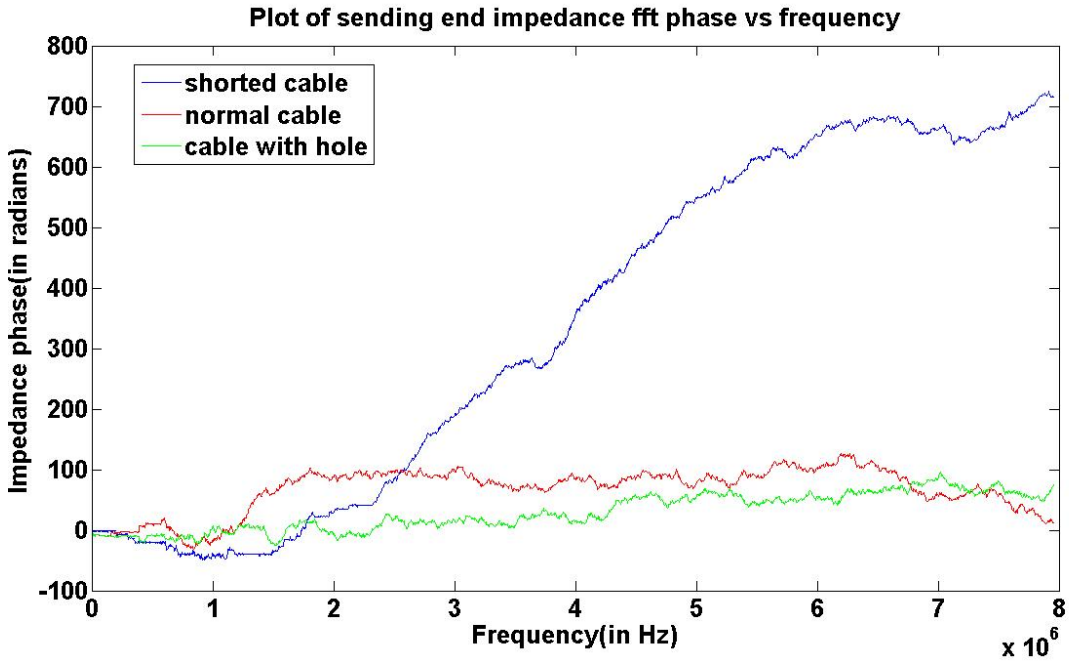

Figure 3.35 Impedance phase with a Gaussian window (fourth sample, differential voltage).

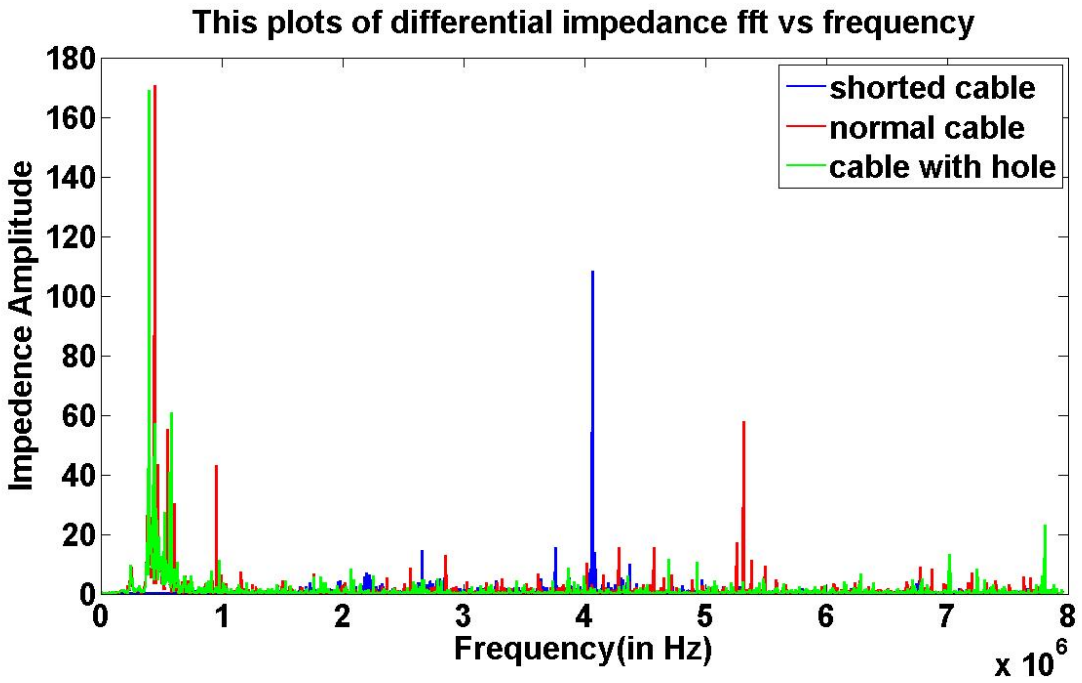

Figure 3.36 Impedance amplitude with a Gaussian window (fifth sample, differential voltage).

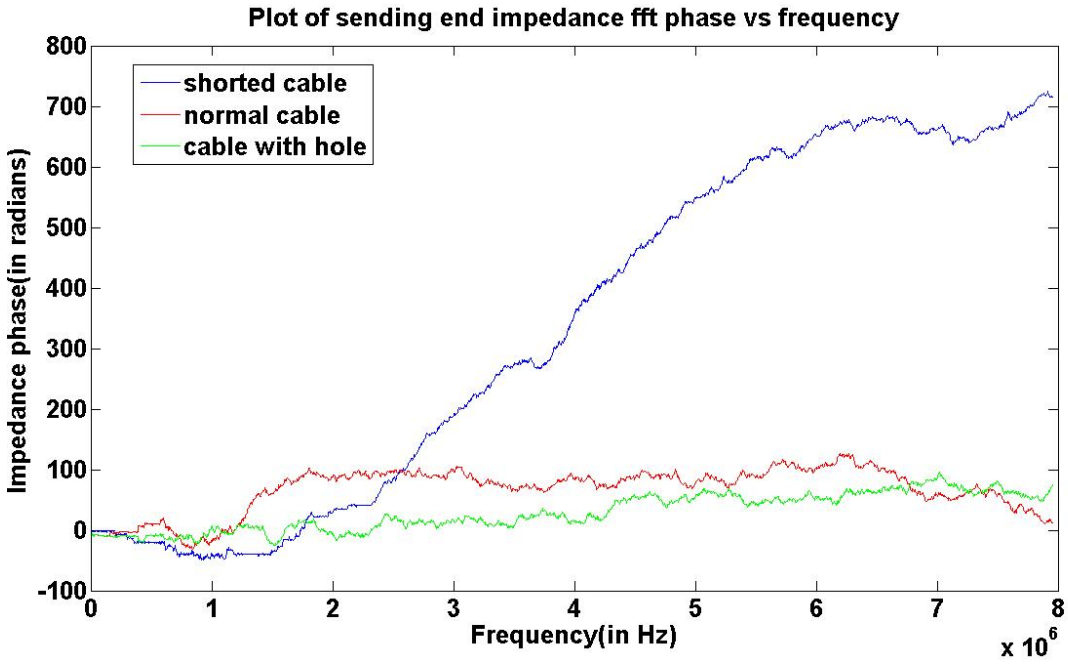

Figure 3.37 Impedance phase with a Gaussian window (fifth sample, differential voltage).

3.3 FFT Observations

a) Both methods of impedance calculation (via the sending end voltage and the differential voltage) can be used for differentiating between the different types of cable defects from phase information.

b) The results obtained from the differential voltage are slightly better than the ones obtained from the sending end voltage.

c) All window types yield reasonable results. However, the Gaussian window seems to have slightly better results than the other windowing techniques in terms of noise deduction.

d) Further study needs to be conducted to find the best way of visualizing the results, especially, the magnitude response

3.4 STFT Results

From the 5 sample data sets that are available and for each type of the underground power cable (normal, shorted, and with holes), the 5th sample data set is used first in this analysis for illustrative purposes. The STFT is used to obtain the magnitude and phase of the cable impedance.

The implementation of the STFT is based on a window size of 128 samples with 50% overlap, i.e., this corresponds to 64 overlapping samples. Note also that, for the shorted cable, the time domain signal (voltage and current) consists of 50000 samples whereas for the normal cable and cable with hole, 5000 samples are available. Thus, for comparison purposes, the shorted cable data are down-sampled (decimated) by a factor of 10 so that the data length for all three types of cables is the same. Considering the window size (128 samples) and the % overlap (64 samples) along with the available data length (5000 samples), the resulting STFT matrix size will be 65x77.

The results provided below correspond to the impedance magnitude and impedance phase for the three types of cables considered in this study for different types of windows. Note that in this study the results obtained from both methods (impedance computation via the sending end voltage and impedance computation via the differential voltage) are nearly identical. Accordingly, only the results of the impedance computed from the differential voltage are illustrated here. Figures 3.37-3.56 correspond to the magnitude response of the impedance as a function of time and frequency and the impedance phase as a function of frequency over a specified time window. With a 65x77 STFT matrix size, the phase response characteristic is selected as the phase response corresponding to the 32nd column of the STFT matrix. Note that in all the phase response plots, *blue* corresponds to the phase response of a normal cable, *red* corresponds to the

phase response of a cable with hole, and *green* corresponds to the phase response of a shorted cable.

By examining these figures, it seems that the three different types of cables can be easily distinguished from the phase response for all windowing types with the Gaussian window having slightly better results in terms of both magnitude and phase responses. Accordingly, all the rest of the sample data sets are analyzed using the Gaussian window and their corresponding results (impedance magnitude and phase responses) are illustrated in Figures 3.57- 3.72.

It is also of interest to examine the behavior of the sending end voltage in the STFT domain (time-frequency domain). The resulting magnitude and phase responses for dataset 1 with a Gaussian window are illustrated in Figures 3.73-3.76. One sees that the different types of cables can be distinguished from the phase response. In addition, the magnitude response for the shorted cable shows distinctive behavior in the spectrum. Similar behavior is also obtained for all datasets analyzed. This method may be used for fault detection. However, further investigation is required.

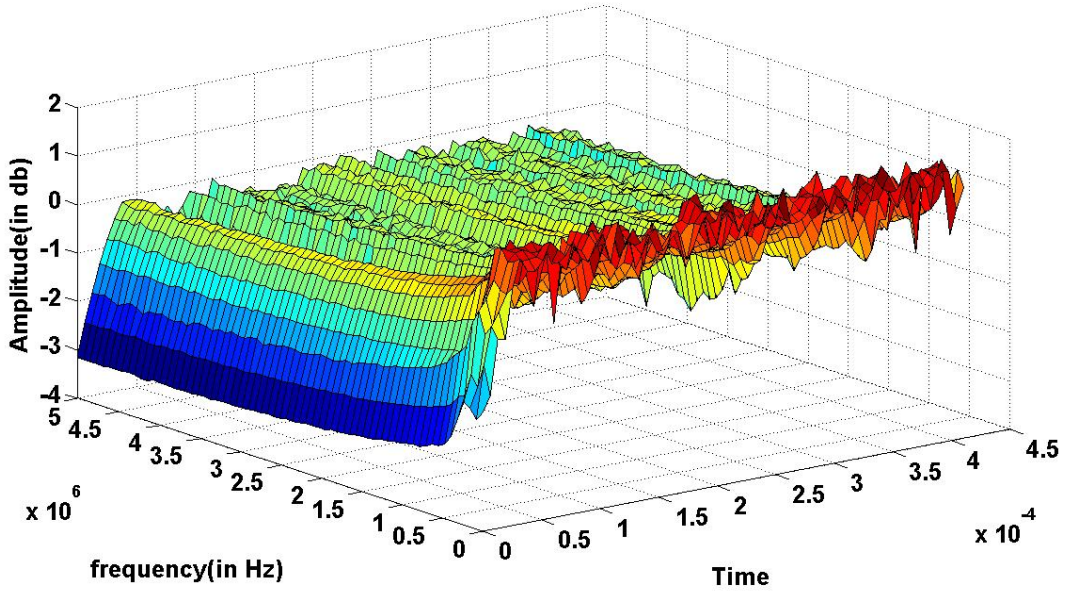

Figure 3.38 Impedance magnitude with a rectangular window (differential voltage, normal cable, dataset 5)

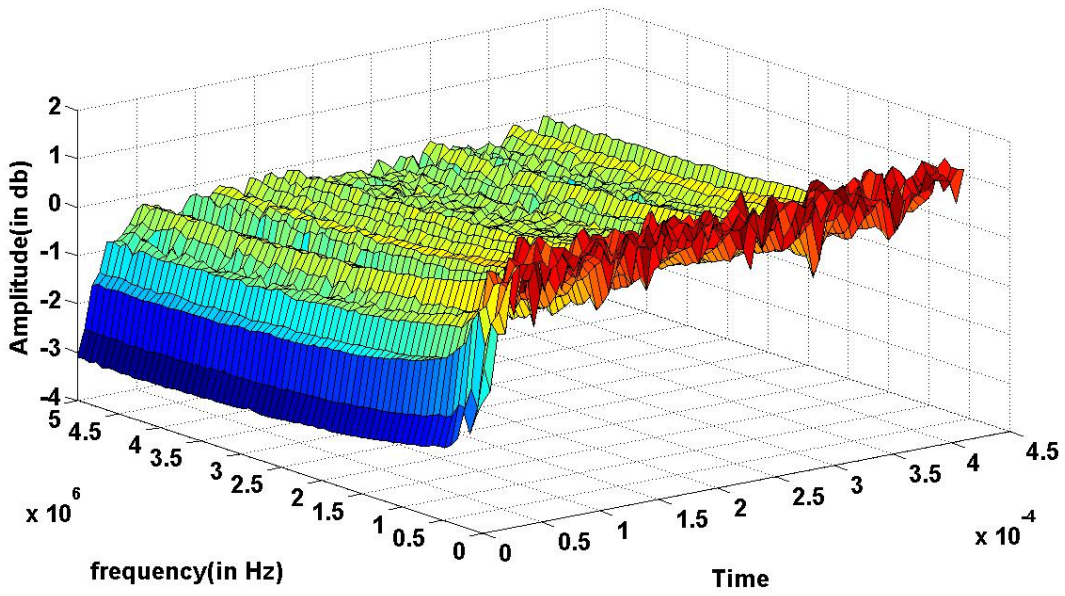

Figure 3.39 Impedance magnitude with a rectangular window (differential voltage, cable with holes, dataset 5).

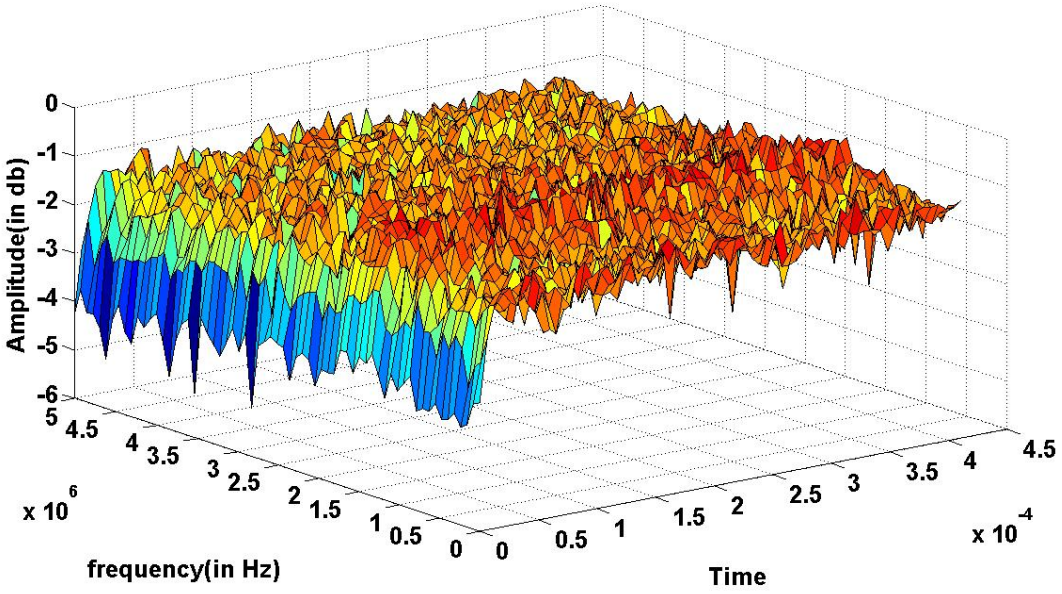

Figure 3.40 Impedance magnitude with a rectangular window (differential voltage, shorted cable, dataset 5)

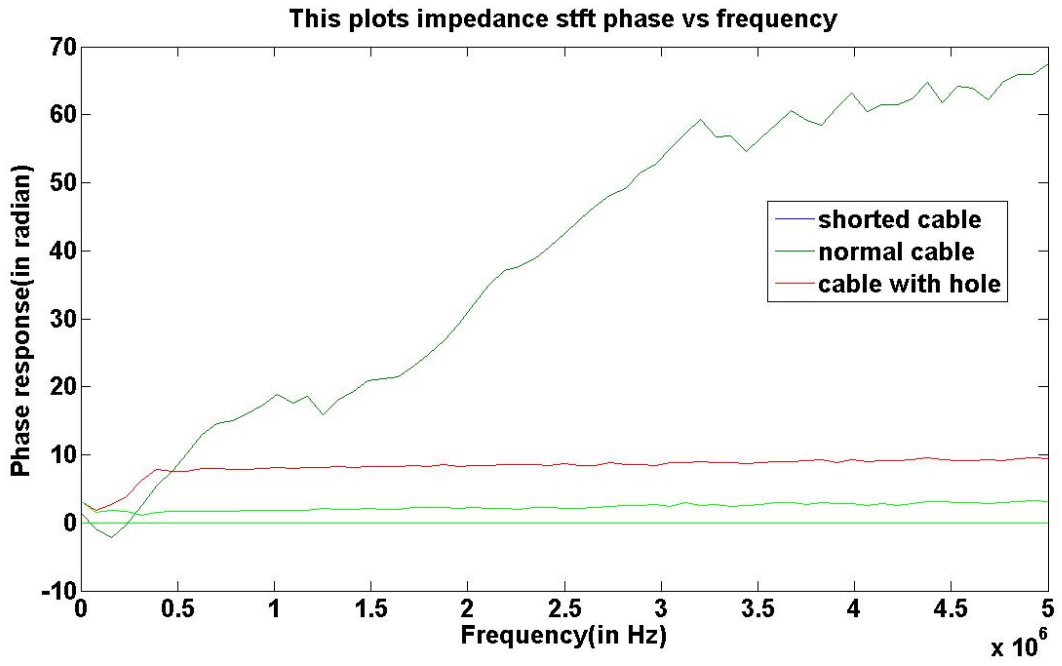

Figure 3.41 Impedance phase with a rectangular window (differential voltage, dataset 5).

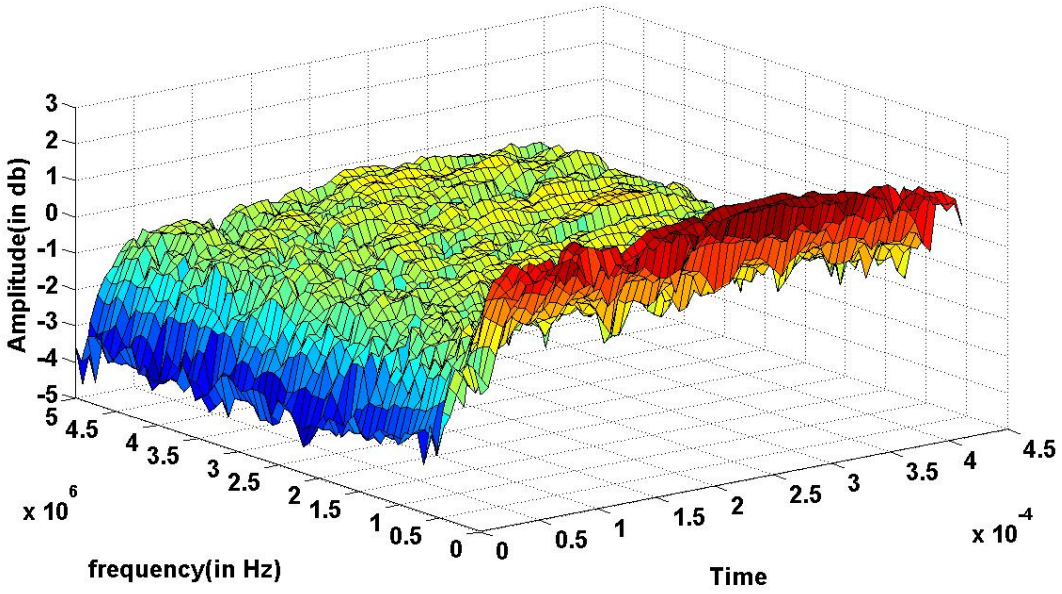

Figure 3.42 Impedance magnitude with a triangular window (differential voltage, normal cable, dataset 5)

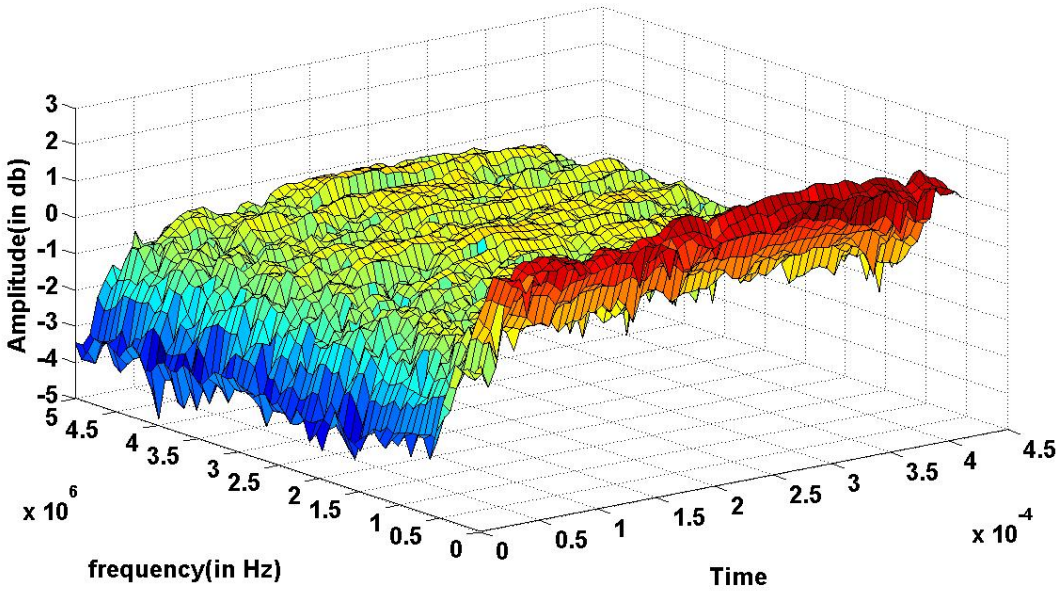

Figure 3.43 Impedance magnitude with a triangular window (differential voltage, cable with holes, dataset 5).

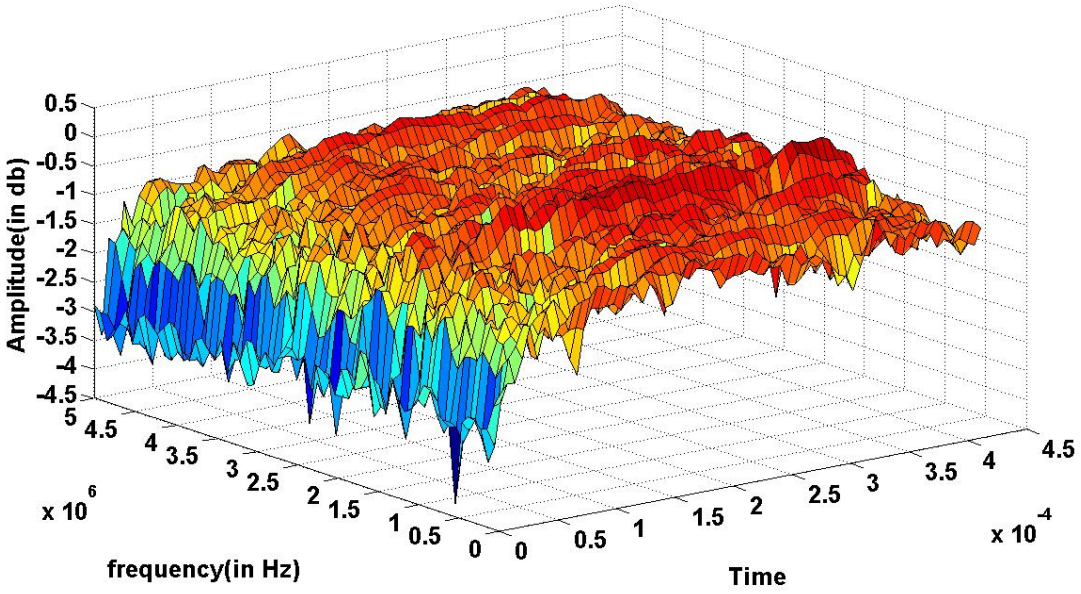

Figure 3.44 Impedance magnitude with a triangular window (differential voltage, shorted cable, dataset 5)

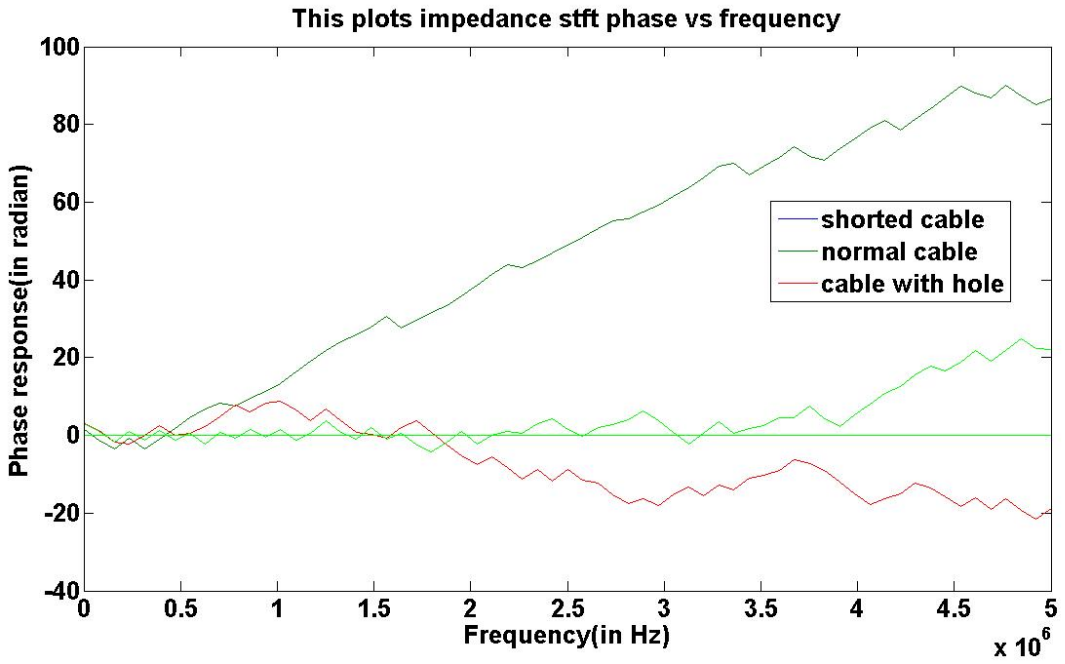

Figure 3.45 Impedance phase with a triangular window (differential voltage, dataset 5).

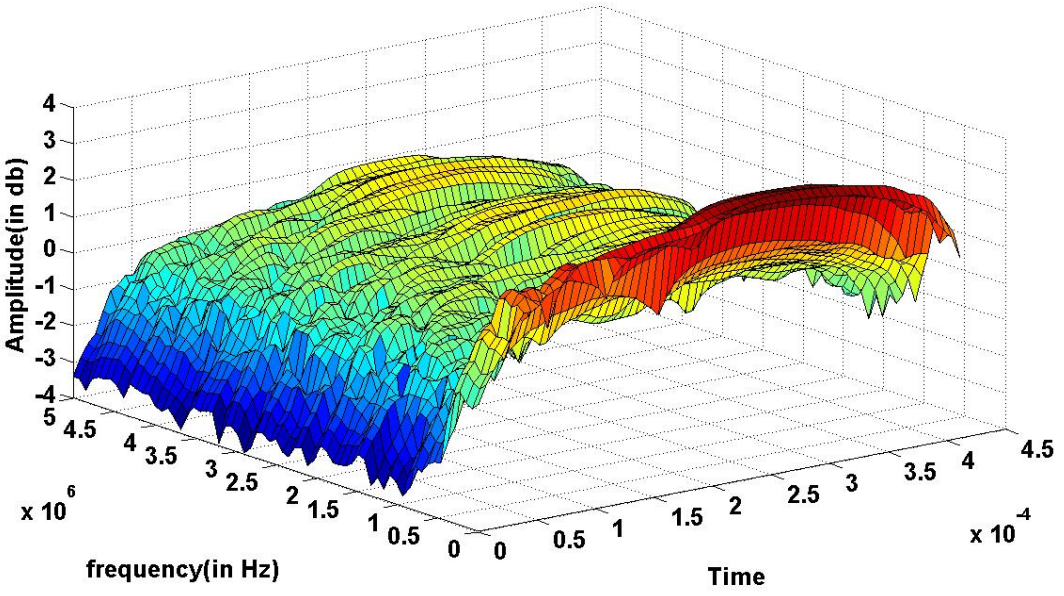

Figure 3.46 Impedance magnitude with a Hanning window (differential voltage, normal cable, dataset 5).

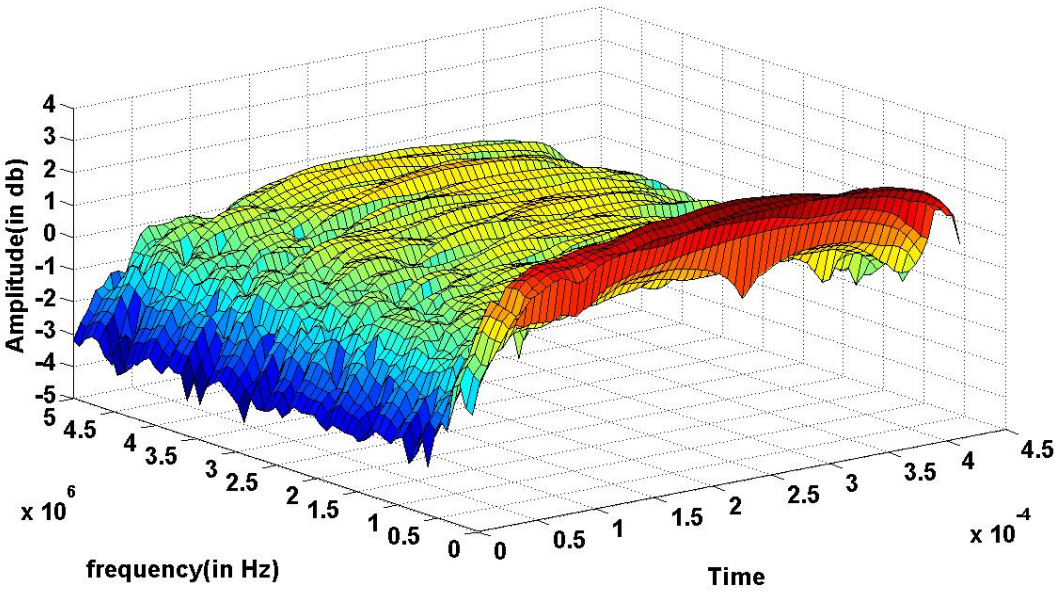

Figure 3.47 Impedance magnitude with a Hanning window (differential voltage, cable with holes, dataset 5).

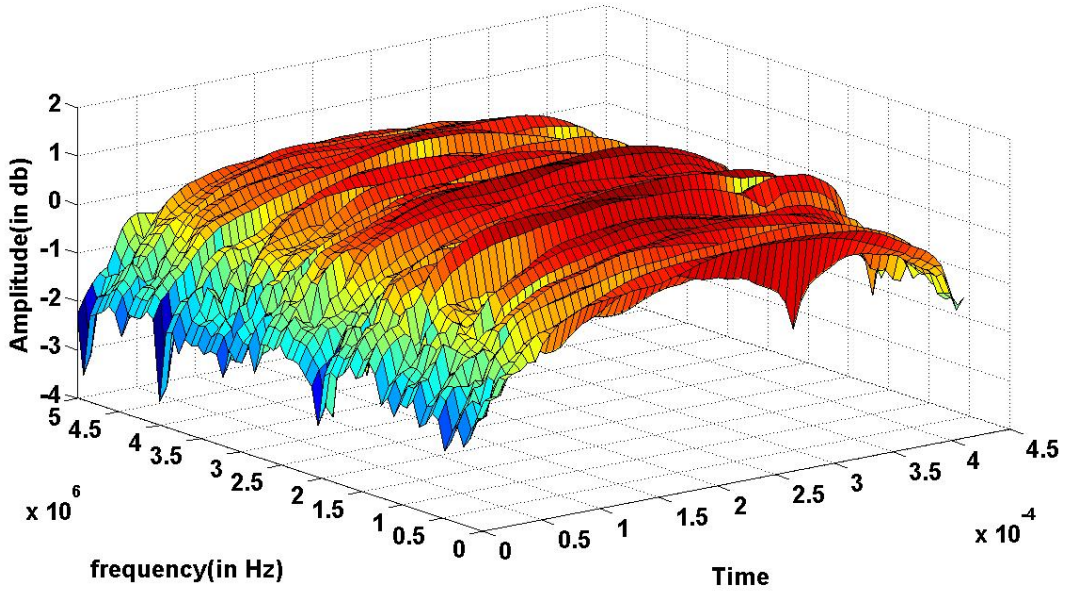

Figure 3.48 Impedance magnitude with a Hanning window (differential voltage, shorted cable, dataset 5).

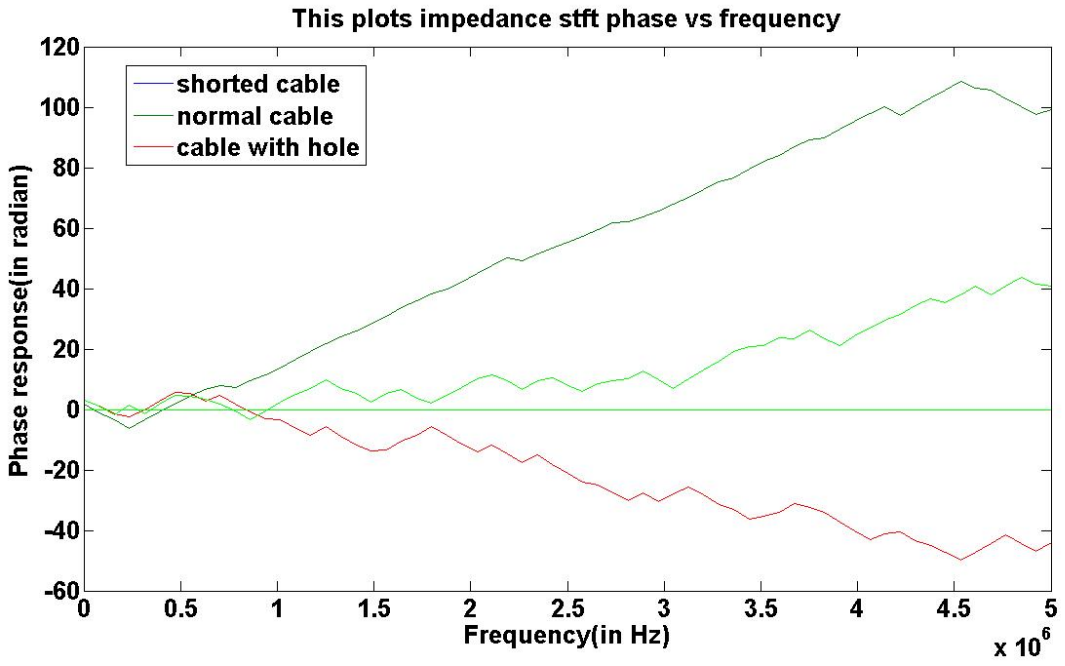

Figure 3.49 Impedance phase with a Hanning window (differential voltage, dataset 5).

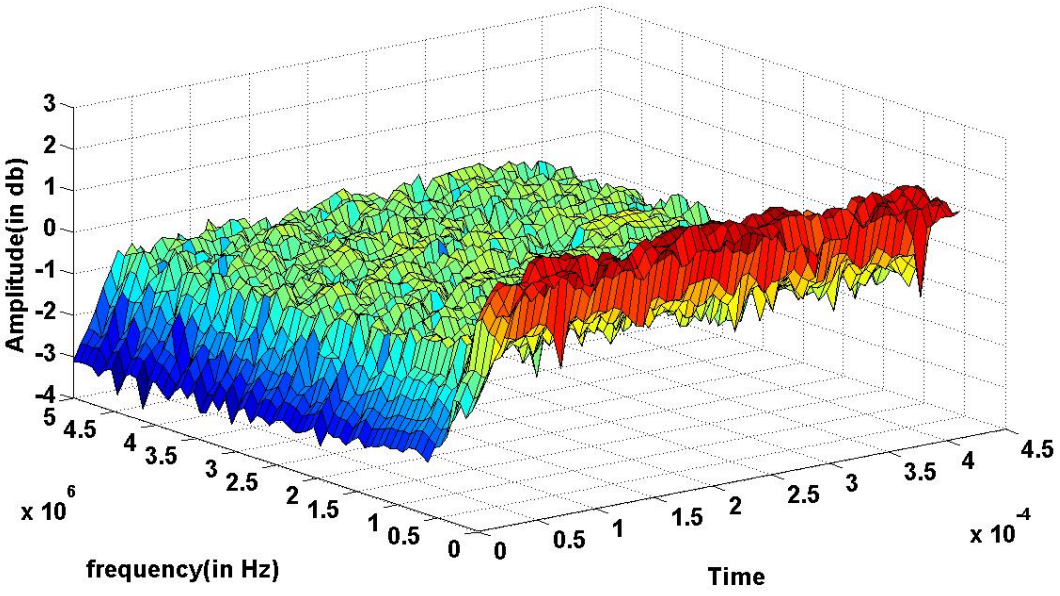

Figure 3.50 Impedance magnitude with a Hamming window (differential voltage, normal cable, dataset 5).

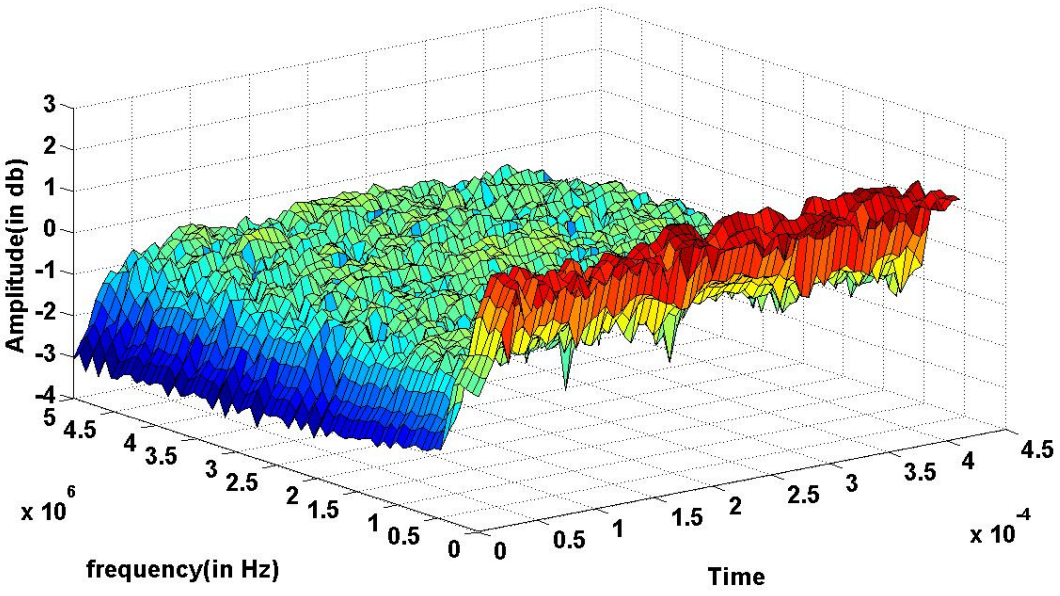

Figure 3.51 Impedance magnitude with a Hamming window (differential voltage, cable with holes, dataset 5)

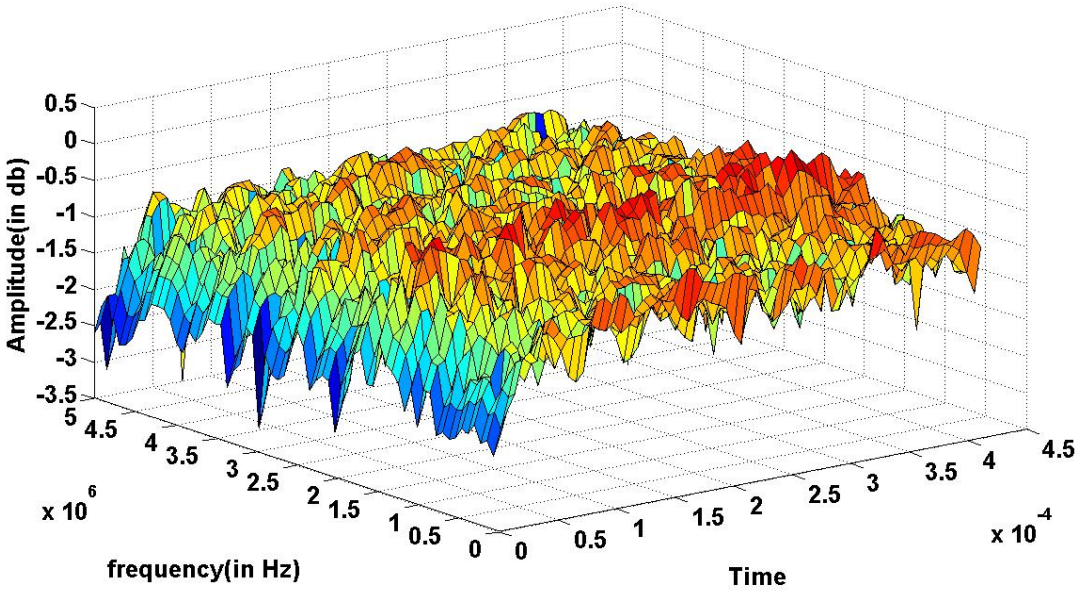

Figure 3.52 Impedance magnitude with a Hamming window (differential voltage, shorted cable, dataset 5).

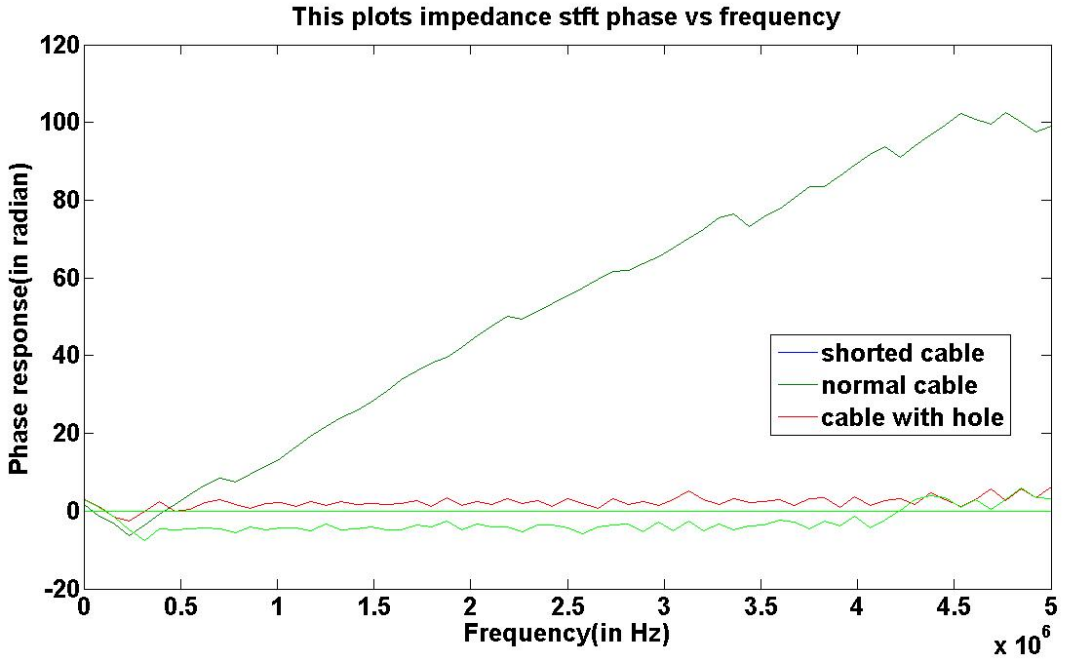

Figure 3.53 Impedance phase with a Hamming window (differential voltage, dataset 5).

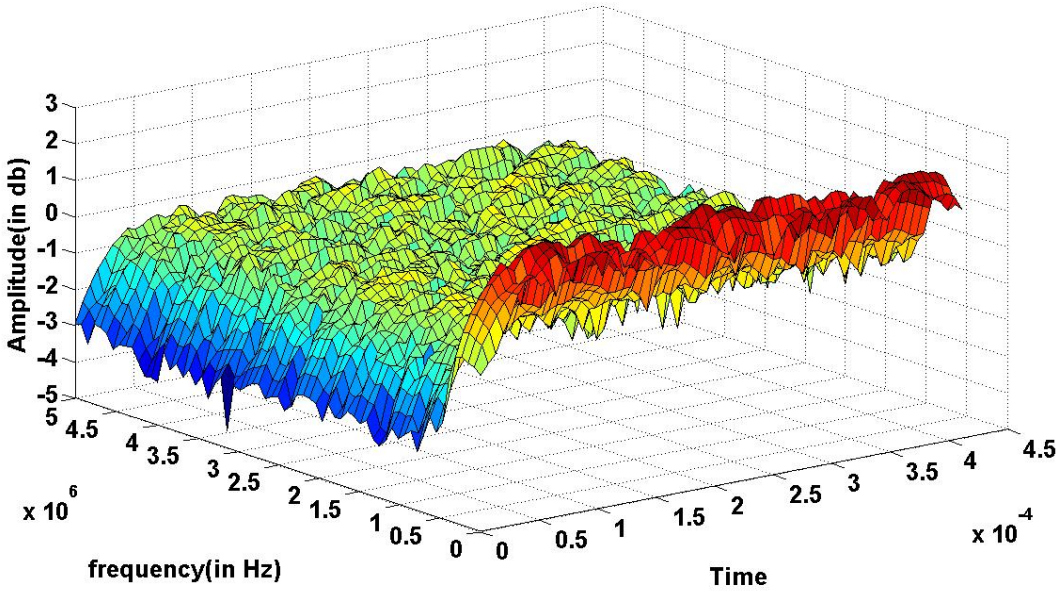

Figure 3.54 Impedance magnitude with a Gaussian window (differential voltage, normal cable, dataset 5).

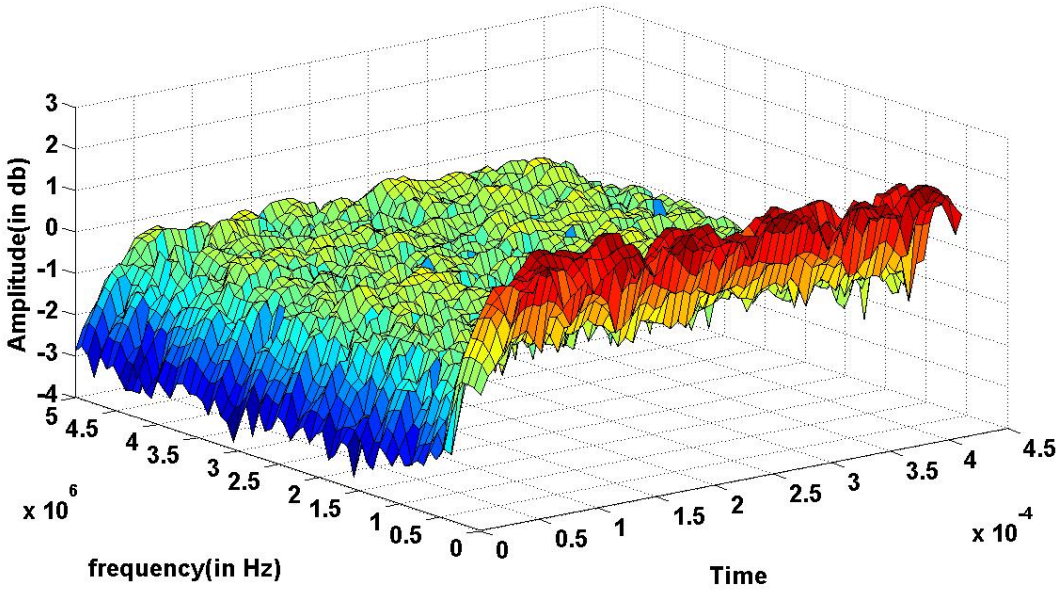

Figure 3.55 Impedance magnitude with a Gaussian window (differential voltage, cable with holes, dataset 5).

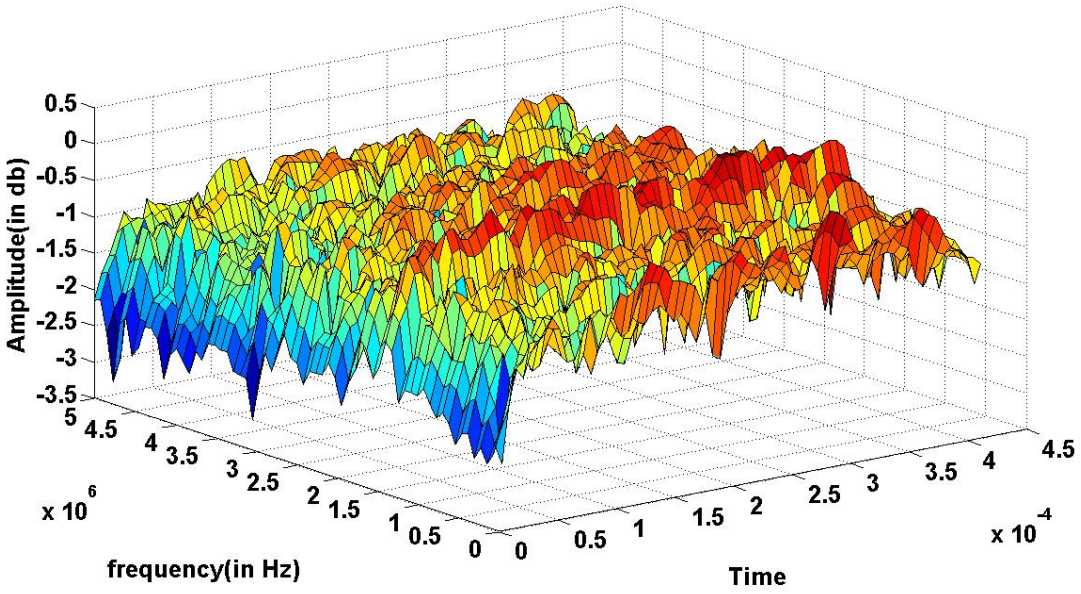

Figure 3.56 Impedance magnitude with a Gaussian window (differential voltage, shorted cable, dataset 5)

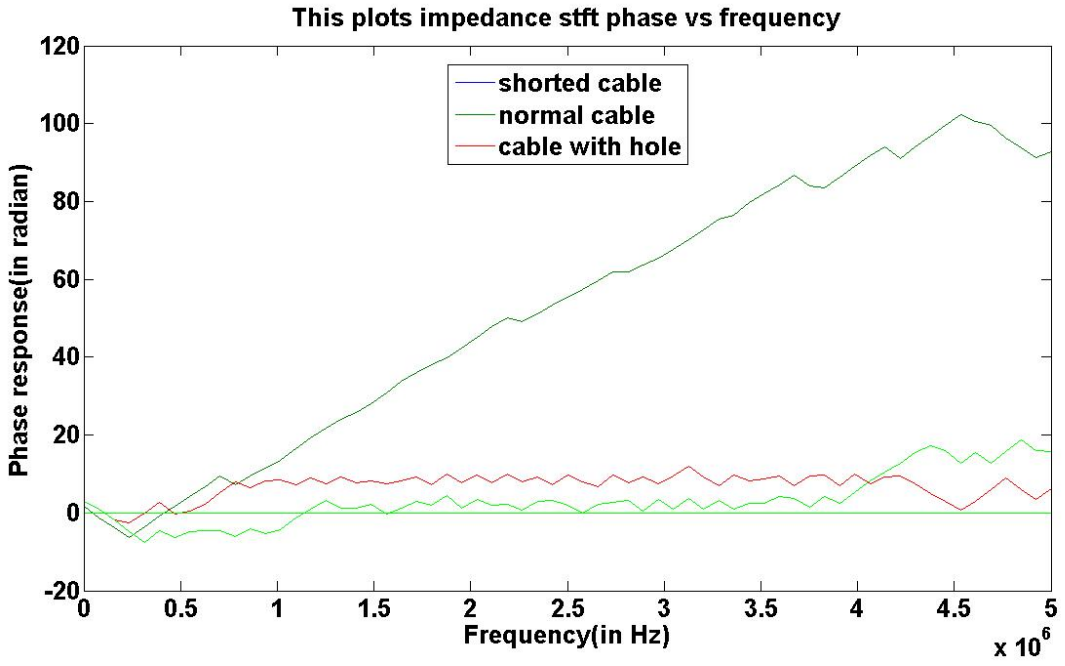

Figure 3.57 Impedance phase with a Gaussian window (differential voltage, dataset 5).

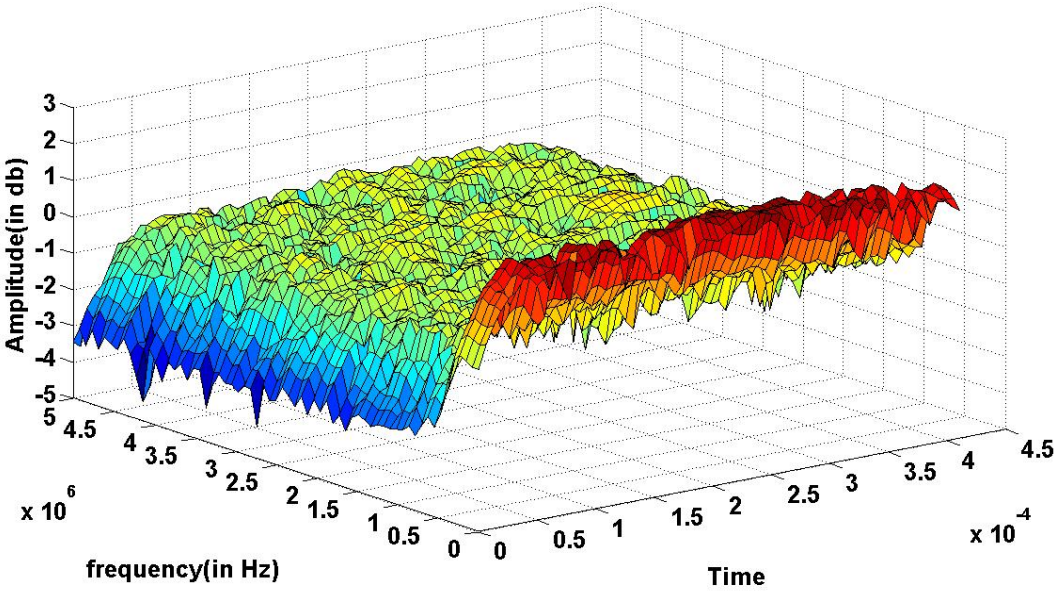

Figure 3.58 Impedance magnitude with a Gaussian window (normal cable, dataset 1).

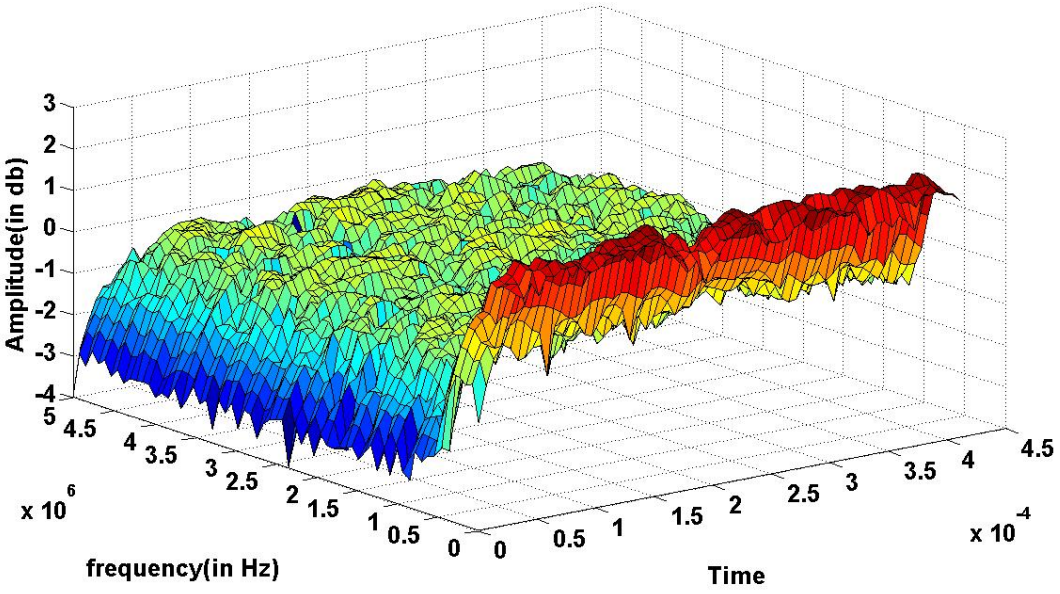

Figure 3.59 Impedance magnitude with a Gaussian window (cable with holes, dataset 1).

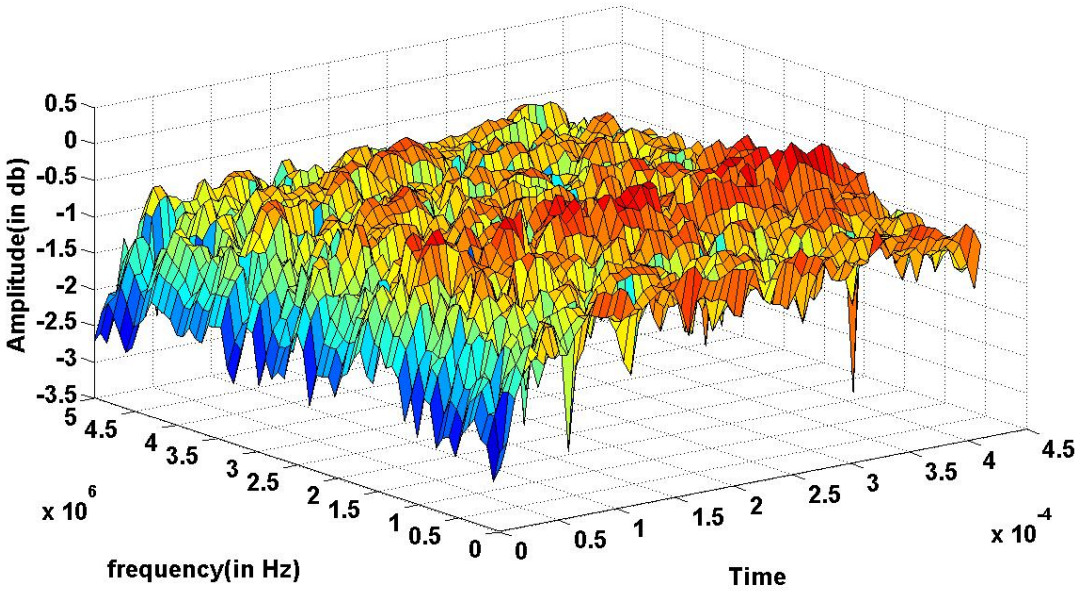

Figure 3.60 Impedance magnitude with a Gaussian window (shorted cable, dataset1).

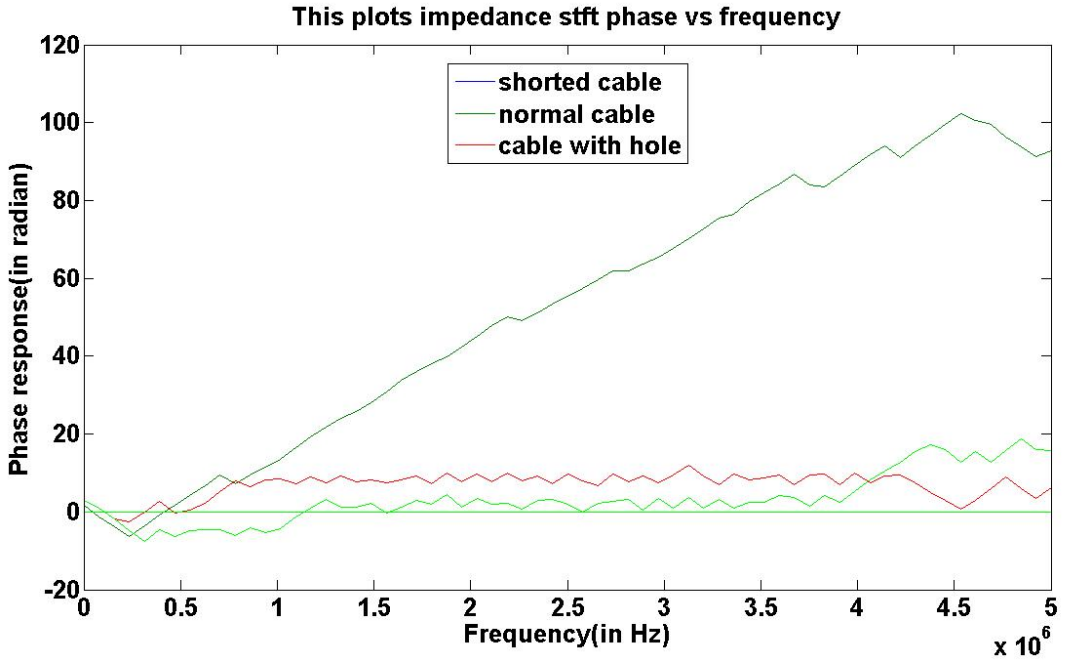

Figure 3.61 Impedance phase with a Gaussian window (dataset1).

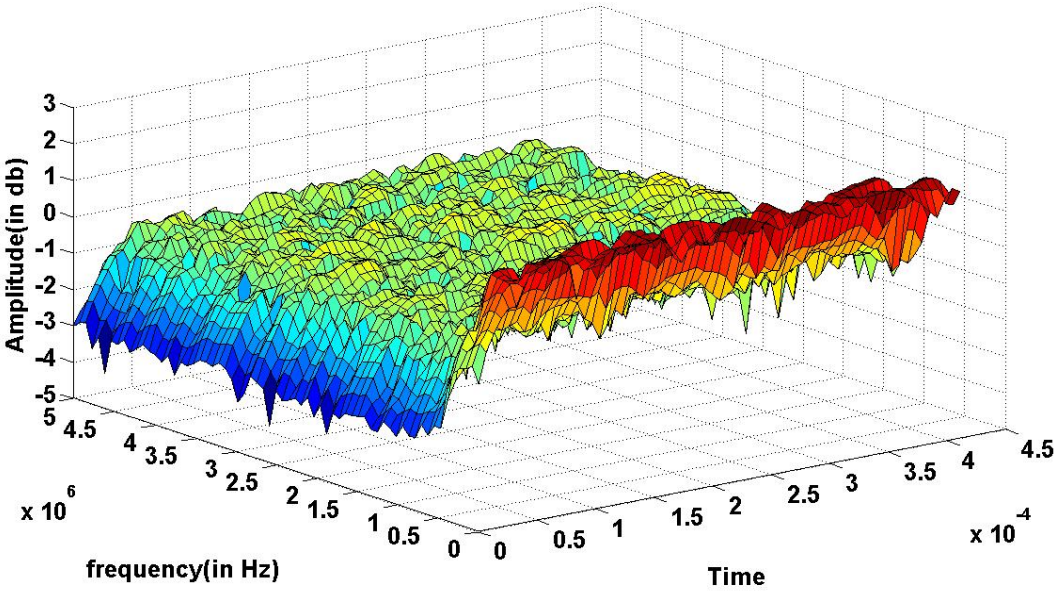

Figure 3.62 Impedance magnitude with a Gaussian window (normal cable, dataset 2).

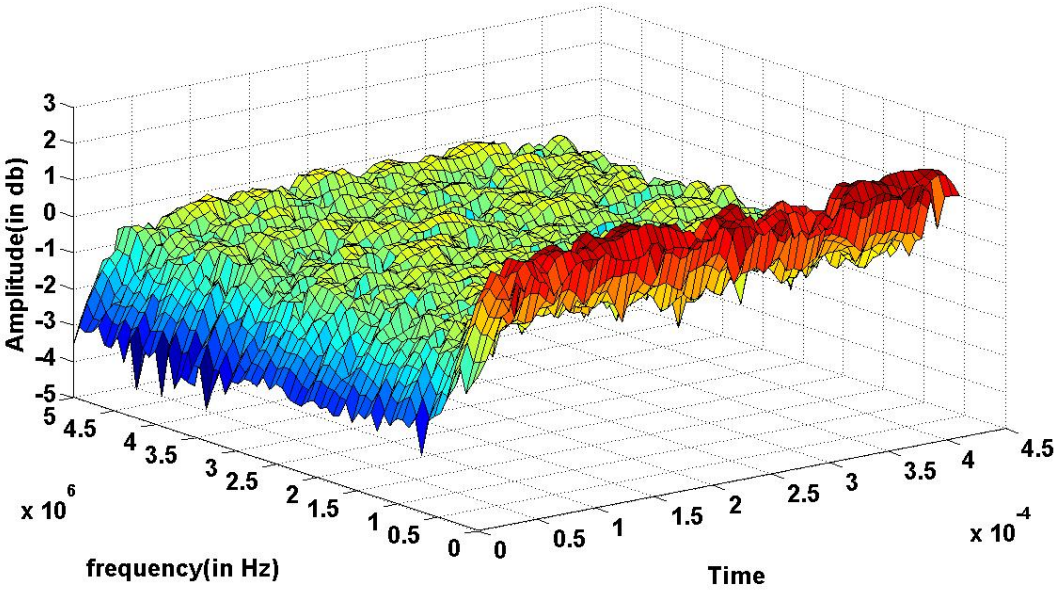

Figure 3.63 Impedance magnitude with a Gaussian window (cable with holes, dataset 2).

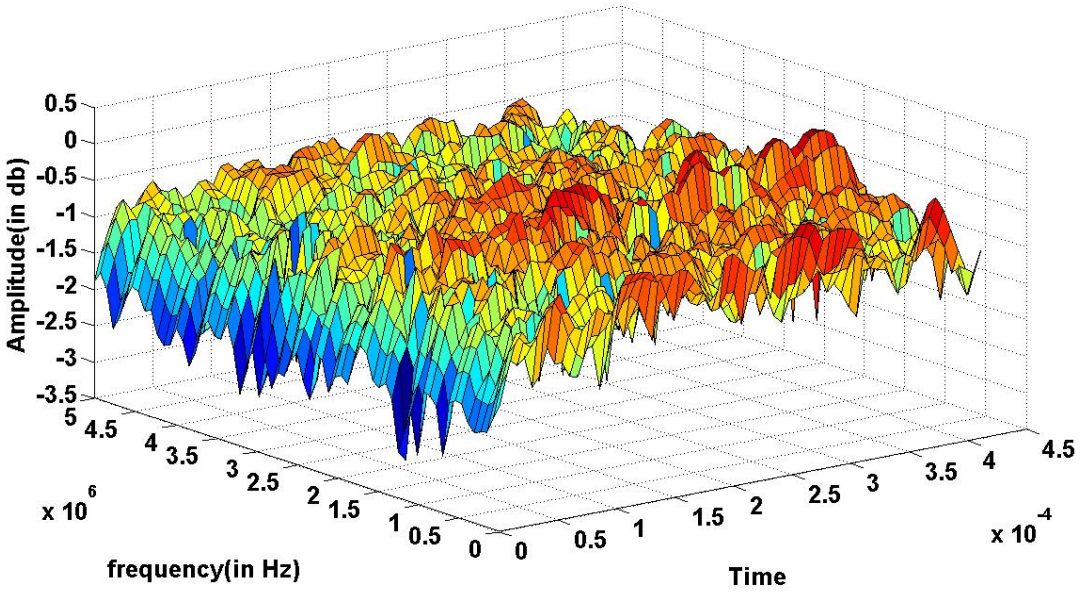

Figure 3.64 Impedance magnitude with a Gaussian window (shorted cable, dataset 2).

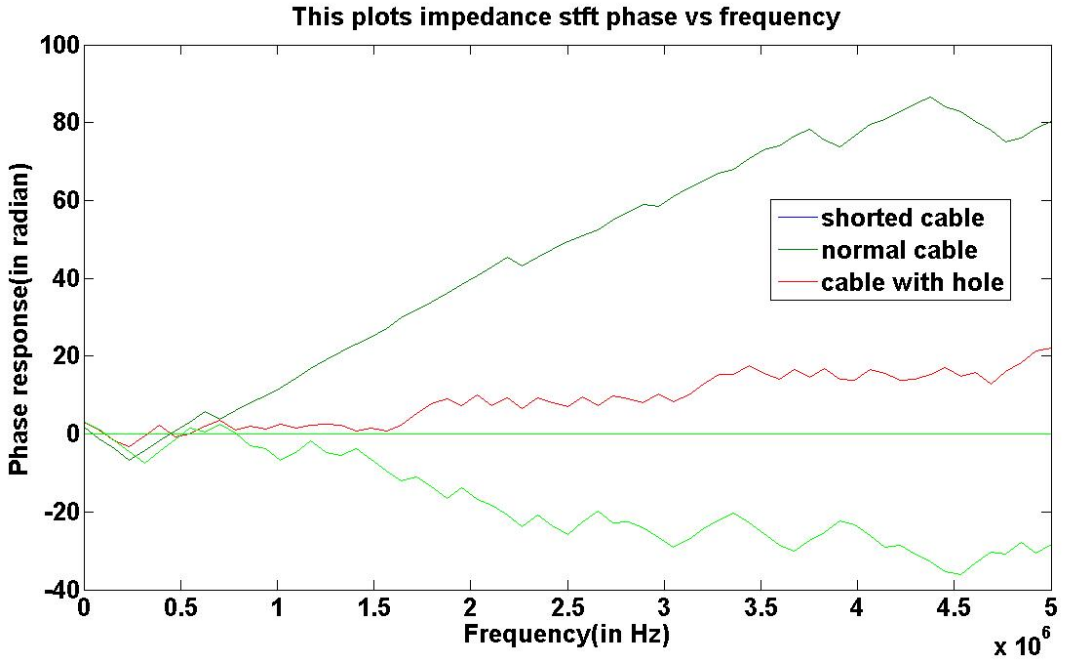

Figure 3.65 Impedance phase with a Gaussian window (dataset 2).

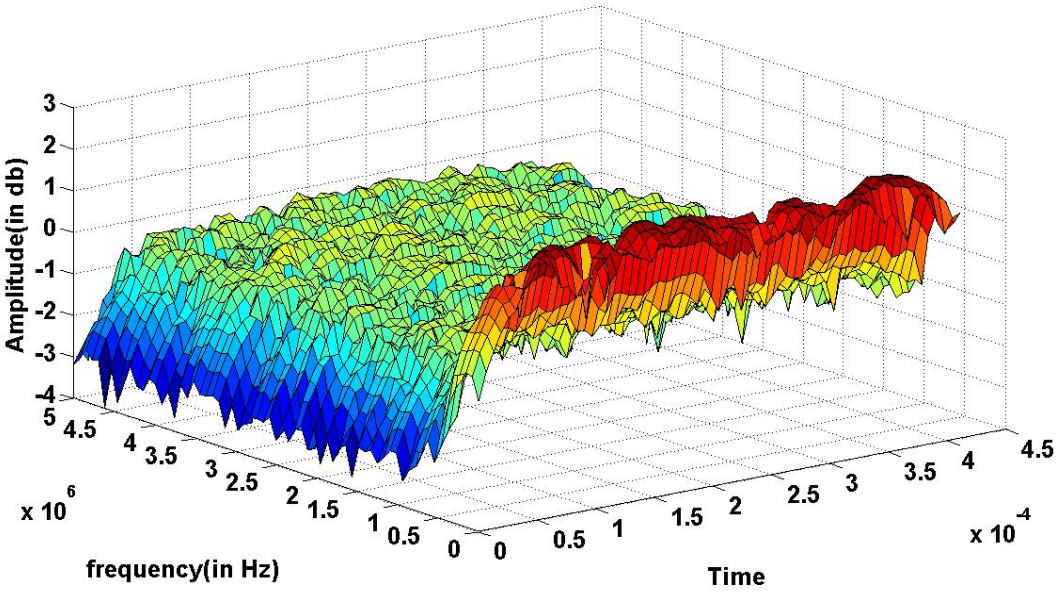

Figure 3.66 Impedance magnitude with a Gaussian window (normal cable, dataset 3).

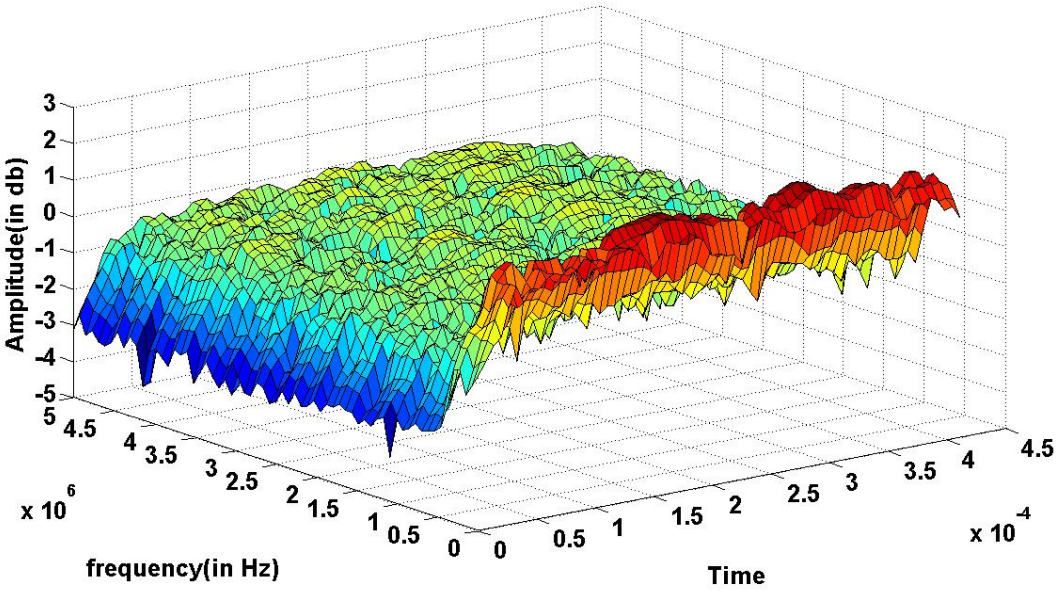

Figure 3.67 Impedance magnitude with a Gaussian window (cable with holes, dataset 3).

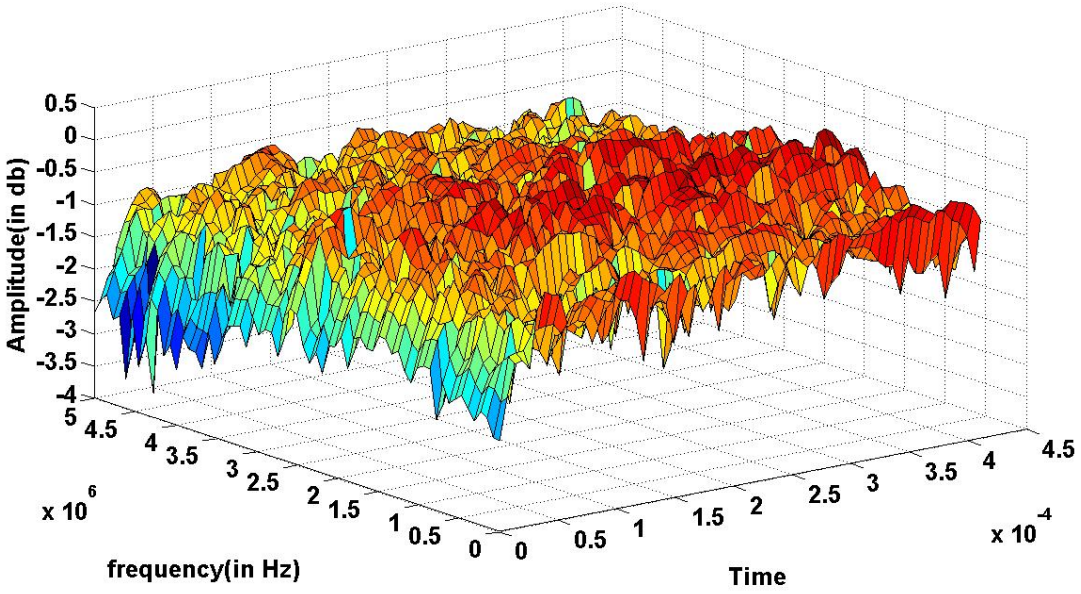

Figure 3.68 Impedance magnitude with a Gaussian window (shorted cable, dataset 3).

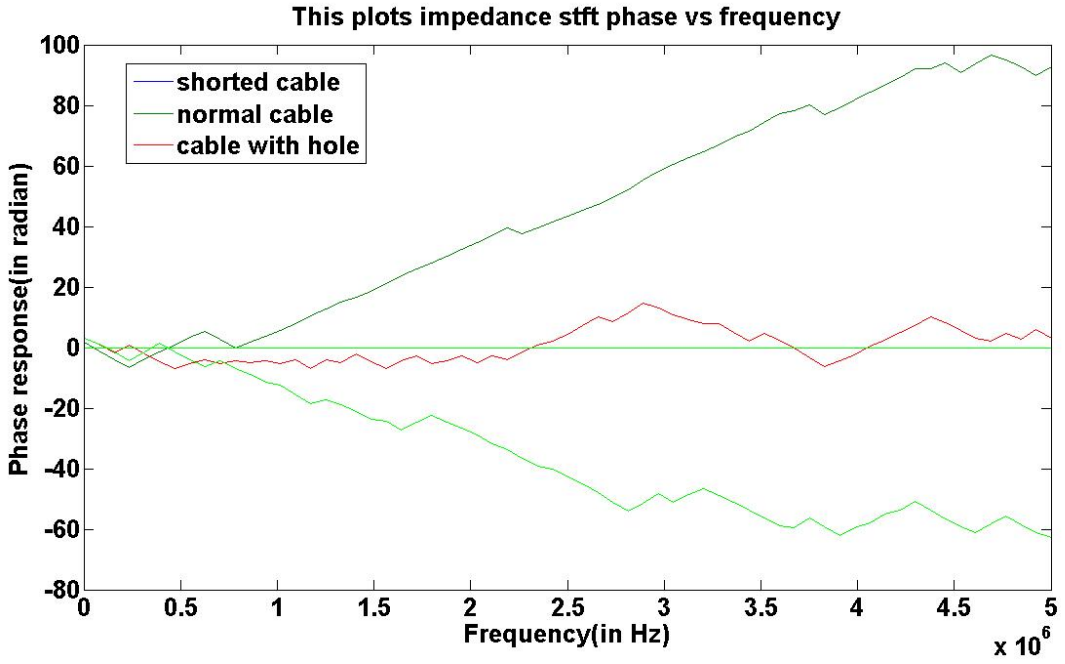

Figure 3.69 Impedance phase with a Gaussian window (dataset 3).

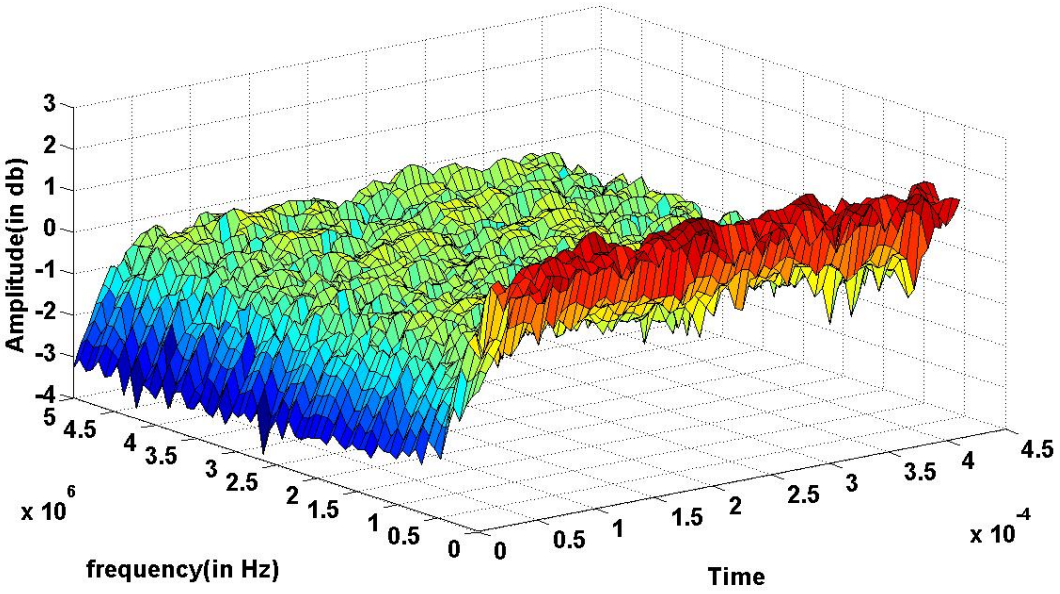

Figure 3.70 Impedance magnitude with a Gaussian window (normal cable, dataset 4).

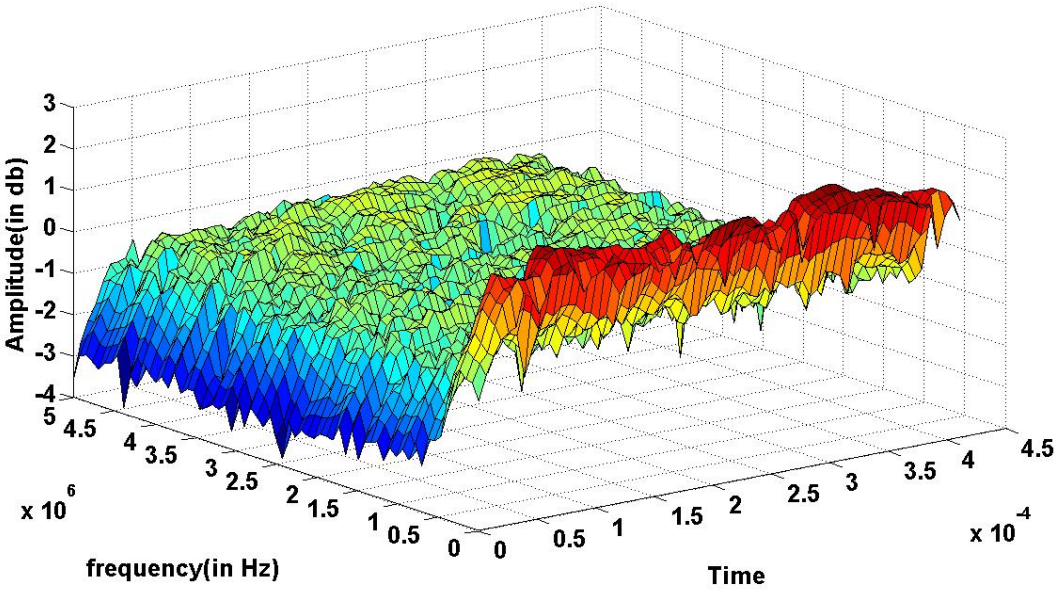

Figure 3.71 Impedance magnitude with a Gaussian window (cable with holes, dataset 4).

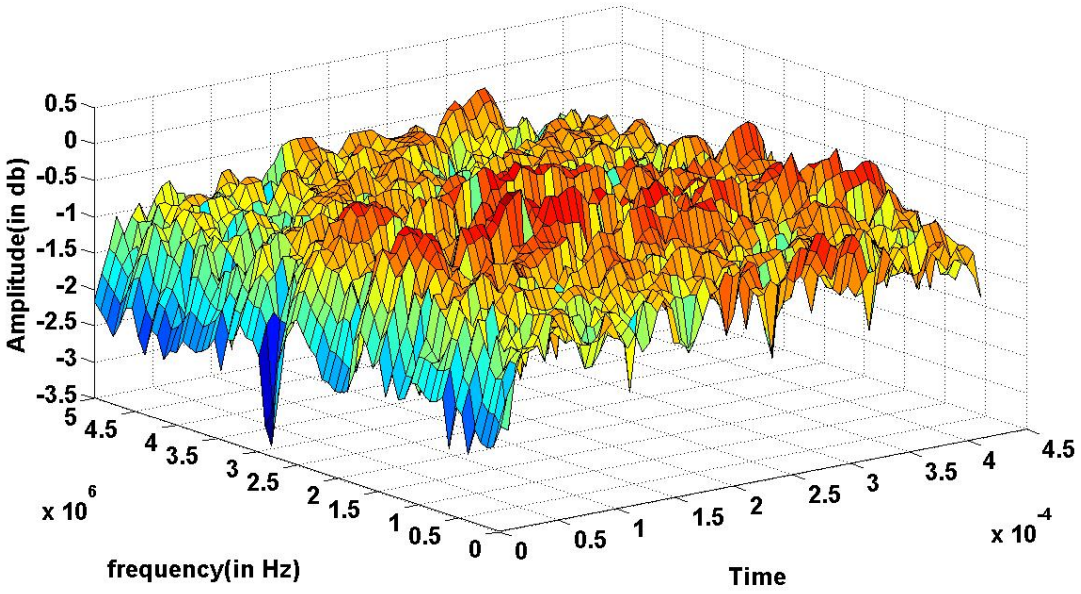

Figure 3.72 Impedance magnitude with a Gaussian window (shorted cable, dataset 4).

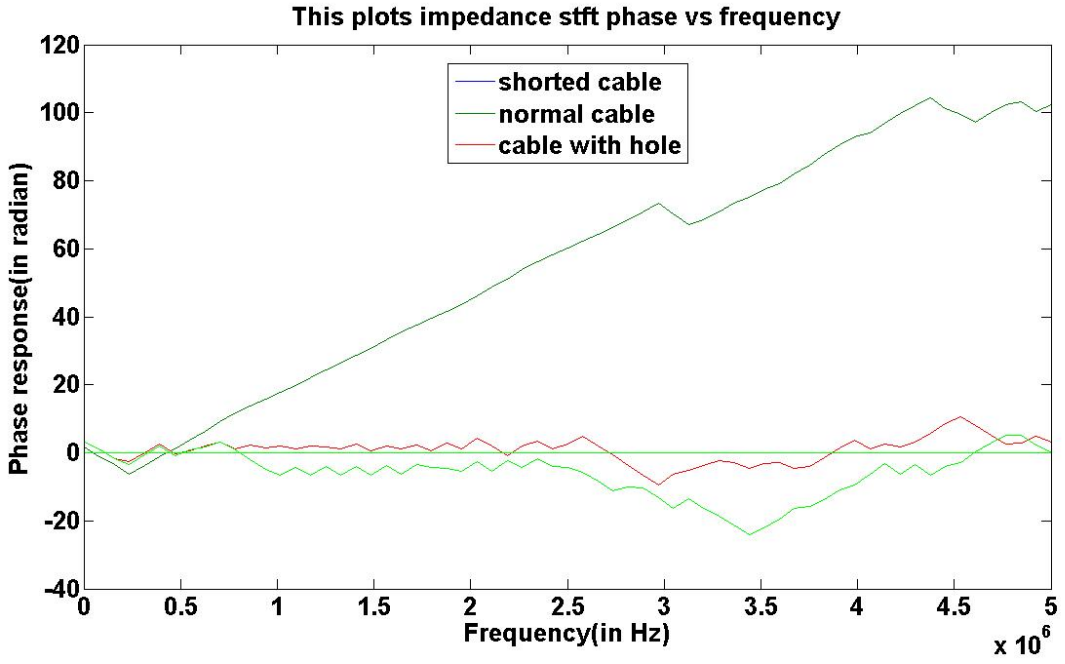

Figure 3.73 Impedance phase with a Gaussian window (dataset 4).

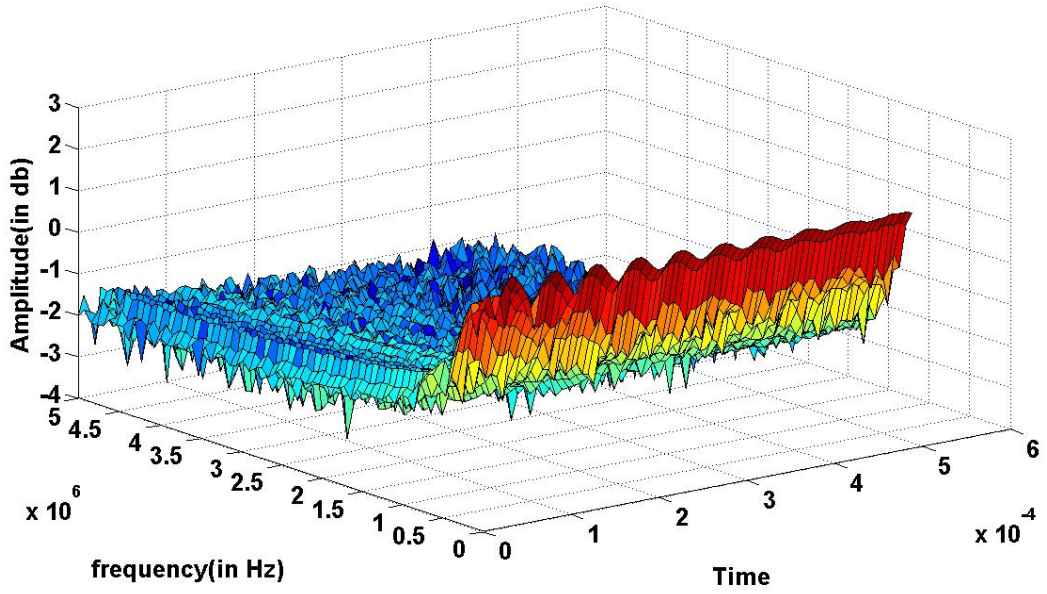

Figure 3.74 Impedance magnitude with a Gaussian window (sending end voltage, normal cable, dataset 1).

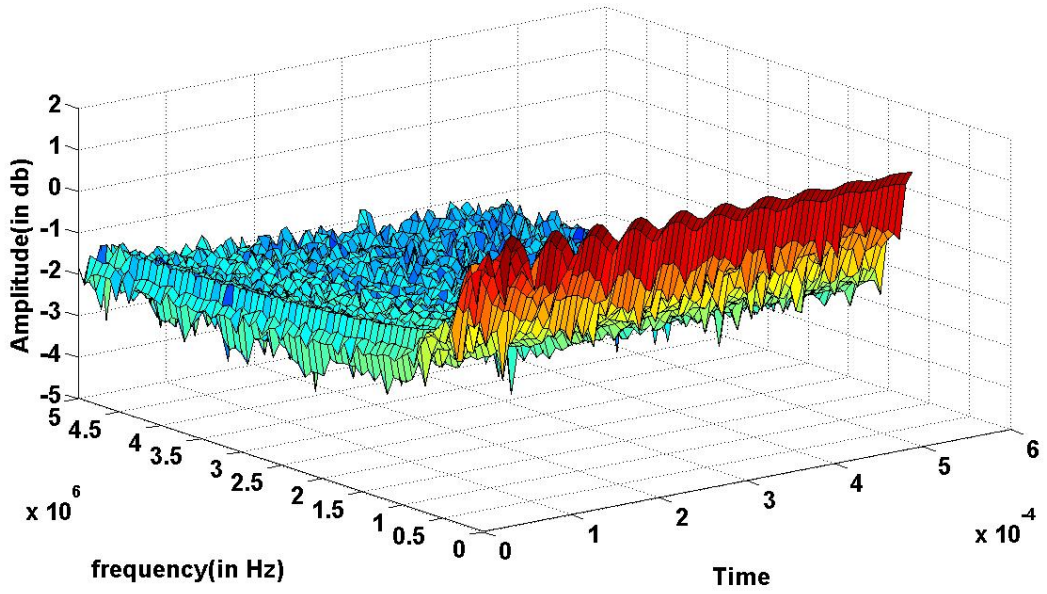

Figure 3.75 Impedance magnitude with a Gaussian window (sending end voltage, cable with holes, dataset 1).

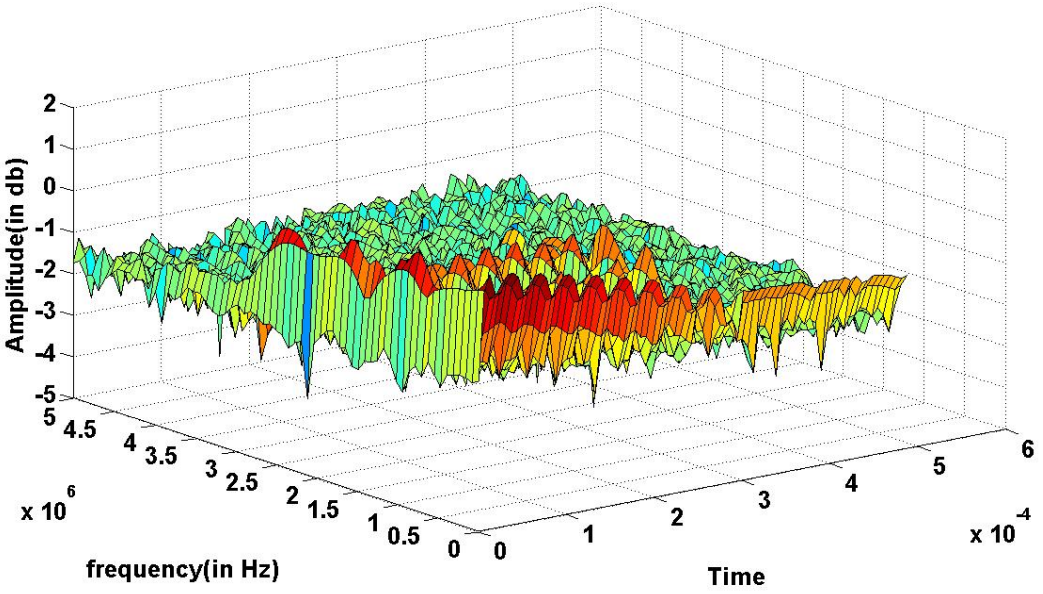

Figure 3.76 Impedance magnitude with a Gaussian window (sending end voltage shorted cable, dataset 1).

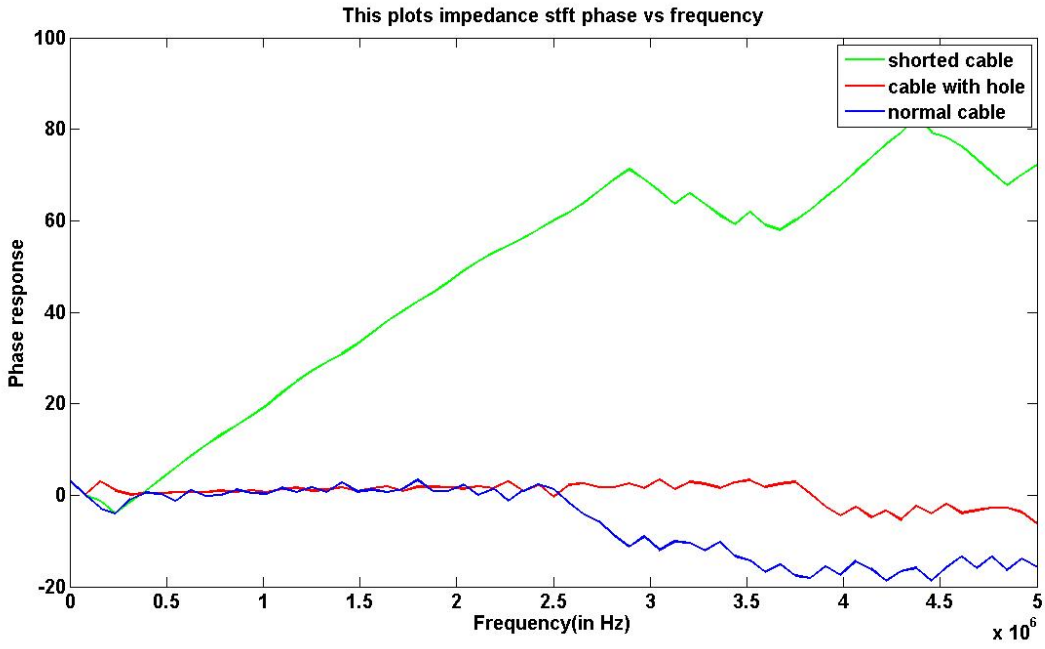

Figure 3.77 Sending end voltage phase with a Gaussian window (data set1).

3.5 STFT Observations

a) Both methods of impedance calculation (via the sending end voltage and the differential voltage) yield nearly identical results and can be used for differentiating between the different types of cable defects, especially from phase information.

b) All windows types yield reasonable results. However, the Gaussian window seems to have slightly better results than the other windowing techniques in terms of noise reduction.

c) Both Hanning and Hamming windows are also good contenders for this type of applications as well. Accordingly, it is better to try out all three windows (Gaussian, Hanning, and Hamming) since the window choice is data dependent.

d) The STFT and the FFT yield identical results for a rectangular window.

e) The shorted cable can be easily distinguished directly from the magnitude response. The cable with holes and normal cable behave very similarly. However, they still can be distinguished from the magnitude response.

f) Overall, 3D visualization of the magnitude response enhances the distinction between the three different types of cables under investigation.

3.6 Discrete Wavelet Transform Results

From the sample data sets and for each type of the underground power cable (normal, shorted, and with holes) that are available, the first sample data set is used initially in this analysis for illustrative purposes. The DWT is used to obtain the magnitude response of the cable impedance. The cable impedance is computed directly from the current and voltage measurements as the ratio of the differential voltage over the

current, where the differential voltage represents the difference between the sending end voltage and the receiving end voltage.

We select Daubechies (4) as the mother wavelet function for its familiarity to faulty waveform. Figures 3.77- 3.91 represent the corresponding DWT implementation of the normal cable, cable with hole, and shorted cable data using all types of windowing. By examining these results, one sees, in most cases, faults can be distinguished from the magnitude response; especially those who correspond to the shorted cable with different windowing techniques. Furthermore, the Hanning window provides clear distinction between all fault types. Accordingly, the Hanning window is used for DWT implementation from then onwards and is tested on all the remaining data sets (datasets 2, 3, 4, and 5). For comparison purposes, results from the Gaussian window are also included. The corresponding plots for the rest of the data sets are illustrated in Figures 3.90-3.103 for the Gaussian window and in Figures 3.104-3.115 for the Hanning window.

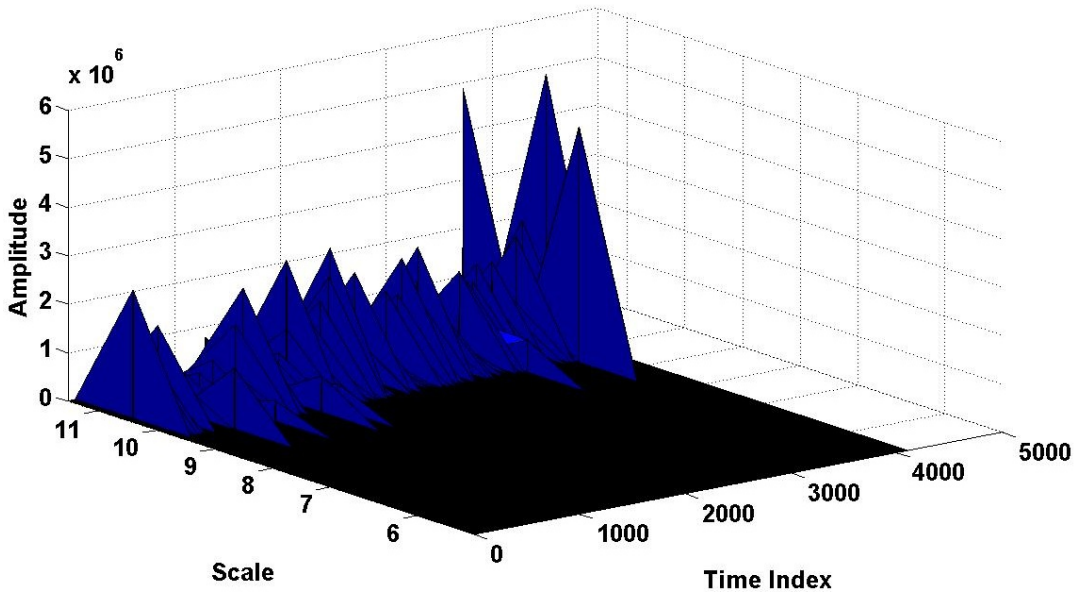

Figure 3.78 Impedance magnitude with a rectangular window (differential voltage, normal cable, dataset 1).

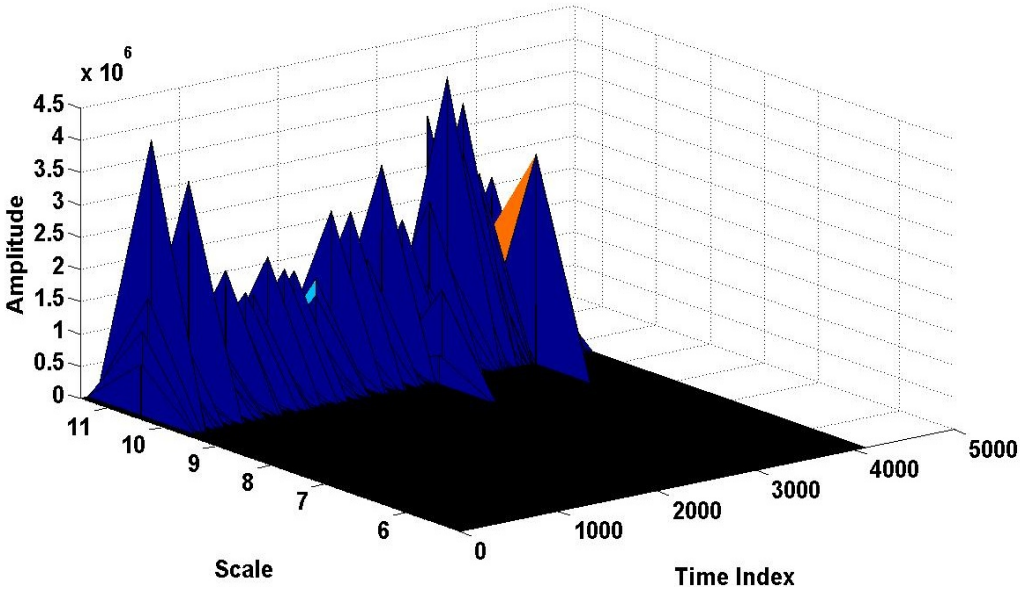

Figure 3.79 Impedance magnitude with a rectangular window (differential voltage, cable with holes, dataset 1).

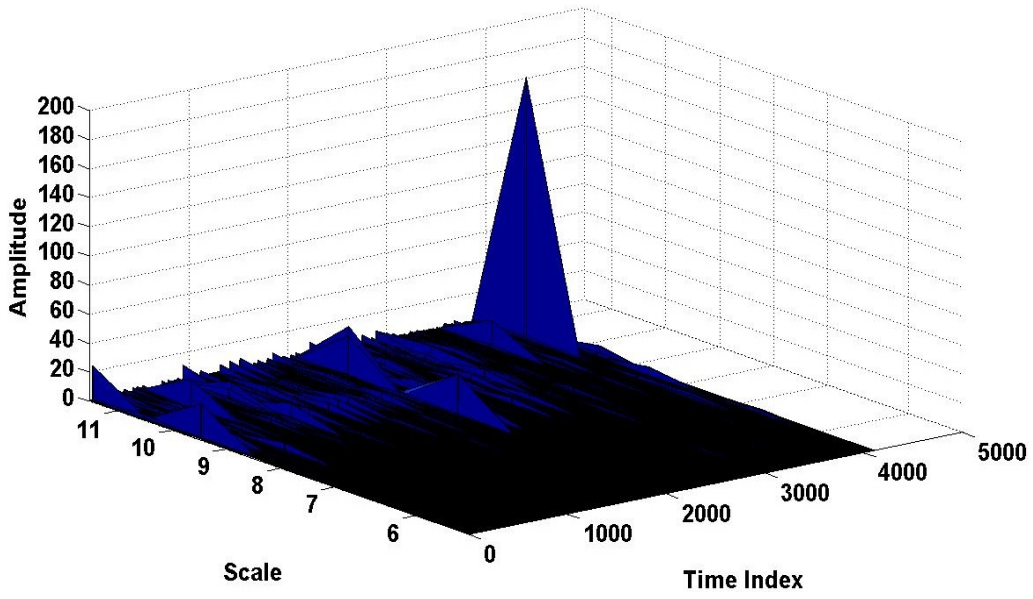

Figure 3.80 Impedance magnitude with a rectangular window (differential voltage, shorted cable, dataset 1).

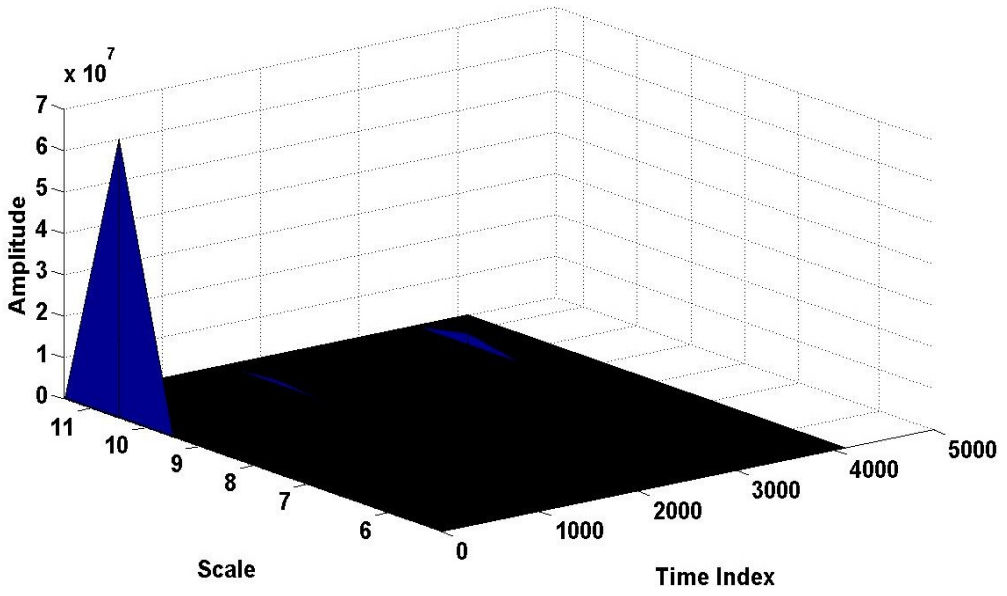

Figure 3.81 Impedance magnitude with a triangular window (differential voltage, normal cable, dataset 1).

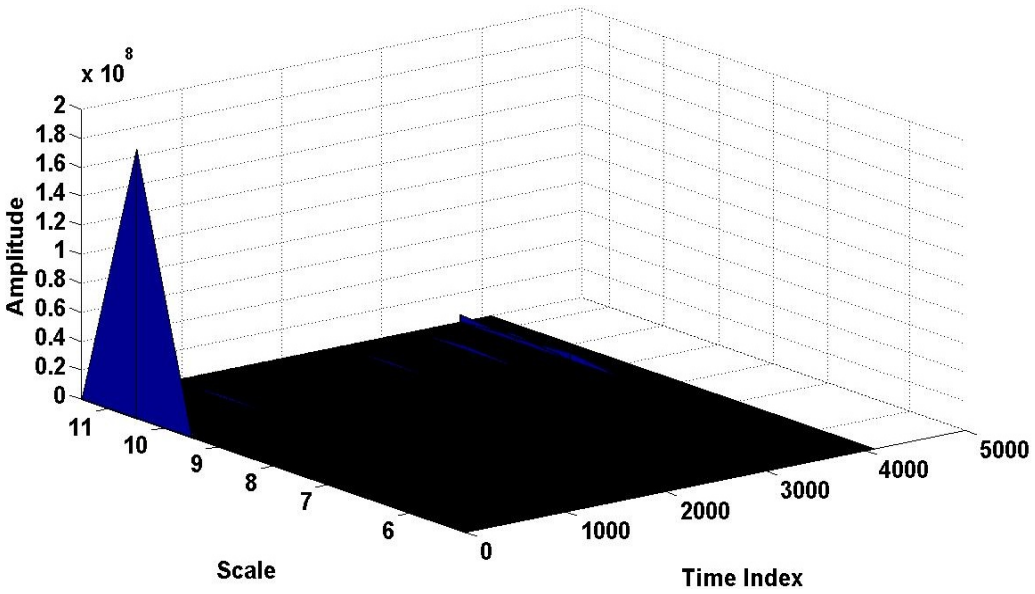

Figure 3.82 Impedance magnitude with a triangular window (differential voltage, cable with holes, dataset 1).

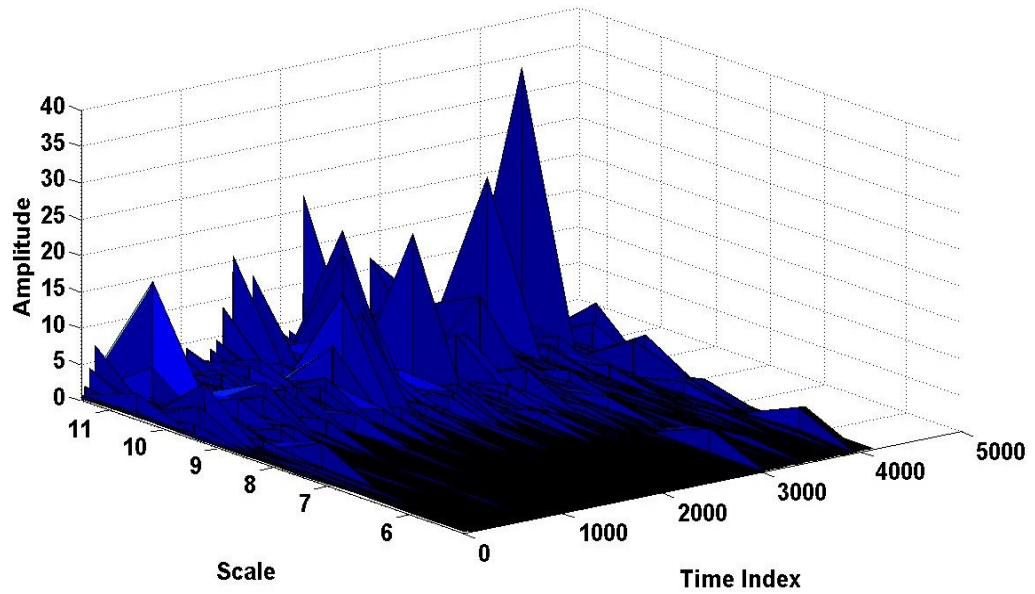

Figure 3.83 Impedance magnitude with a triangular window (differential voltage, shorted cable, dataset 1).

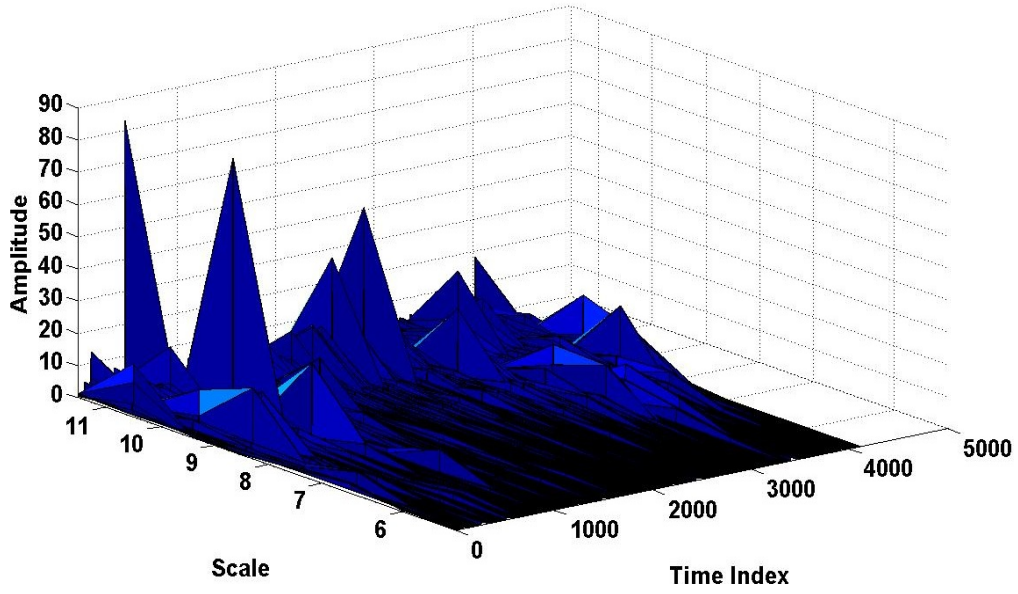

Figure 3.84 Impedance magnitude with a Hanning window (differential voltage, normal cable, dataset 1).

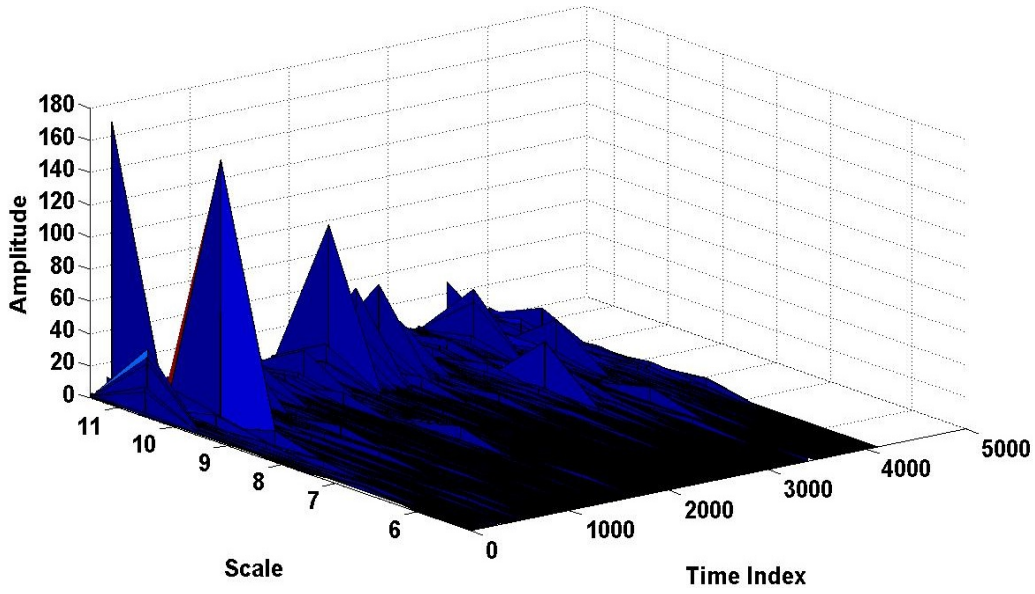

Figure 3.85 Impedance magnitude with a Hanning window (differential voltage, cable with holes, dataset 1).

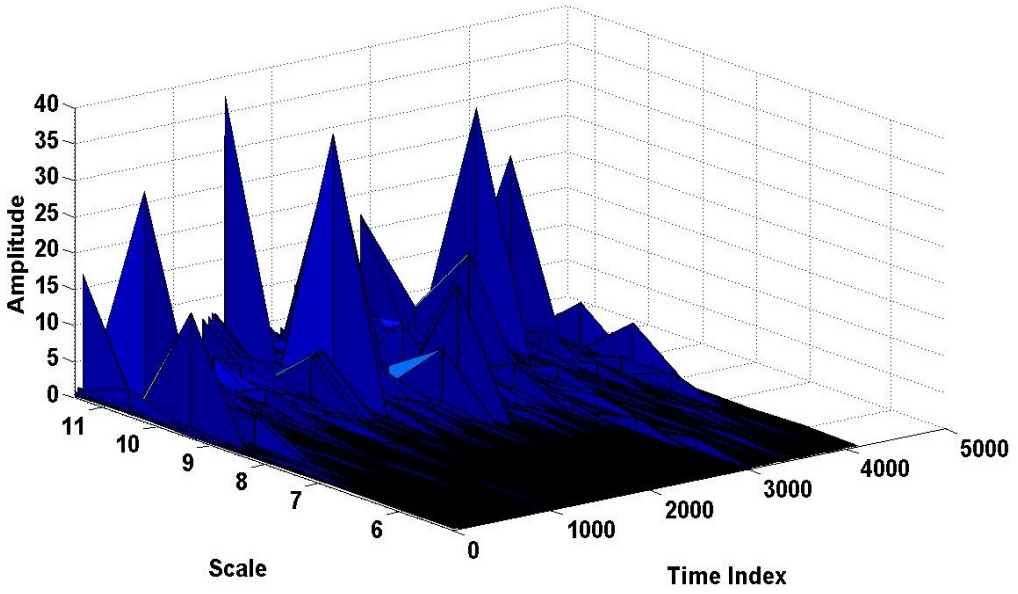

Figure 3.86 Impedance magnitude with a Hanning window (differential voltage, shorted cable, dataset 1).

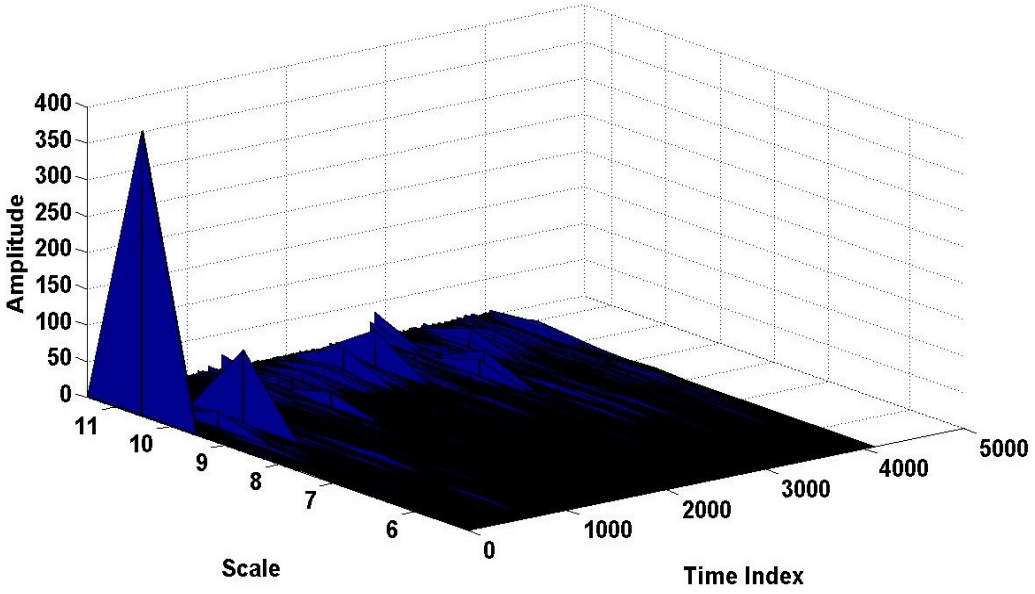

Figure 3.87 Impedance magnitude with a Hamming window (differential voltage, normal cable, dataset 1).

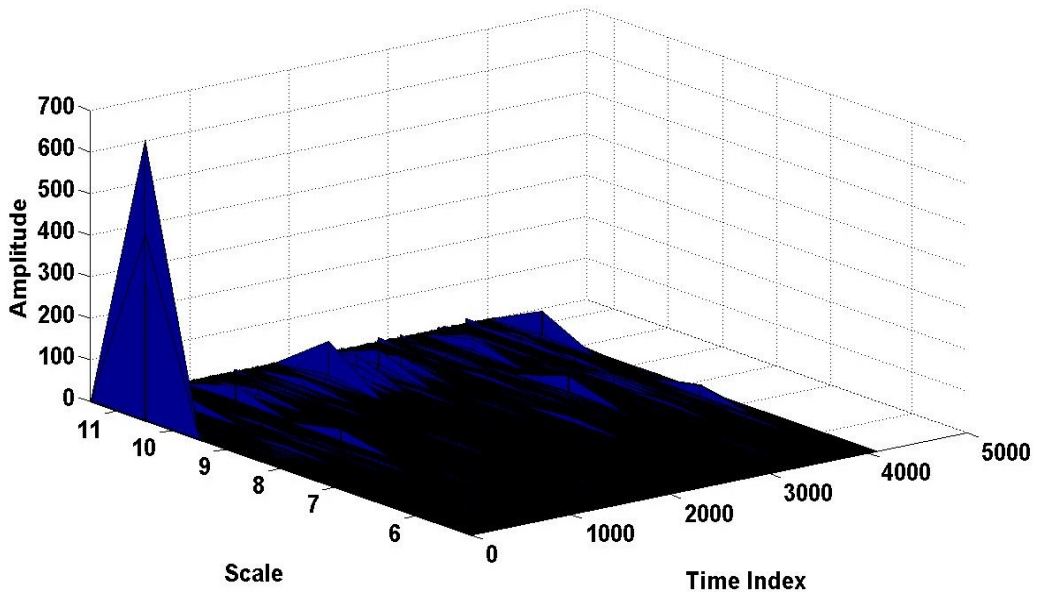

Figure 3.88 Impedance magnitude with a Hamming window (differential voltage, cable with holes, dataset 1).

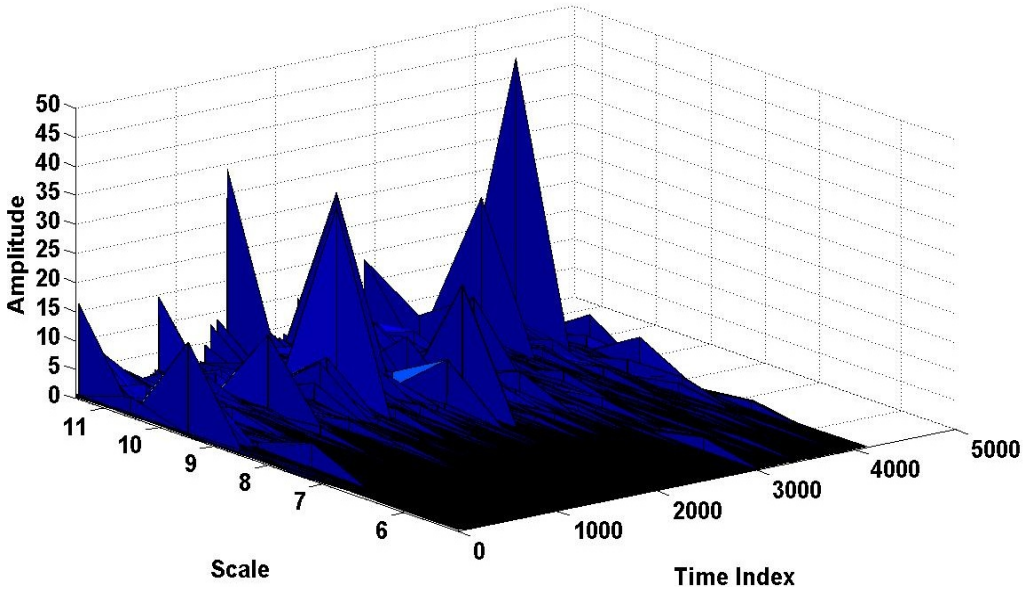

Figure 3.89 Impedance magnitude with a Hamming window (differential voltage, shorted cable, dataset 1).

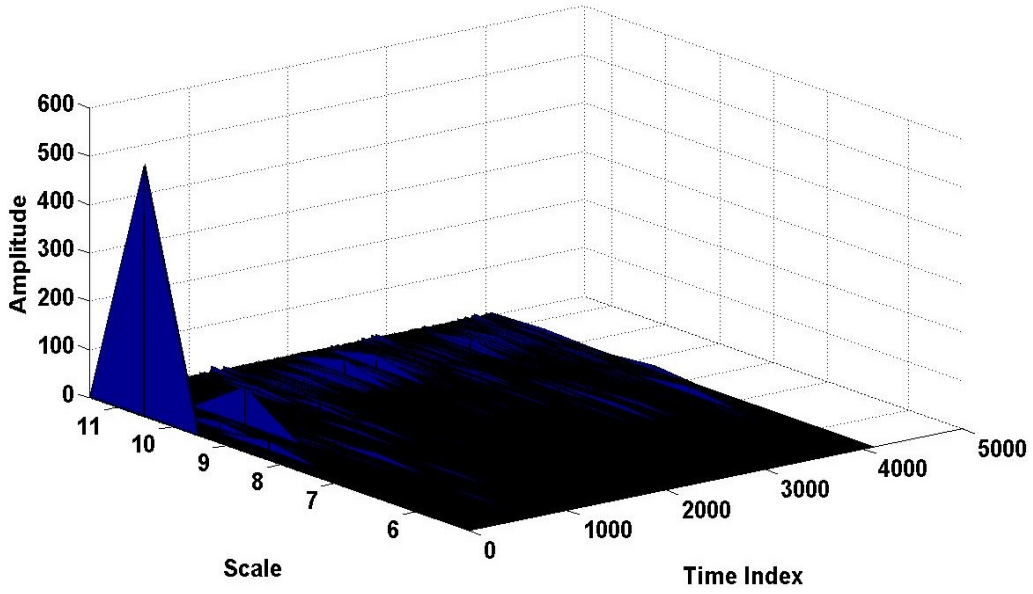

Figure 3.90 Impedance magnitude with a Gaussian window (differential voltage, normal cable, dataset 1).

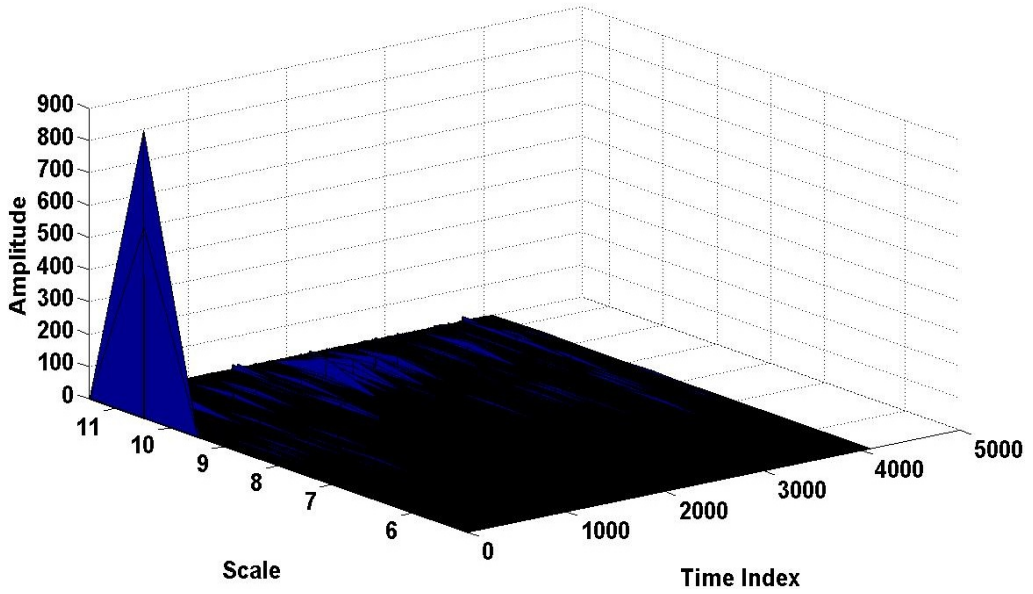

Figure 3.91 Impedance magnitude with a Gaussian window (differential voltage, cable with holes, dataset 1).

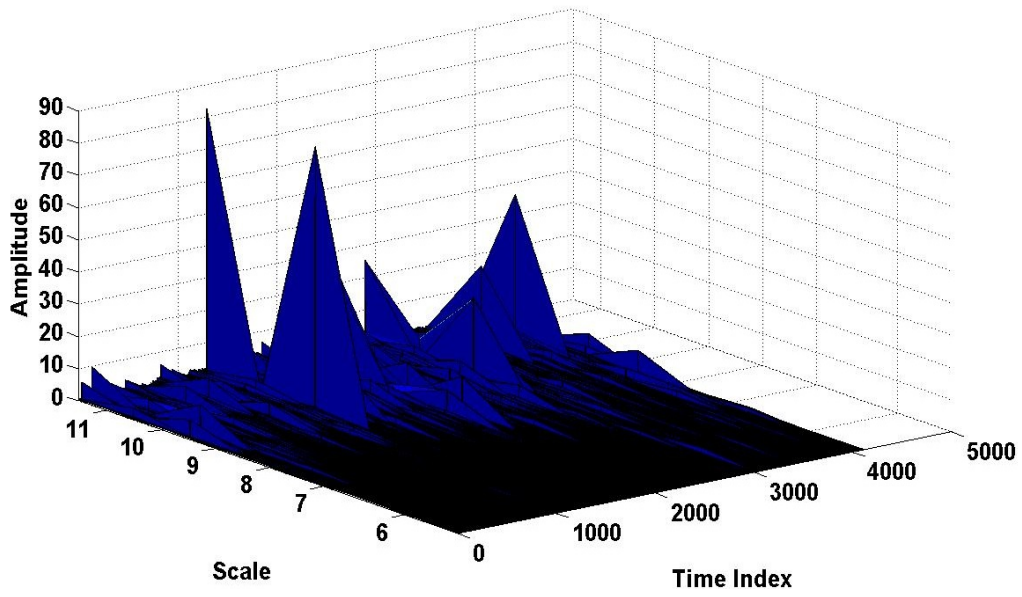

Figure 3.92 Impedance magnitude with a Gaussian window (differential voltage, shorted cable, dataset 1).

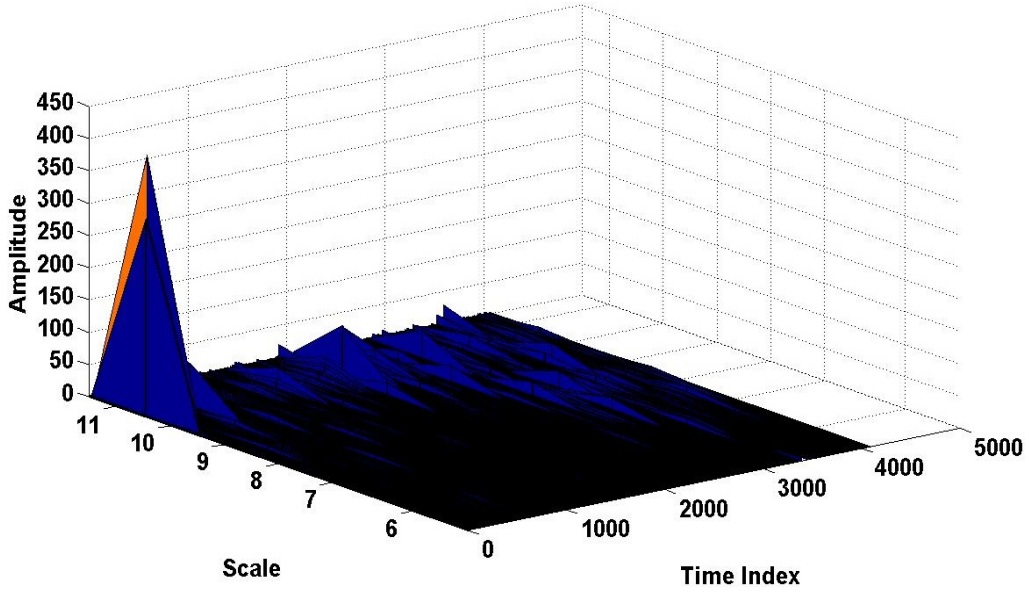

Figure 3.93 Impedance magnitude with a Gaussian window (differential voltage, normal cable, dataset 2).

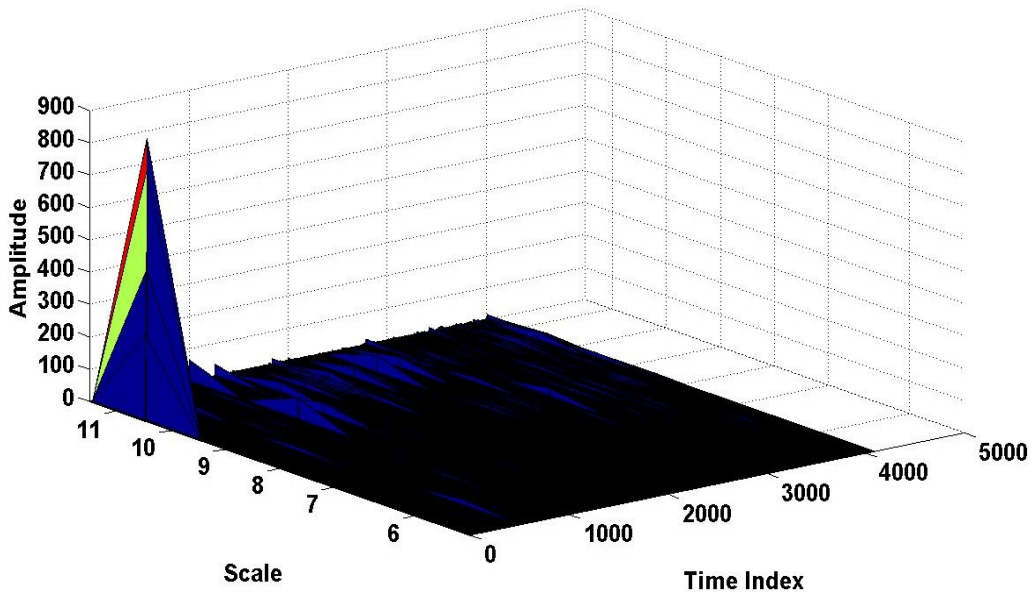

Figure 3.94 Impedance magnitude with a Gaussian window (differential voltage, cable with holes, dataset 2).

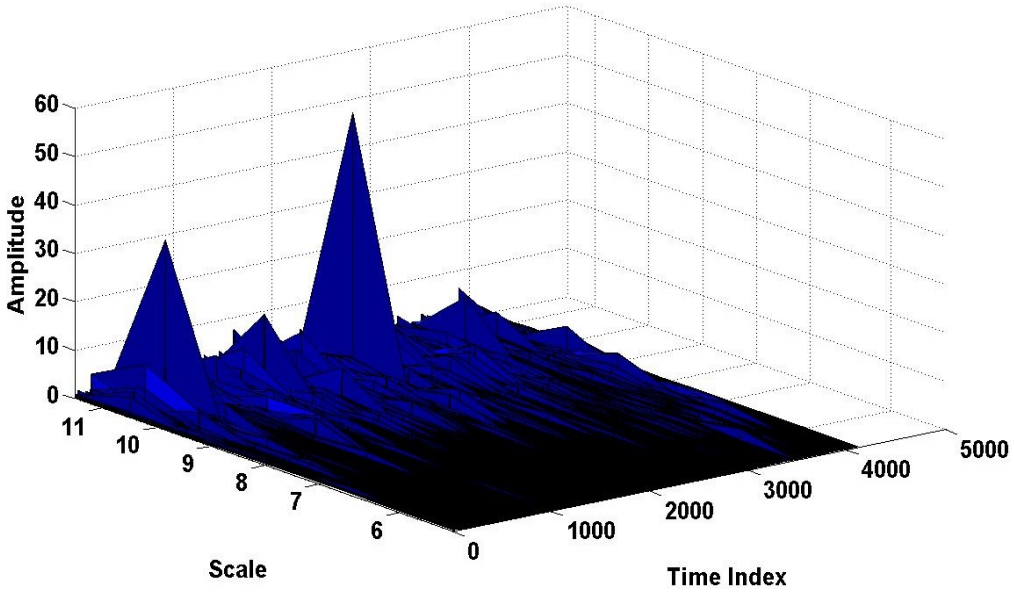

Figure 3.95 Impedance magnitude with a Gaussian window (differential voltage, shorted cable, dataset 2).

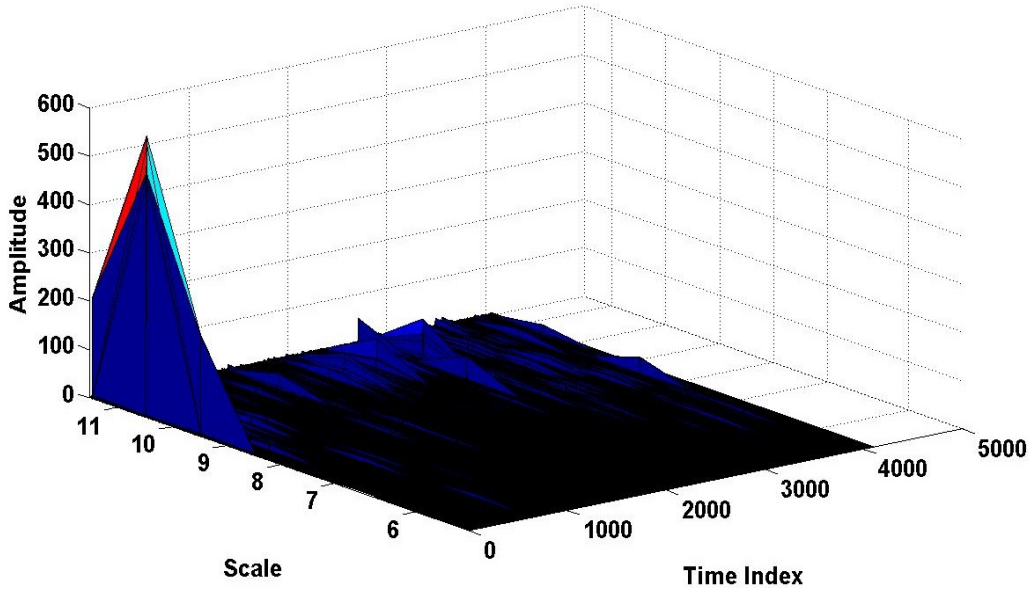

Figure 3.96 Impedance magnitude with a Gaussian window (differential voltage, normal cable, dataset 3).

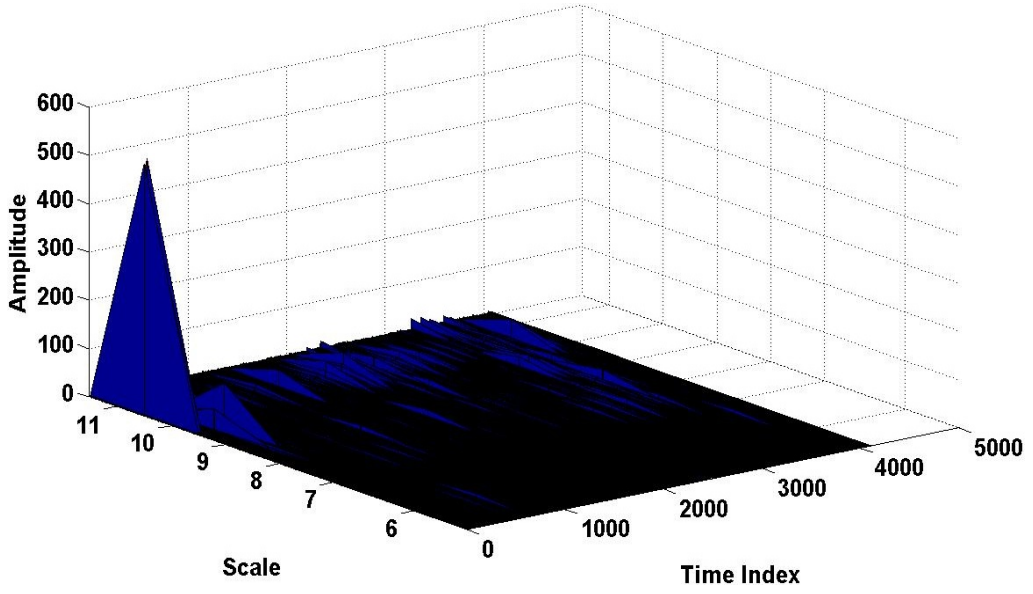

Figure 3.97 Impedance magnitude with a Gaussian window (differential voltage, cable with holes, dataset 3).

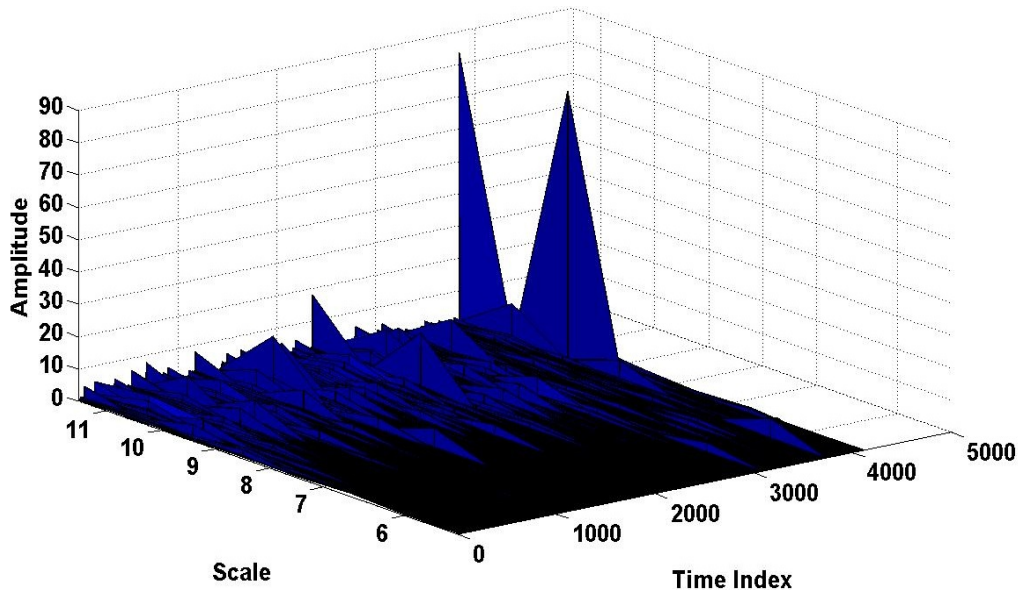

Figure 3.98 Impedance magnitude with a Gaussian window (differential voltage, shorted cable, dataset 3).

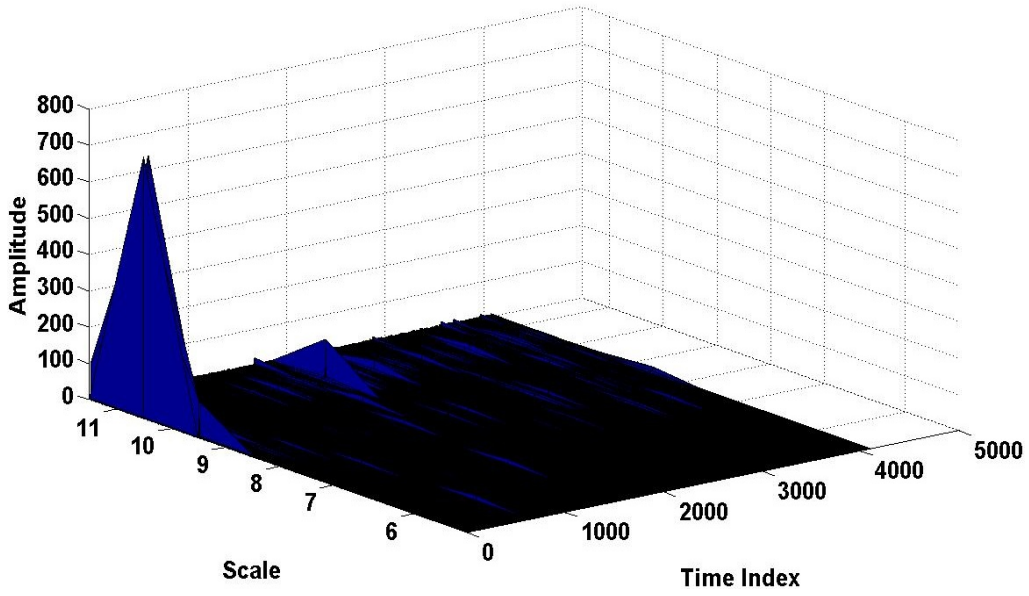

Figure 3.99 Impedance magnitude with a Gaussian window (differential voltage, normal cable, dataset 4).

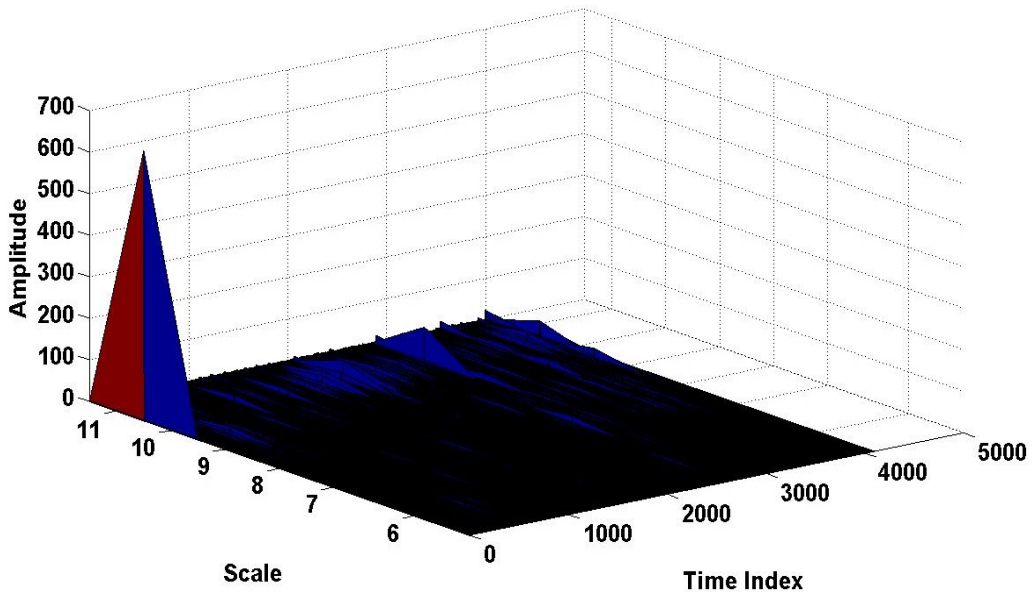

Figure 3.100 Impedance magnitude with a Gaussian window (differential voltage, cable with holes, dataset 4).

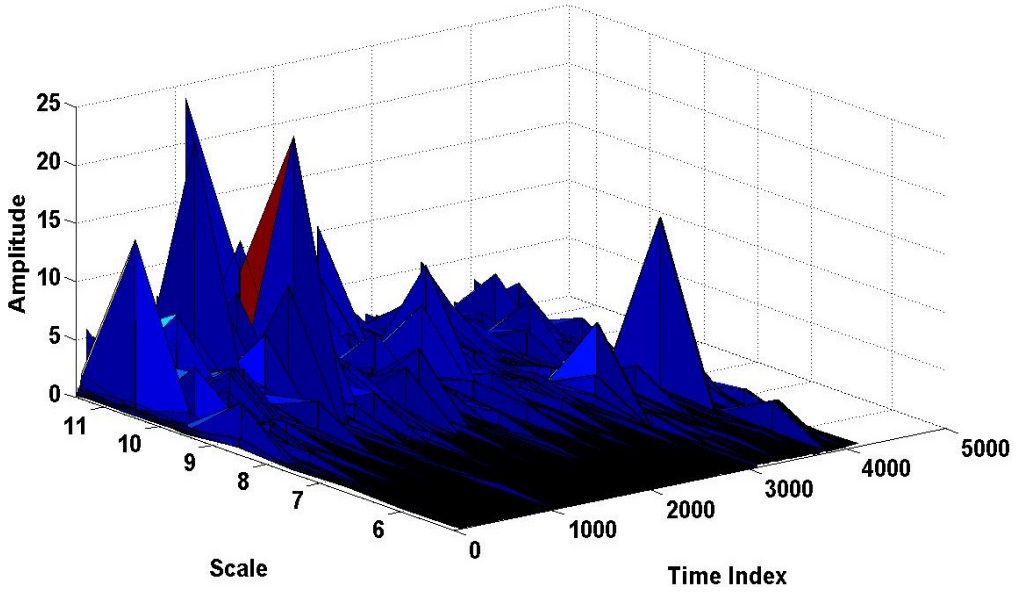

Figure 3.101 Impedance magnitude with a Gaussian window (differential voltage, shorted cable, dataset 4).

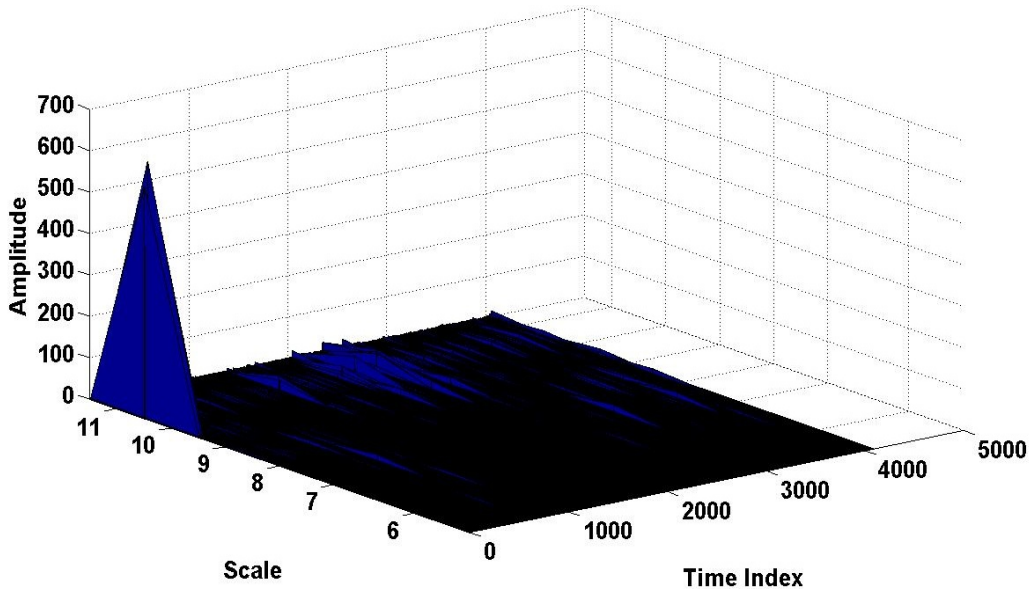

Figure 3.102 Impedance magnitude with a Gaussian window (differential voltage, normal cable, dataset 5).

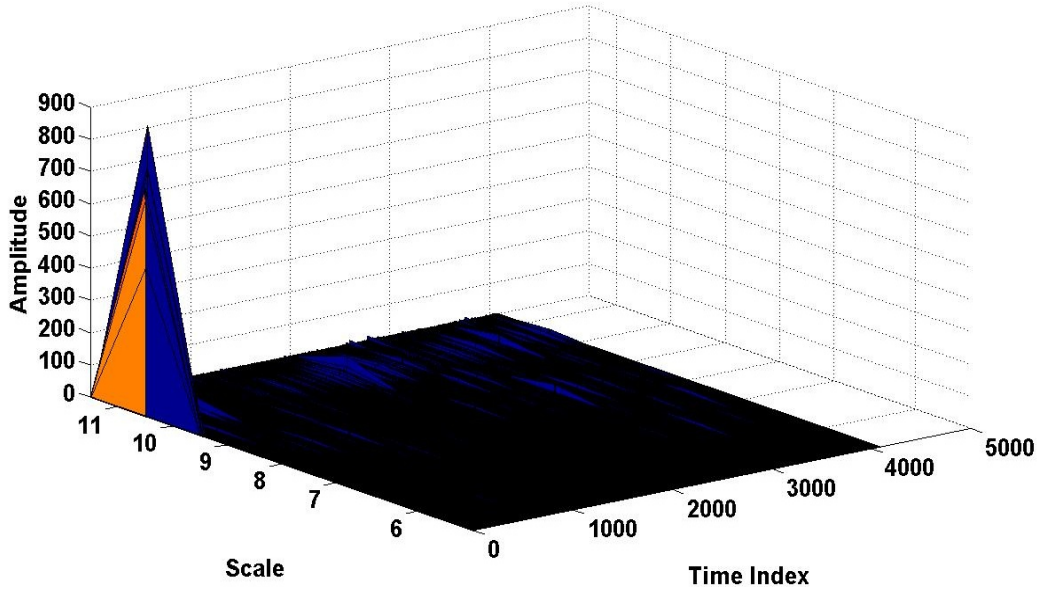

Figure 3.103 Impedance magnitude with a Gaussian window (differential voltage, cable with holes, dataset 5).

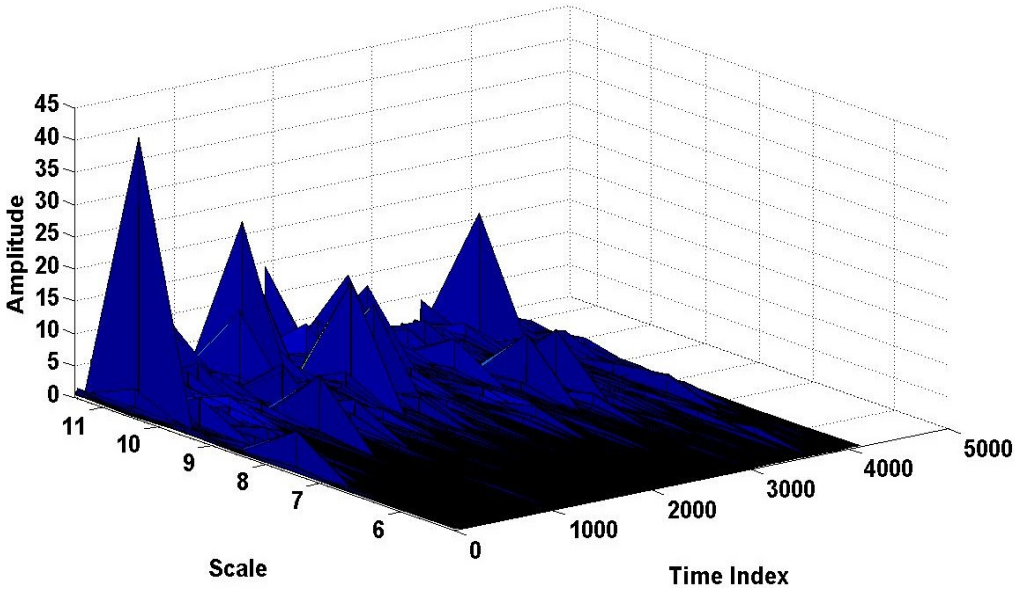

Figure 3.104 Impedance magnitude with a Gaussian window (differential voltage, shorted cable, dataset 5).

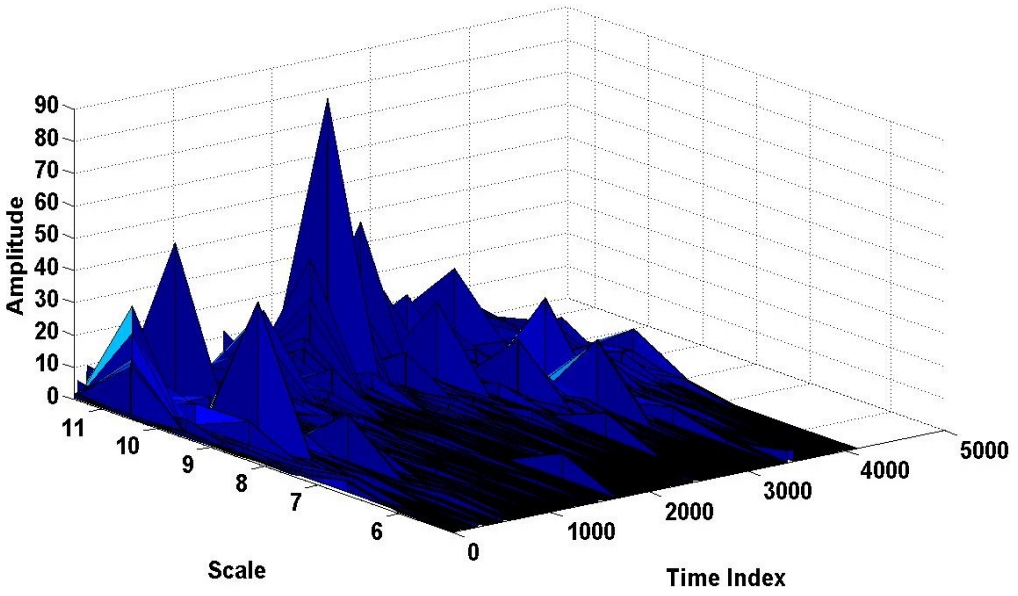

Figure 3.105 Impedance magnitude with a Hanning window (differential voltage, normal cable, dataset 2).

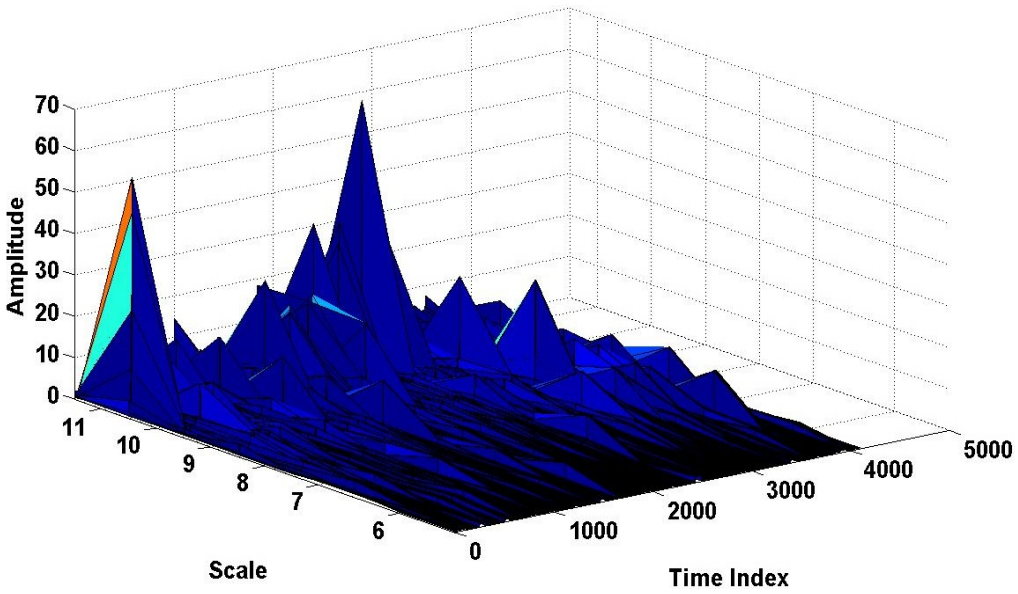

Figure 3.106 Impedance magnitude with a Hanning window (differential voltage, cable with holes, dataset 2).

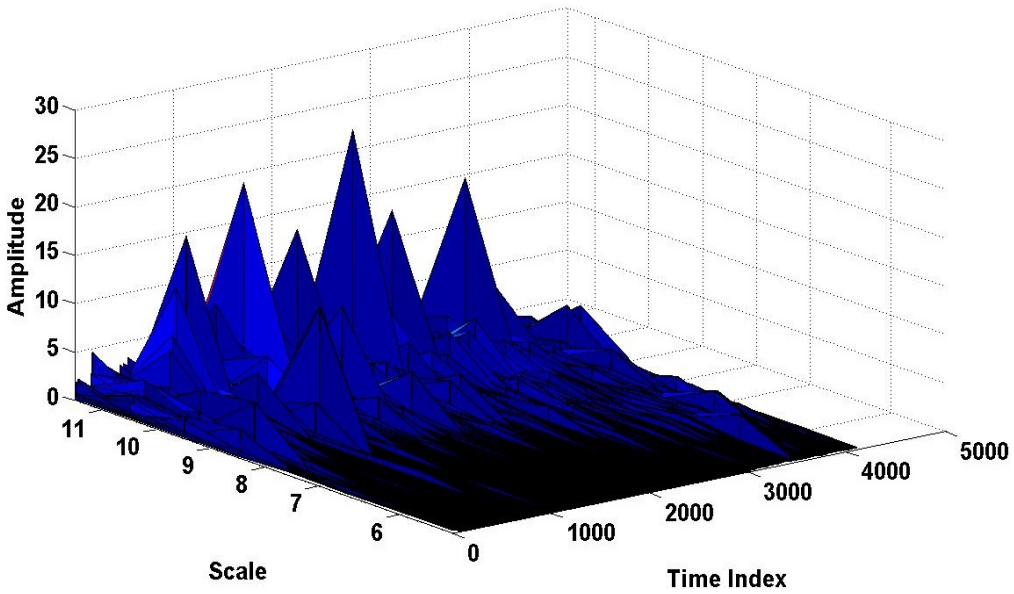

Figure 3.107 Impedance magnitude with a Hanning window (differential voltage, shorted cable, dataset 2).

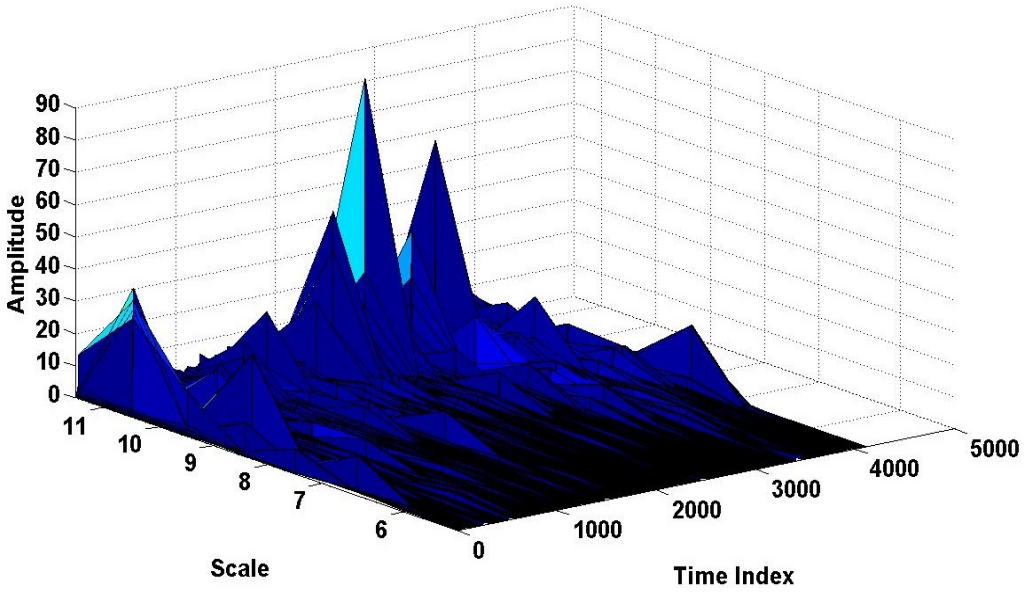

Figure 3.108 Impedance magnitude with a Hanning window (differential voltage, normal cable, dataset 3).

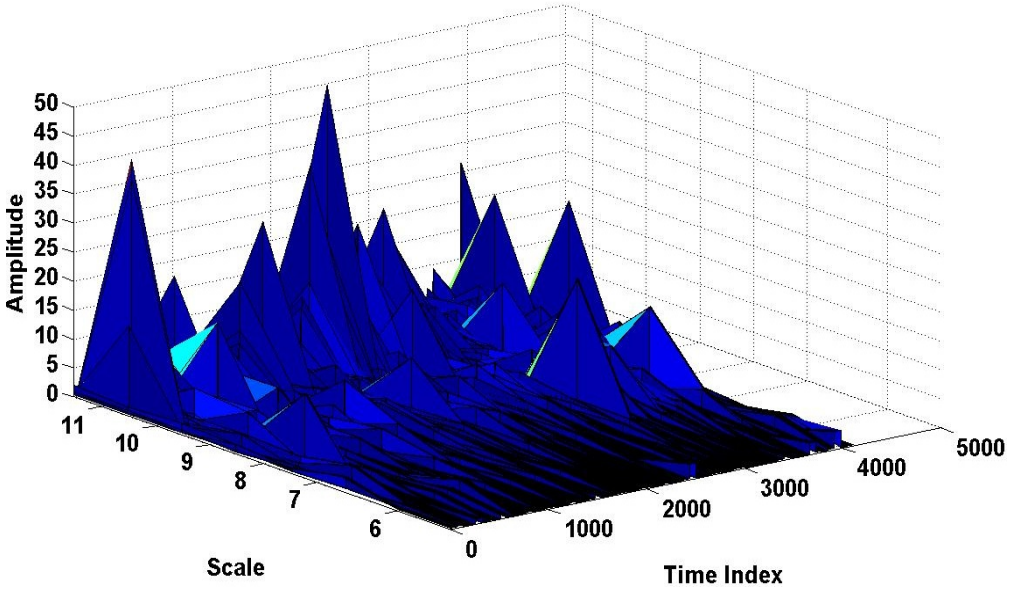

Figure 3.109 Impedance magnitude with a Hanning window (differential voltage, cable with holes, dataset 3).

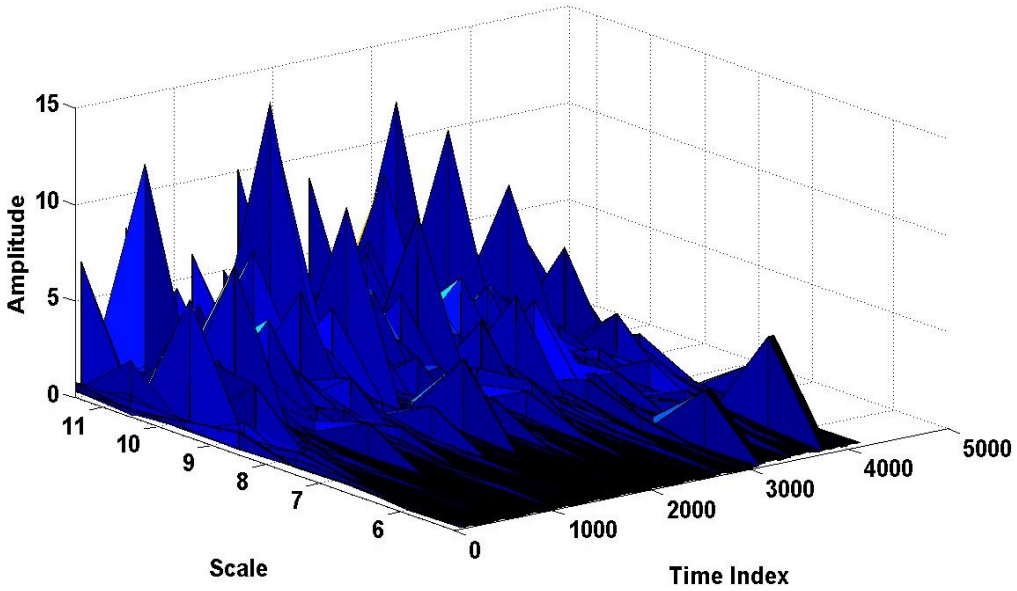

Figure 3.110 Impedance magnitude with a Hanning window (differential voltage, shorted cable, dataset 3).

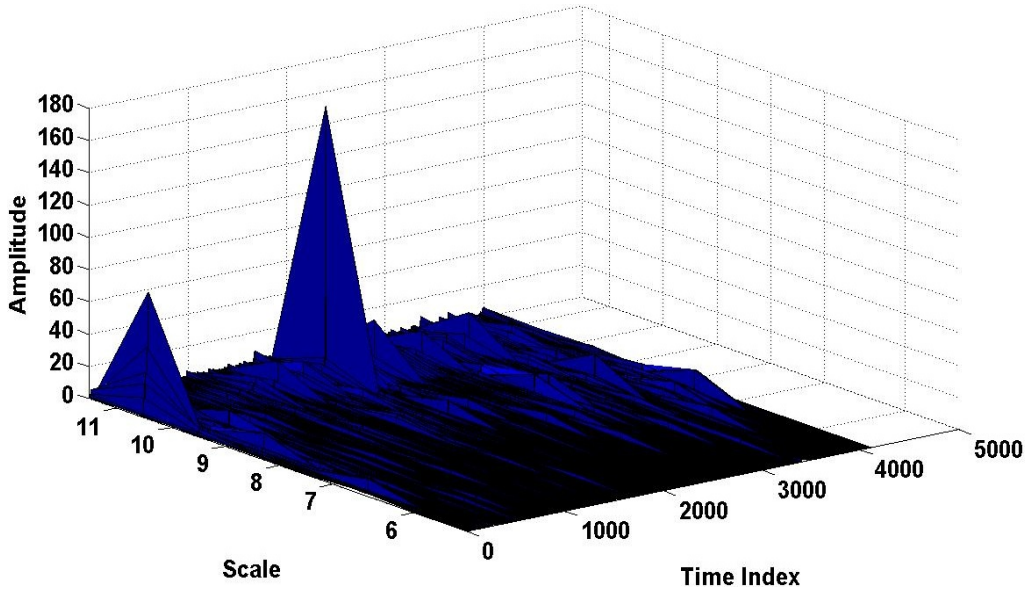

Figure 3.111 Impedance magnitude with a Hanning window (differential voltage, normal cable, dataset 4).

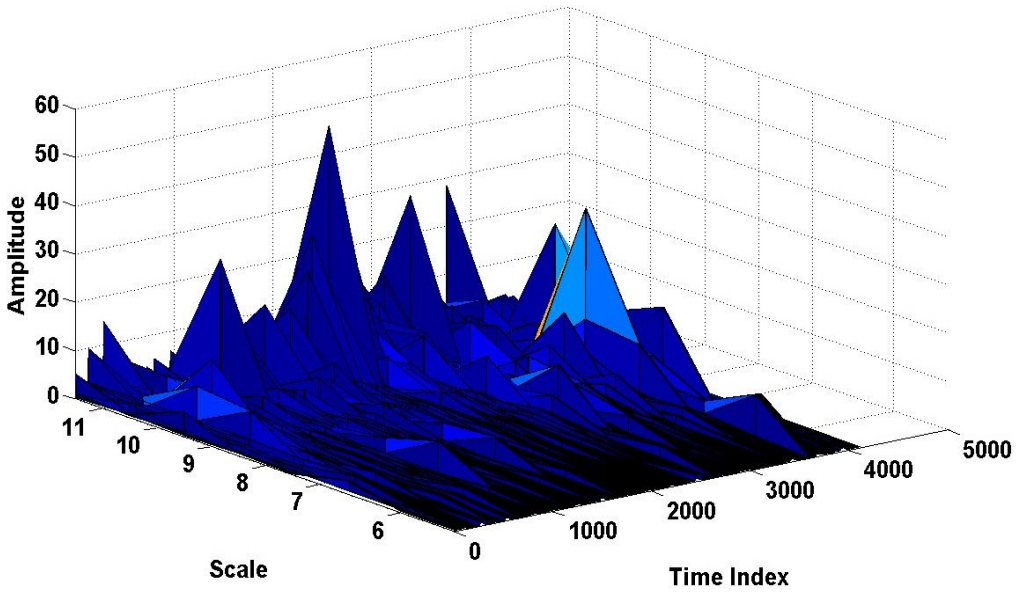

Figure 3.112 Impedance magnitude with a Hanning window (differential voltage, cable with holes, dataset 4).

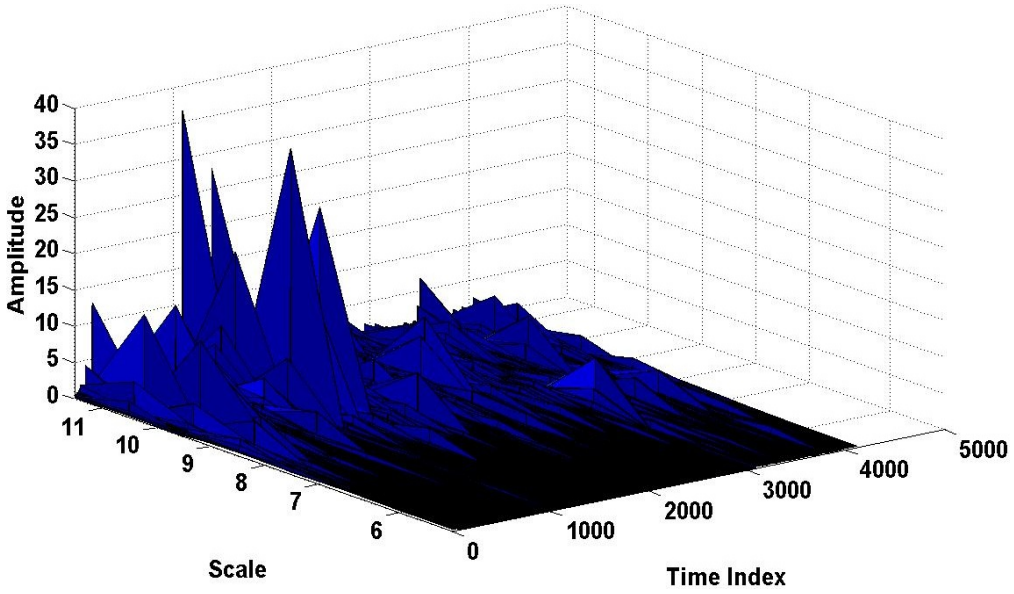

Figure 3.113 Impedance magnitude with a Hanning window (differential voltage, shorted cable, dataset 4).

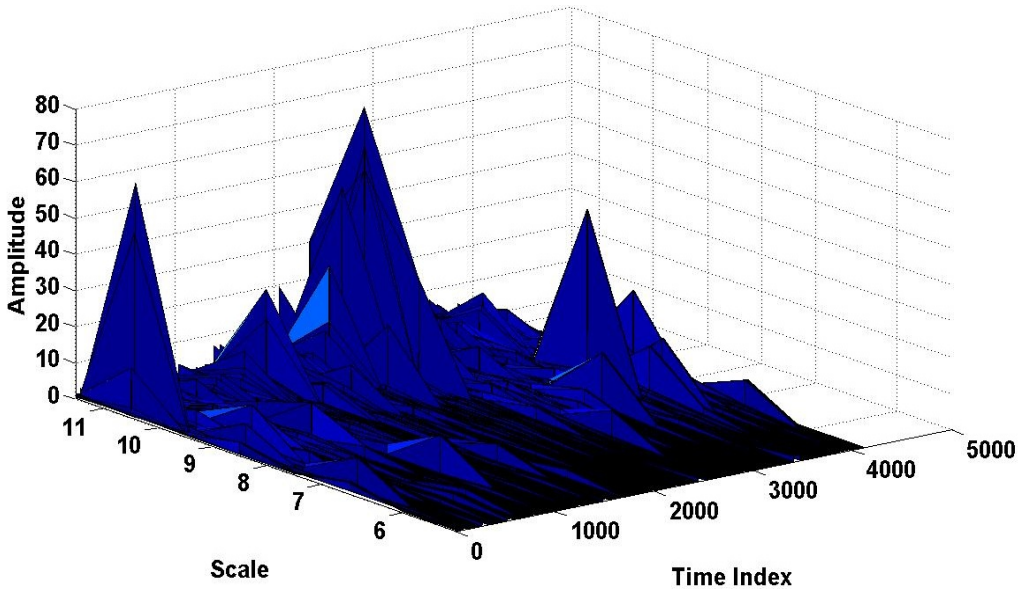

Figure 3.114 Impedance magnitude with a Hanning window (differential voltage, normal cable, dataset 5).

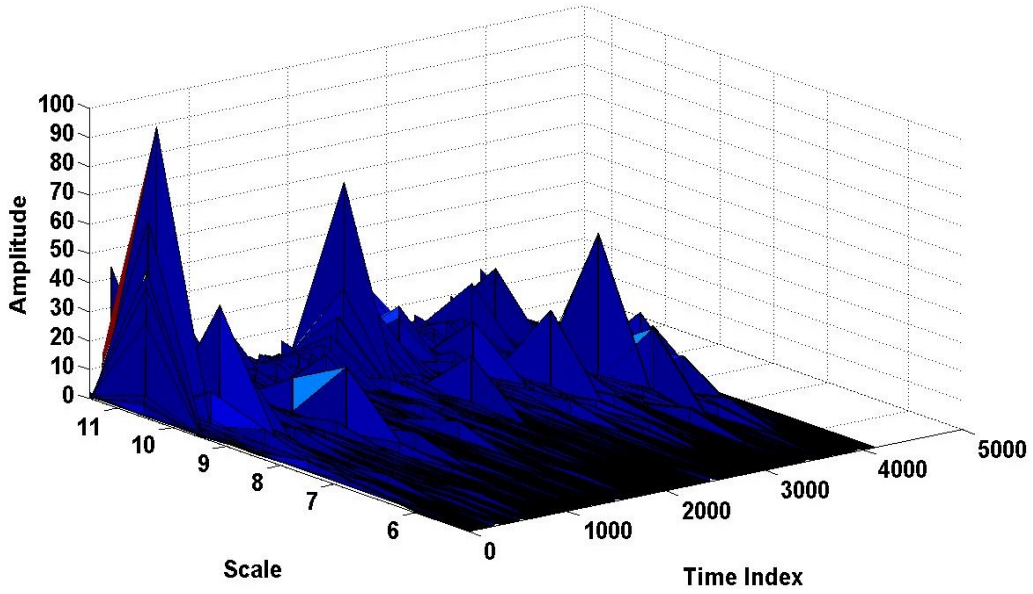

Figure 3.115 Impedance magnitude with a Hanning window (differential voltage, cable with holes, dataset 5).

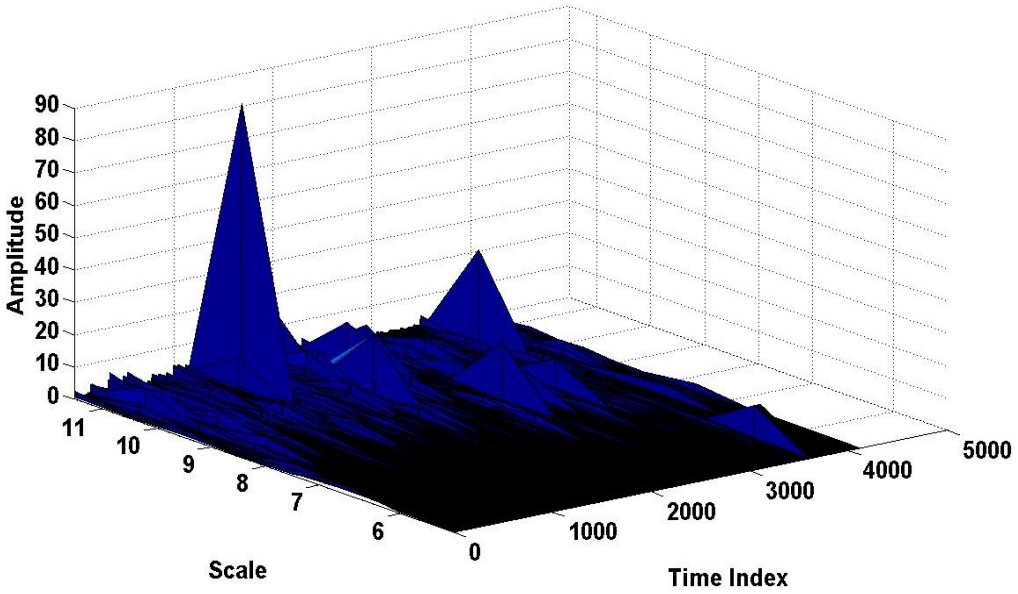

Figure 3.116 Impedance magnitude with a Hanning window (differential voltage, shorted cable, dataset 5).

3.7 Wavelet Transform Observations:

a) A 3D visualization of the magnitude response enhances the distinction between all cables' types and someone can easily differentiate between the different cables.

b) The Hanning window is mainly used since fault types can be easily distinguished. This window provides better results based on the magnitude response. Results from other windows provide also promising results.

c) The peak values maybe used as a measure of fault distance as they represent high amplitude at certain time index and scale values, especially for the shorted cable (distinguishable).

CHAPTER IV

SUMMARY

4.1 Conclusion:

All three cable types have been analyzed using fast Fourier transformation, short-time Fourier transformation, and wavelet transformation. Furthermore, identification and classification of various faults are investigated. Different types of windows are applied to the original fault signals. In general, a Gaussian window is found to have good response from the test data. Both Hanning and Hamming windows are also quite worthy contender.

Based on the FFT results, a Gaussian window gives encouraging results based on the phase response. The magnitude response obtained from FFT is not of much help as we are not able to differentiate between different cable types with it. The phase response, on the other hand, shows distinct results for different cable faults. Thus, we are able to identify and classify fault using the FFT phase response. This kind of diagnostic tool can be of great help in designing smart grids which can do self-healing. Classifying faults also helps us to tackle different cable faults differently.

Similar to the FFT, the STFT also shows good results based on the phase response. Hence, the phase response is quite helpful in identifying and classifying different fault types. Based on the magnitude response, both the FFT and the STFT fail to distinguish between the different types of cable faults. An exception to this conclusion is the shorted cable, which can be easily differentiated with the STFT impedance magnitude

response. Again, for the STFT, the Gaussian window proves to be a promising window function which can be used fault classification. Hamming and Hanning again are worthy contender as well.

On the other hand, the wavelet transform impedance magnitude plots provide a clear distinction between various fault types. Peaks of various sizes are easily identified. The magnitude response is helpful in fault classification via the wavelet transform as compared to the FFT and the STFT where the magnitude response is not of much help. Unlike the other two methods, the wavelet transform proves to respond better with a Hanning window. The Gaussian window still gives us considerable results but the outputs from a Hanning window is best for classifying different fault types.

4.2 Future Work

With multiresolution analysis, additional work can be further exploited. For example, one can further investigate the use of different mother wavelets and study their effect on fault detection. It is also of interest to investigate fault localization in real or near-real time. This will help in making this system implementable. Furthermore, a sensitivity analysis can be also further investigated to validate this method. Future works proposed for this research are

1) Investigate the use of different mother wavelets with the expectation to come up with a suitable one for this application. In our study, we have simply used the level 4 Daubechies (db4) mother wavelet and accordingly only magnitude information has been used for fault detection. Complex mother wavelets or adopting a different wavelet transformation implementation will provide us with

phase information that can probably be better suited for this analysis and provide more insight to fault detection.

2) Investigate the use of the localization property of the wavelet transform to predict the location of the faults. In general, the localization property of the wavelet transform provides information in both time and frequency, thus predicting faults location can be achieved with some additional manipulation to some extent.
3) Perform a sensitivity analysis to better assess the accuracy of the diagnostic tool. This requires additional measurements for cables with different lengths. Thus, building a library of cable measurements taking into consideration different fault types, locations, and different cable lengths so that spectrum matching can be used for near real time applications. This will make the system more practical and more reliable for field applications; thus fault detection can be possibly achieved without requiring a power outage.
4) Begin coordination with the high voltage laboratory to investigate the possibility of using this diagnostic tool on measured data obtained from their system. Thus, field implementation could be achieved.

REFERENCES

1. Abhishek Pandey and Nicolas Younan "Underground Cable Fault Detection and Identification via Fourier Analysis," International Conference on High Voltage Engineering and Application, New Orleans, pp 618 – 621, 2010.

2. Abhishek Pandey and Nicholas H. Younan, "Fault identification and classification of Power Cables using Short-Time Fourier Transformation," (ISH 2011 Hannover, Germany) (accepted).

3. Abhishek Pandey and Nicholas H. Younan, "Underground Cable Fault Detection and Identification via Wavelet Analysis," (CEIDP 2011 Cancun, Mexico) (accepted).

4. Abhishek Pandey and Nicholas H. Younan, "Underground Cable Fault Detection and Identification via Fourier Analysis," Journal of High Voltage Engineering for China", (selected and invited by ICHVE – 2010, New Orleans)(submitted).

5. Abhishek Pandey and Nicholas H. Younan, "Use of Wavelet Transform in Underground Cable Fault Detection and Identification," IEEE Transaction on Dielectrics and Electrical Insulation", (in preparation).

6. Thomas Owen Bialek, "Evaluation and modelling of high-voltage cable insulation using a high-voltage impulse," Ph.D. Dissertation, Mississippi State University, 2005.

7. J. Moshtagh and R.K Aggrawal ,"A new approach to fault location in a single core underground cable system using combined fuzzy logic and wavelet analysis," University of Bath, IEE, Michael Faraday House, Six Hills Way, Stevenage, SGI 2AY, 2004**.**

8. C. K. Jung, J. B. Lee, X. H. Wang and Y. H. Song, "A study on fault location algorithm on underground power cable system," *Proceedings of IEEE Power engineering society general meeting*, pp 2165-2171, 2005.

9. Lee Jae-Duck, Ryoo HeeSuk, Choi SangBong, Nam KeeYoung, Jeong SeongHwan, Kim DaeKyeong, "Signal processing technology for fault location system in underground power cable," *Transmission and Distribution Conference and Exhibition, 2005/2006 IEEE PES* ,pp-839.

10. Mahmoud Gilany, Doaa khalil Ibrahim, and El Sayed Tag Eldin, "Travelling wave-based fault location scheme for multiend-aged underground cable system," *IEEE Trans. On Power Delivery*, Vol 22 No.1, January 2007.

11. Willaim R.Stagi, "Cable injection technology," *IEEE Latin American Conference.*, 2007.

12. Mirrasoul J.Mousavi, Karen L. Butler-Purry, Ricardo Gutierrez-Osuna and Massieh Najafi, "Classification of load change transient and incipient abnormalities in underground cable using pattern analysis techniques," Texas A&M University, Department of Electrical Engineering, Power System Automation Laboratory , College Station, TX 77843-3123

13. KL Butler and S S Dey, "Using Discrete Wavelet Transforms to Characterize Equipment Failures for Maintaining Distribution System Reliability," *Proc. 4th Int. Conf. Power Syst. Oper. Planning*, Texas A&M University, Department of Electrical Engineering, Power System Automation Laboratory , College Station, TX 77843-3123

14. E.O. Bringham and R.E. Morrow "The Fast Fourier Transform," *IEEE Spectrum*, Vol 4, pp 63- 70.

15. Robi Polikar, "The Wavelet Tutorial" by, Rowan University http://users.rowan.edu/~polikar/WAVELETS/WTtutorial.html

16. Oppenheim, Alan V., Schafer, Ronald W. and Buck, John A. (1999). *Discrete-time signal processing*. Upper Saddle River, N.J.: Prentice Hall. pp. 468–471. ISBN 0-13-754920-2.

17. Thomas Theußl, Helwig Hauser and Eduard Gr ller "Mastering windowing: Improving Reconstruction," Institute of Computer Graphics, Vienna University of Technology.